

UNCLASSIFIED

AD NUMBER

ADB259398

NEW LIMITATION CHANGE

TO

Approved for public release, distribution
unlimited

FROM

Distribution authorized to U.S. Gov't.
agencies only; Proprietary Info.; Jul
2000. Other requests shall be referred to
U.S. Army Medical Research and Material
Command, 504 Scott St., Fort Detrick, MD
21702-5012.

AUTHORITY

USAMRMC ltr, 26 Aug 2002

THIS PAGE IS UNCLASSIFIED

AD _____

GRANT NUMBER: DAMD17-96-1-6038

TITLE: Growth Suppression and Therapy Sensitization of Breast Cancer

PRINCIPAL INVESTIGATOR: Ruth A. Gjerset, Ph.D.

CONTRACTING ORGANIZATION: Sidney Kimmel Cancer Center
San Diego, California 92121

REPORT DATE: July 2000

TYPE OF REPORT: Annual Report

PREPARED FOR: U.S. Army Medical Research and Materiel Command, Fort Detrick, Frederick, Maryland
21702-5012

DISTRIBUTION STATEMENT: Distribution authorized to U.S. Government agencies only (proprietary information, Jul 00). Other requests for this document shall be referred to U.S. Army Medical Research and Materiel Command, 504 Scott Street, Fort Detrick, Maryland 21702-5012.

The views, opinions and /or findings contained in this report are those of the author(s) and should not be construed as an official Department of the Army position, policy or decision unless so designated by other documentation.

DTIC QUALITY INSPECTED 4

20001107 060

NOTICE

USING GOVERNMENT DRAWINGS, SPECIFICATIONS, OR OTHER DATA INCLUDED IN THIS DOCUMENT FOR ANY PURPOSE OTHER THAN GOVERNMENT PROCUREMENT DOES NOT IN ANY WAY OBLIGATE THE U.S. GOVERNMENT. THE FACT THAT THE GOVERNMENT FORMULATED OR SUPPLIED THE DRAWINGS, SPECIFICATIONS, OR OTHER DATA DOES NOT LICENSE THE HOLDER OR ANY OTHER PERSON OR CORPORATION; OR CONVEY ANY RIGHTS OR PERMISSION TO MANUFACTURE, USE, OR SELL ANY PATENTED INVENTION THAT MAY RELATE TO THEM.

LIMITED RIGHTS LEGEND

Award Number: DAMD17-96-1-6038

Organization: Sidney Kimmel Cancer Center

Those portions of the technical data contained in this report marked as limited rights data shall not, without the written permission of the above contractor, be (a) released or disclosed outside the government, (b) used by the Government for manufacture or, in the case of computer software documentation, for preparing the same or similar computer software, or (c) used by a party other than the Government, except that the Government may release or disclose technical data to persons outside the Government, or permit the use of technical data by such persons, if (i) such release, disclosure, or use is necessary for emergency repair or overhaul or (ii) is a release or disclosure of technical data (other than detailed manufacturing or process data) to, or use of such data by, a foreign government that is in the interest of the Government and is required for evaluational or informational purposes, provided in either case that such release, disclosure or use is made subject to a prohibition that the person to whom the data is released or disclosed may not further use, release or disclose such data, and the contractor or subcontractor or subcontractor asserting the restriction is notified of such release, disclosure or use. This legend, together with the indications of the portions of this data which are subject to such limitations, shall be included on any reproduction hereof which includes any part of the portions subject to such limitations.

THIS TECHNICAL REPORT HAS BEEN REVIEWED AND IS APPROVED FOR PUBLICATION.

Nimisha Chen Miron
10/19/05

REPORT DOCUMENTATION PAGE			Form Approved OMB No. 0704-0188
<p>Public reporting burden for this collection of information is estimated to average 1 hour per response, including the time for reviewing instructions, searching existing data sources, gathering and maintaining the data needed, and completing and reviewing the collection of information. Send comments regarding this burden estimate or any other aspect of the collection of information, including suggestions for reducing this burden, to Washington Headquarters Services, Directorate for Information Operations and Reports, 1215 Jefferson Davis Highway, Suite 1204, Arlington, VA 22202-4302, and to the Office of Management and Budget, Paperwork Reduction Project (0704-0188), Washington, DC 20503.</p>			
1. AGENCY USE ONLY (Leave Blank)	2. REPORT DATE	3. REPORT TYPE AND DATES COVERED	
	July 2000	Annual (July 1, 1999 to June 30, 2000)	
4. TITLE AND SUBTITLE		5. FUNDING NUMBERS	
Growth Suppression and Therapy Sensitization of Breast Cancer		DAMD17-96-1-6038	
6. AUTHOR(S)			
Ruth A. Gjerset, Ph.D.			
7. PERFORMING ORGANIZATION NAME(S) AND ADDRESS(ES)		8. PERFORMING ORGANIZATION REPORT NUMBER	
Sidney Kimmel Cancer Center San Diego, California 92121			
9. SPONSORING/MONITORING AGENCY NAME(S) AND ADDRESS(ES)		10. SPONSORING/MONITORING AGENCY REPORT NUMBER	
U.S. Army Medical Research and Materiel Command Fort Detrick, Frederick, Maryland 21702-5012			
11. SUPPLEMENTARY NOTES			
12a. DISTRIBUTION / AVAILABILITY STATEMENT		12b. DISTRIBUTION CODE	
Distribution authorized to U.S. Government agencies only (proprietary information, Jul 00). Other requests for this document shall be referred to U.S. Army Medical Research and Materiel Command, 504 Scott Street, Fort Detrick, Maryland 21702-5012.			
13. ABSTRACT (Maximum 200 Words)			
<p>The goal of this project is to provide a rationale and pre-clinical evaluation of p53-based approaches to growth suppression and therapy sensitization of breast cancer, including combination approaches in which p53 gene therapy is combined with traditional chemotherapy or with inhibitors of DNA repair. We have observed <i>in vitro</i> that p53 + doxorubicin provided an additive to synergistic suppression of breast cancer cell viability. The scope of the fourth year's work was to extend these observations to <i>in vivo</i> breast cancer models in nude mice. Using a sub-cutaneous model with MDA-MB-435 breast cancer cells, we observed that direct intratumoral injection of p53 adenovirus led to a significant suppression of tumor growth that was enhanced in animals that received doxorubicin in addition. Using the MDA-MB-435 orthotopic nude mouse model for breast cancer metastasis, we observed that systemic administration of Adp53 in combination with doxorubicin led to a significant suppression of lung metastases. Taken together these results suggest that p53 gene therapy in combination with conventional therapy could have broad application for breast cancer treatment. We are presently investigating how DNA repair inhibitors affect p53-mediated apoptosis in breast cancer.</p>			
14. SUBJECT TERMS		15. NUMBER OF PAGES 75	
Breast Cancer		16. PRICE CODE	
17. SECURITY CLASSIFICATION OF REPORT	18. SECURITY CLASSIFICATION OF THIS PAGE	19. SECURITY CLASSIFICATION OF ABSTRACT	20. LIMITATION OF ABSTRACT
Unclassified	Unclassified	Unclassified	Limited

FOREWORD

Opinions, interpretations, conclusions and recommendations are those of the author and are not necessarily endorsed by the U.S. Army.

RG Where copyrighted material is quoted, permission has been obtained to use such material.

RG Where material from documents designated for limited distribution is quoted, permission has been obtained to use the material.

RG Citations of commercial organizations and trade names in this report do not constitute an official Department of Army endorsement or approval of the products or services of these organizations.

RG In conducting research using animals, the investigator(s) adhered to the "Guide for the Care and Use of Laboratory Animals," prepared by the Committee and Care and Use of Laboratory Animals of the Institute of Laboratory Resources, national Research Council (NIH Publication No. 86-23, Revised 1985).

For the protection of human subjects, the investigator(s) adhered to policies of applicable Federal Law 45 CFR 46.

In conducting research utilizing recombinant DNA technology, the investigator(s) adhered to current guidelines promulgated by the National Institutes of Health.

RG In the conduct of research utilizing recombinant DNA, the investigator(s) adhered to the NIH Guidelines for Research Involving Recombinant DNA Molecules.

RG In the conduct of research involving hazardous organisms, the investigator(s) adhered to the CDC-NIH Guide for Biosafety in Microbiological and Biomedical Laboratories.

Ruth G. Gjerset
PI - Signature

7.23.2000
Date

TABLE OF CONTENTS

	<u>Page #</u>
FRONT COVER	
REPORT DOCUMENTATION PAGE	2
FOREWORD	3
TABLE OF CONTENTS	4
INTRODUCTION	5
BODY OF REPORT	6-10
KEY RESEARCH ACCOMPLISHMENTS	11
REPORTABLE OUTCOME	12
CONCLUSIONS	13-14
REFERENCES	15
APPENDIX COVER PAGE	16

Growth Suppression and Therapy Sensitization of Breast Cancer
DAMD17-96-1-6038
Progress Report #4

INTRODUCTION

This project is designed to provide a rationale and pre-clinical evaluation of p53-based approaches to growth suppression and therapy sensitization of breast cancer, including combination approaches in which p53 gene therapy is combined with traditional chemotherapy or inhibitors of DNA repair. p53 abnormalities occur in about 40% of breast cancers (1-4), and are a feature of more aggressive tumors with increased aneuploidy and genetic instability (5,6). Gene therapy approaches aimed at restoring wild-type p53 function to tumors with abnormal endogenous p53 would therefore have broad application, particularly for advanced disease. We have also observed that p53 adenovirus suppresses the *in vitro* growth of breast cancer cells with endogenous wild-type p53, suggesting that p53-based approaches would have application to wild-type p53-expressing tumors as well. Because p53 gene transfer appears to have minimal consequences for normal cells, and because p53 adenovirus has been used successfully in animal models and Phase I clinical trials for various cancers without toxicity (7,8), p53 based approaches for breast cancer therapy hold promise as effective biological therapies with minimal to no adverse side effects.

Loss of p53 plays a key role in tumor progression and also promotes resistance to DNA damaging chemotherapeutic drugs such as cisplatin and doxorubicin. This is most likely due to the function of p53 as a modulator of apoptosis following DNA damage (9-13). Karyotypic instability, which occurs in breast cancer and increases with disease progression, generates strand breaks and other forms of DNA damage that can stabilize p53 and activate it for transcriptional transactivation and induction of apoptosis. Loss of p53 function would then favor the growth of karyotypically unstable cancer cells by removing the trigger for apoptosis (possibly an abnormal DNA structure generated by the mechanisms that destabilize the genome of these cells) as proposed in (14). This notion is consistent with studies of mammary tumorigenesis in wnt-1 transgenic mice where a correlation between loss of p53 function and increased genomic instability and aneuploidy was observed, suggesting that p53 deficiency relaxes constraints on chromosome number and organization during tumorigenesis.

Loss of p53-mediated DNA damage-induced apoptosis also promotes resistance to radiation and DNA damaging chemotherapeutic drugs. We and others have shown that restoration of p53 function in tumor cells that have lost p53, restores apoptosis in response to DNA damaging therapies such as cisplatin and 5-fluorouracil (15,16). We have also shown that restoration of p53 function in T47D breast cancer cells and MDA-MB-435 breast cancer cells, both of which express endogenous mutant p53, enhances sensitivity to the DNA damaging drug doxorubicin (adriamycin), the standard therapy for breast cancer. Because resistance to doxorubicin and other chemotherapies occurs in breast cancer, and constitutes one of the biggest obstacles to successful therapy of this disease, we have set up subcutaneous and orthotopic (mammary fat pad) models for breast cancer in nude mice (described below) and have carried out studies (tasks

6,7) to test the efficacy of a combined p53 adenovirus + doxorubicin approach in inhibiting primary tumor growth as well as metastatic disease.

The central hypothesis of this project is that the level of DNA damage is a key determinant of a tumor cell's susceptibility to p53-mediated apoptosis. In tumor cells with unstable genomes the endogenous DNA damage would trigger p53-mediated apoptosis unless the damage is repaired. We postulated therefore that agents that inhibit DNA repair (for example, inhibitors of c-Jun downstream targets, see below) would promote p53-mediated apoptosis by increasing the endogenous level of DNA damage in these cells. Chemotherapeutic agents that directly damaged DNA (cisplatin, doxorubicin) would also enhance p53-mediated apoptosis. In support of this hypothesis, we have reported on studies showing that cell lines inhibited in DNA repair have increased genomic instability and are more sensitive to p53-mediated apoptosis through expression of bax, and we have published these results (17, copy attached).

Overall our results provide a strong rationale for the combined use of p53 along with DNA damaging chemotherapies or inhibitors of DNA repair for the treatment of breast cancer. As part of a no cost extension to this study, we will complete studies on the combined effects of p53 and DNA repair inhibition in breast cancer.

BODY OF REPORT

Our objectives for the fourth year, as outlined in the Statement of Work included (task 6, Specific Aim 4 continued) carrying out *in vivo* tumor models demonstrating the efficacy of p53 gene therapy in combination with the DNA damaging chemotherapeutic, doxorubicin. We have also initiated the construction of gene transfer vectors for mutant Jun and c-Jun that will enable us to examine how inhibition of c-Jun downstream targets affects the response of breast cancer cells to p53 and chemotherapy.

Results

Inhibition of subcutaneous tumor growth by Adp53 in the presence and absence of doxorubicin.

A subcutaneous tumor model was used to extend the *in vitro* observations to an *in vivo* situation and to provide a point of reference for the subsequent metastasis model. For the subcutaneous model, 10^6 MDA MB 435 cells were implanted under the skin of the back of female nude mice. About 10 days post implantation, or when the average tumor size was about 40 mm^3 , animals were randomized into 4 groups of 10 animals each and administered treatment (designated day 1). Doxorubicin was administered intravenously

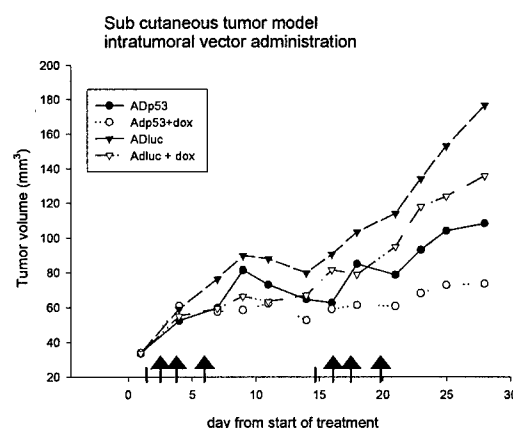


Figure 1. Growth of subcutaneous tumors of MDA-MB-435 cells (provided by Janet Price, M.D. Anderson Cancer Center) in nude mice. Animals were treated intratumorally with AdLuc (control vector) or Adp53 on days indicated by arrows. Some groups received intravenous doxorubicin on days indicated by a vertical line

(100 μ l of a 2 mg/ml solution, or 10 mg/kg) on days 1,15. Vector (Adp53 or AdLuc at 3×10^8 pfu per mg) were administered intratumorally (in 100 μ l PBS) on days 2,4, and 7, and again on days 16, 18, and 21. p53-Adenovirus and AdLuc adenovirus (control) was supplied by Introgen Therapeutics. Tumors were measured at 2 -3 day intervals and volumes were calculated and plotted in Figure 3. Using an Anova variance analysis of all data points at each time point, we observed significant differences in the 4 treatment groups beginning at day 21 ($p < 0.05$) and continuing after that ($p < 0.01$ on days 23, 25, 28). In the Adp53 + doxorubicin treatment group, tumor growth was largely arrested over the period of treatment. The results suggest an additive to synergistic benefit from the combination of Adp53 and doxorubicin relative to Ad p53 alone or relative to dox alone (AdLuc +dox).

Inhibition of breast cancer metastases by Adp53 and doxorubicin. In order to determine whether systemically administered Adp53 (tail vein) in combination with doxorubicin improved the outcome for metastatic disease, we employed an orthotopic mammary fat pad model using the same MDA-MB-435 cells provided by Janet Price (M.D. Anderson Cancer Center, Houston, Texas). These cells were selected by Dr. Price for increased metastatic potential. As reported by Dr. Price, and as we confirmed (see Progress Report Year 3), these cells form lung metastases in a high proportion of animals (50-80%) following mammary fat pad implantation. Furthermore, we have also confirmed that tail vein administration of a control adenovirus (β -gal adenovirus) is able to reach the lung of injected animals, supporting the use of Adp53 to treat lung metastases. Figure 2 shows the results of β -gal immunohistochemistry on formaldehyde-fixed, paraffin-imbedded sections of lung tissue taken from animals two days following tail vein injection of 10^9 pfu of Ad β gal. A similarly treated section of normal mouse lung is shown for comparison.

We then tested the efficacy of Adp53 combination therapy with doxorubicin in eradicating breast cancer lung metastases. 5×10^5 cells were implanted in the mammary fat pads of female nude mice (protocol described by Janet Price and colleagues (18)). At 8 weeks post implantation primary tumors that had attained a size of 600-900 mm^3 were excised, although these tumors grew back in the second half of the experiment. At 9½ weeks post-implantation, animals were randomized into treatment groups of 7-8 animals each and treatment was initiated (day 1). Doxorubicin was administered intravenously on days 1 and 21. Vector was administered at 2-3 day intervals for the duration of the experiment (from day 3 and ending on day 46). In order to equalize potential vector-related toxicities resulting from systemic administration of vector, we administered equivalent amount of vector to control (AdLuc) animals and Adp53 animals (2.5×10^{10} vp of vector per animal per injection in 100 μ l PBS). This corresponded to 3×10^8 pfu in the case of Adp53 and 10^9 pfu in the case of AdLuc. The treatment protocol is summarized below:

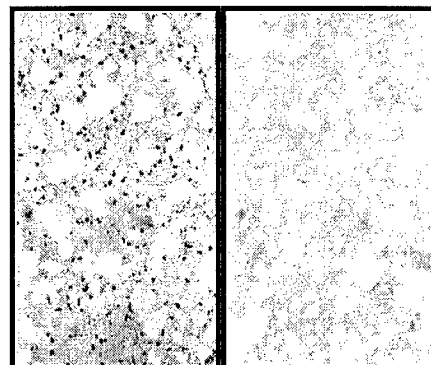


Figure 2. Immunohistochemical stain for β -galactosidase expression in lung sections from mice injected intravenously with 10^9 pfu of Ad β gal (left). A similarly stained section of lung from an untreated animal is shown to the right.

Treatment schedule for MD MB 435 metastases
 (3 cycles of treatment in weeks 1, 3, 5)
 9 animals per group

1) no treatment 2) doxorubicin only 3) Ad-p53 4) Ad-Luc (control vector) 5) Ad-p53 + doxorubicin 6) Ad-Luc + doxorubicin	} Doxorubicin 10 mg/kg day 1, 15, 29 (100 µl) Vector 3x per week during weeks 1-6. Vector dose: 5×10^{10} vp per injection $= 5 \times 10^8$ pfu for Adp53 and 2×10^9 pfu for AdLuc
---	--

Metastases were monitored at 15-16 weeks post-implantation (i.e., 7-8 weeks post tumor excision) by sacrificing the animals, removing the lungs, and fixing the lungs in 10% formaldehyde for paraffin imbedding and histological analysis. Longitudinal and transverse sections were prepared and analyzed for the incidence of metastases (Table 1). As shown in the table, lung metastases were observed in all treatment groups except the group that had been treated with Adp53 + doxorubicin. A Fisher exact test showed that the reduction in metastases was significant to $p = 0.07$ for the Adp53+ doxorubicin group relative to the other groups. Amongst the other groups, the incidences of metastases were not statistically significant.

Two deaths that occurred in the AdLuc + dox treatment group and appeared to be disease-related. Because these animals were not analyzed for lung metastases, the incidence scored for that group (Table 1) could under represent the actual incidence for that group.

Table 1
 Incidence of lung metastases in nude mice, 16 weeks following mammary fat pad implantation of 10^5 MDA-MB-435 breast cancer cells.

<i>Animal group</i>	<i>N/group</i>	<i>Incidence (histology) (%)</i>	<i>Average animal weight (gm) per group</i>
No treatment	8	38	26
Dox	8	50	26
Adp53	8	50	26
AdLuc	8	38	26
Adp53 + dox	7	0	24
AdLuc + dox	6 (2 deaths)	17	26

Treatment was initiated at 8 weeks post-implantation of tumor cells, and just after excision of the primary tumors. Treatment consisted of vector, 10^{11} viral particles (10^9 pfu) of p53 adenovirus (or AdLuc control) administered 3 times per week by tail vein injection. Some of the animals received doxorubicin intravenously (100 µl of a 2 mg/ml stock, or 10 mg/kg) once every three weeks for a total of three doses.

Overall toxicity, assessed by weighing the animals at the end of the treatment (Table 1), was minimal, as all groups showed similar average weights. Toxicity to the liver, the organ preferentially targeted by adenovirus, was assessed by histological examination of formaldehyde-fixed liver sections. No toxic effects of prolonged exposure to vector were apparent in any of the treatment groups.

Enhancement of p53-mediated apoptosis by DNA repair inhibition. We have previously observed in T98G glioblastoma cells that inhibition of c-Jun downstream targets following modification of cells with a non-phosphorylatable mutant of c-Jun (denoted m-Jun) leads to inhibition of DNA repair, enhanced sensitivity to the DNA damaging drug, cisplatin, increased genome instability, and enhanced p53-mediated apoptosis. To extend these observations to a breast cancer model, we have constructed retroviral vectors encoding the c-Jun and m-Jun sequences from a bicistronic gene also encoding green fluorescent protein (GFP). The strategy for vector construction is shown in Figure 3.

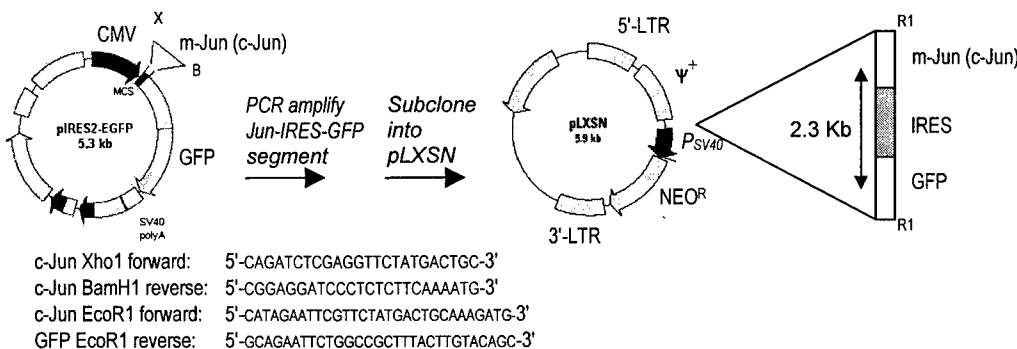


Figure 3. Scheme showing the construction of bicistronic retroviral constructs (pLXSN) encoding m-Jun or c-Jun and Green Fluorescent Protein, beginning with the bicistronic plasmid pIRES2-EGFP (Clontech Laboratories, Inc.)

The 995 base pair coding sequence for c-Jun or m-Jun has been PCR amplified from normal cellular cDNA or from pLHC(m-Jun), respectively, using the forward and reverse primers that create Xho1 (X) and BamH1 (B) restriction sites for subcloning (Primers synthesized by Genosys Biotechnologies, Inc., Woodlands, TX). Primers have been selected with the aid of MacVector software. Following amplification, restriction digestion and purification of the PCR fragment, it was inserted between the Xho1 and the BamH1 sites in the multi-cloning site of pIRES2-EFGP (Clontech Laboratories Inc.), which incorporates an internal ribosome binding site (IRES) and generates a bicistronic message in which the subcloned gene of interest is translated from the same transcript as Green Fluorescent Protein. In the case of the m-Jun vector, the entire bicistronic region, including m-Jun, IRES (584 bp), and GFP (726 bp), has been PCR amplified from this vector, using primers that generate EcoR1 sites at the 5' and 3' ends, so that it could be inserted into the EcoR1 site of the retroviral plasmid pLXSN. Orientation was verified by restriction digestion. All vector constructs will be sequenced prior to using them in biological experiments (service available through the Microarray Facility of Sidney Kimmel Cancer Center). A similar strategy is being used to generate a bicistronic retroviral construct for c-Jun. The retroviral construct will then be used to generate modified retrovirus using the GP-293 packaging cell line (gag-pol-modified human embryonic kidney cells) cotransduced with the pLXSN construct and pVSV-G (both available from Clontech Laboratories, Inc.). The pVSV-G plasmid encodes the envelope glycoprotein from vesicular stomatitis virus (VSV), which does not require a receptor for entry into a cell. The system allows production of pantropic virus of high titer (up to 10^8 or higher cfu/ml following concentration). As controls for biological experiments, we will use parental unmodified cells, and cells modified with empty constructs, lacking the m-Jun (or c-Jun) sequences. We will then transduce the tumorigenic cell line MDA-MB-435, which we have previously used, to generate modified populations expressing m-Jun or c-Jun. The efficiency of gene transduction of the culture can be directly

visualized using an inverted fluorescence microscope. Once the cultures have been selected, overexpression of Jun protein will be verified by Western analysis using a murine monoclonal antibody to the C-terminal domain of c-Jun, available from Santa Cruz Biotechnologies (Santa Cruz CA), using procedures provided by the manufacturer.

The cell lines will then be used to assay DNA repair, and drug sensitivity *in vitro*. Based on the results of the *in vitro* experiments, we will then extend the results to include an *in vivo* subcutaneous tumor model in nude mice, in which the efficacy of p53-based therapy is evaluated in tumors expressing mutant Jun or normal cellular c-Jun.

These results could have clinical implication for late stage tumors where DNA repair mechanisms may be upregulated in response to exposure to DNA damaging therapies (17-21). Such tumors may require concurrent down regulation of DNA repair in order to respond optimally to p53 therapy. Down regulation of specific AP-1 regulated DNA synthesis and repair genes may provide a means to inhibit DNA repair and enhance sensitivity to p53.

Key Research Accomplishments

We have observed the following:

- Restoration of wild-type p53 expression enhances sensitivity of breast cancer cells to doxorubicin, a DNA damaging drug, and the standard therapy for breast cancer.
- Inhibition of DNA repair in tumor cells enhances sensitivity to DNA damaging drugs, as well as p53-mediated induction of bax and apoptosis.
- Inhibition of c-Jun downstream targets (through inhibition of c-Jun N terminal phosphorylation) leads to DNA repair defects, increased gene amplification, and increased p53-mediated apoptosis.
- Inhibition of c-Jun N terminal phosphorylation inhibits cisplatin-induced expression of GADD45, suggesting that this may be one downstream target of phosphorylated c-Jun.
- Pretreatment of T47D breast cancer cells with 9-cis retinoic acid leads to increased cisplatin adduct formation in the promoter region of the 9-cis retinoic acid-responsive gene, retinoic acid receptor β (RAR β), suggesting that retinoids such as 9-cis retinoic acid, through their pleiotropic effects on gene expression, generate new targets for cisplatin, and enhance its cytotoxicity through inhibition of the transcription initiation complex.
- MDA-MB-435 cells, expressing endogenous mutant p53, are growth inhibited and sensitized to doxorubicin following restoration of wild-type p53 function. They also provide a useful *in vivo* model for breast cancer metastasis.
- Subcutaneous tumors of MDA-MB-435 cells are suppressed by intratumoral administration of Adp53, and this suppression is enhanced in the presence of doxorubicin.
- Systemic administration of Adp53 suppresses lung metastases in a mouse orthotopic model of metastatic breast cancer, and suppression is enhanced when combined with doxorubicin.

- Reportable Outcomes

Manuscripts:

- (1) Gjerset, R.A., Lebedeva, S., Haghghi, A., Turla, S.T., and Mercola, D. (1999) Inhibition of the Jun kinase pathway blocks DNA repair, enhances p53-mediated apoptosis and promotes gene amplification. *Cell Growth and Differentiation* 10:545-554.
- (2) Haghghi, A., Lebedeva, S., and Gjerset, R.A. (1999) Preferential platination of an activated cellular promoter by cis-diamminedichloroplatinum. *Biochemistry* 38: 12432-12438.
- (3) Gjerset, R.A., and Mercola, D. (2000) Sensitization of tumors to chemotherapy through gene therapy. In "Cancer Gene Therapy: Past Achievements and Future Challenges", N. Habib, ed., Plenum Publishing Corporation, New York, London, Moscow. pp. 273-291.
- (4) Gjerset, R.A., Haghghi, A., Lebedeva, S., Mercola, D. Gene Therapy Approaches to sensitization of human prostate carcinoma to cisplatin, *In "Methods in Molecular Biology: Genomics Protocols"*, M. Starkey and R. Elaswarapu, eds. The Humana Press, Inc. Totowa, N.J. (*in press*).
- (5) Lebedeva, S., Bagdasaraova, S., Tyler, T., Mu, S., Wilson, D.R., and Gjerset, R.A. Tumor Suppression and Therapy Sensitization of localized and metastatic breast cancer by adenovirus p53. (*in preparation*).

Abstracts, posters, oral presentations:

- (1) Haghghi, A., Lebedeva, S., Mercola, D., Saadatmandi, N., Gjerset, R. "T98G glioblastoma cells defective in DNA repair show enhanced p53-mediated growth suppression and apoptosis." Presented at the AACR Special Conference on DNA repair Defects, San Diego CA, January 14-18, 2000.

Conclusions

We have shown that restoration of wild-type p53 activity sensitizes breast cancer cells to doxorubicin, a common DNA damaging chemotherapeutic drug used in the treatment of breast cancer. These observations extend our earlier observation on p53-mediated sensitization to cisplatin (15), and suggest a broad applicability of p53 as a general sensitizer to DNA damaging therapies.

We have extended these *in vitro* studies to *in vivo* tumor models in nude mice. We used a subcutaneous tumor model with MDA-MB-435 cells to evaluate regression of pre-established tumors by Adp53. When vector was administered intratumorally at two to three day intervals in weeks one and three, we saw significantly slower tumor growth in animals treated with Adp53 compared to animals treated with AdLuc. Suppression by Adp53 was further enhanced when animals were treated intravenously with doxorubicin prior to treatment with vector in weeks one and three. Because we have observed that systemic administration of adenovirus achieves gene transfer to lung tissue, we then tested the efficacy of systemically administered Adp53 to suppress breast cancer lung metastases. For this we used an orthotopic model with MDA-MB-435 cells, where lung metastases occur in a high percentage of tumor-bearing animals. We observed a significant suppression of lung metastases in animals treated with both Adp53 and doxorubicin compared to animals treated with Adp53, AdLuc, doxorubicin, or AdLuc+doxorubicin. Thus Adp53 gene therapy may have broad potential for the treatment of breast cancer in combination with conventional chemotherapy.

Materials and Methods.

Cell culture. MDA-MB-435 breast cancer cells used in this work were purchased either from ATCC or received from Dr. Janet Price (MD Anderson Cancer Center) and grown under 10% CO₂ in DMEM medium supplemented with 10% fetal calf serum, non-essential amino acids, glutamine, pyruvate and gentamycin.

Subcutaneous tumor model in nude mice. Tumor cells were harvested and washed once in PBS (Phosphate-buffered saline) at a concentration of 10⁷ cells per ml and maintained on ice. 10⁶ cells (100 µl of the suspension) were injected subcutaneously under the skin of the back of female nude mice (4-5 weeks, Harlan-Sprague Dawley). Tumors were monitored for growth by measuring their width and length at 2-3 day intervals and calculating the volume based on the formula v = L · w². Enough animals are implanted so that each treatment arm would be comprised of at least 10 animals. When the average tumor size reached 40 mm³ in volume, the animals were randomized into treatment groups and treatment was initiated. The first day of treatment was designated day 1. Adp53 or AdLuc (Clinical grade adenovirus provided by Introgen Therapeutics, Inc.) was then administered intratumorally at a dose of 2 x 10⁸ pfu per injection in 100 µl PBS. Vector was administered on days 2,4,7 and again on days 16, 18, 21. Doxorubicin 100 µl, equivalent to 10 mg/kg, (2mg/ml stock solution, Bedford Laboratories, obtained through local pharmacies) was administered intravenously on days 1 and 15. Tumor growth was monitored at 2-3 day intervals.

Orthotopic tumor model. 4-5 week female nude (Harlan Sprague Dawley) were used. A metastatic clone of MDA-MB-435 cells was provided by Janet Price (M.D. Anderson, Houston, TX)). When these cells are implanted orthotopically in the mammary fat pad of female nude mice, metastases form in the lung in a high percentage of the animals. The model thus provides an excellent model for human breast cancer and has been previously described (18). Animals were anesthetized with isoflourane. A small incision was made in the middle of the chest and 10^5 cells in 50 μ l PBS were implanted under the skin in the mammary fat pad. The incision was closed with a surgical staple, and removed about 1 week later. Animals were monitored for tumor growth by measuring the length and width of tumors calculating volumes based on the formula Volume = ($\frac{1}{2}$) length x (width)². At 8 weeks post implantation primary tumors that had attained a size of 600-900 mm³ were excised, although these tumors grew back in the second half of the experiment. At 9½ weeks post-implantation, animals were randomized into treatment groups of 7-8 animals each and treatment was initiated (day 1). Doxorubicin was administered intravenously on days 1 and 21. Vector was administered at 2-3 day intervals for the duration of the experiment (from day 3 and ending on day 46). In order to equalize potential vector-related toxicities resulting from systemic administration of vector, we administered equivalent amount of vector to control (AdLuc) animals and Adp53 animals (2.5×10^{10} vp of vector per animal per injection in 100 μ l PBS). This corresponded to 3×10^8 pfu in the case of Adp53 and 10^9 pfu in the case of AdLuc.

Immunohistochemistry of β -galactosidase. One Balb/C mouse was injected intravenously (tail vein) with 10^9 pfu of Ad β gal (provided by Introgen Therapeutics, Inc.). Two days following vector administration, the animal was sacrificed and lungs were removed and fixed in 3.7 % formaldehyde, followed by paraffin imbedding and sectioning onto slides. The slides were then deparaffinized by heating them at 60° C for one hour, following by stepwise treatment in xylene, EtOH (100%), EtOH (95%), EtOH (80%), and distilled H₂O. Slides were dried around the section and sections were encircled using a PAP Pen. Slides were blocked with H₂O₂ (3%) for 10 minutes, rinsed in PBS, and treated with Super Block (Scy Tek Laboratories, Logan, UT) for 5 minutes (room temperature). Slides were rinsed with PBS and treated with anti β -galactosidase antibody (Eppendorf-5', Inc., Boulder, CO) at 4°C for 24 hours. Slides were rinsed in PBS and treated with Link (biotinylated goat anti-rabbit, BioGenex; San Ramon, CA) for 20 minutes at room temperature. Slides were rinsed in PBS and treated with Label (HRP-streptavidin (BioGenex) for 20 minutes at room temperature. Slides were rinsed at treated with substrate (AEC, BioGenex) for 30 minutes. Slides were rinsed in distilled water, dried around the section, and mounted with coverslips using Aqueous Mounting Medium (BioGenex).

References

1. Bartek, J., Iggo, R., Gannon, J., and Lane J.P. (1990) Genetic and immunochemical analysis of mutant p53 in human breast cancer lines. *Oncogene*, 5:893-899.
2. Coles, C., Condie, A., Chetty, U., Steel, C.M., Evans, A.J. and Prosser, J. (1992) *Cancer Research* 52:5291-5298.
3. Singh, S., Simon, M., Meybohm, I., Jantke, I., Jonat, W., Maass, H., and Goedde, H.W. (1993) Human breast cancer: frequent p53 allele loss and protein overexpression. *Human Genet.*, 90:635-640.
4. Moll, U.M., Riou, G., and Levine, A.J. (1992) Two distinct mechanisms alter p53 in breast cancer: mutation and nuclear exclusion. *Proc. Natl. Acad. Sci., USA* 89:7262-7266.
5. Hendersin, I.C., Harris, J.R., Kinne, D.W., and Hellman, S. Cancer of the breast. In *Cancer, Principles and Practice of Oncology*. DeVita, V.T., Hellman, S., and Rosenberg, S.A., eds., J.P. Lippincott Comp., Philadelphia, 3rd ed., pp. 1197-1268.
6. Donehower, L.A., Godley, L.A., Aldaz, C.M., Pyle, R., Shi, Y-P., Pinkel, D., Gray, J., Bradley, A., Medina, D., Varmus, H.E. (1995) Deficiency of *p53* accelerates mammary tumorigenesis in *wnt-t* transgenic mice and promotes chromosomal instability. *Genes and Development*, 9: 882-895.
7. Swisher, S.G., Roth, J.A., Nemunaitis, J., et al. (1999) Adenovirus-mediated p53 gene transfer in advanced non-small-cell lung cancer. *J. Natl. Cancer Inst.* 91: 763-771.
8. Clayman G.L., el-Naggar, A.K., Lippman, S.M., et al. (1998) Adenovirus-mediated p53 gene transfer in patients with advanced head and neck squamous cell carcinoma. *J. Clin. Oncol.* 16:2221-2232
9. Lowe S.W., Ruley H.E., Jacks T., Housman, D.E. (1993) p53-mediated apoptosis modulates the cytotoxicity of anti-cancer agents. *Cell* 74: 957-967.
10. Lotem, J. and Sachs, L. (1993) Hematopoietic cells from mice deficient in wild-type p53 are more resistant to induction of apoptosis by some agents. *Blood* 82:1092-1096.
11. Clarke, A.R., Purdie, C.A., Harrison, D.J., Morris, R.G., Bird, C.C., Hooper, M.L., Wyllie, A.H. (1993) Thymocyte apoptosis induced by p53-dependent and independent pathways. *Nature* 362: 849-852.
12. Yonish-Rouach E, Resnitzky D, Lotem J, Sachs, L., Kimchi, A., Oren, M. (1991) Wild-type p53 induces apoptosis of myeloid leukemic cells that is inhibited by interleukin-6. *Nature* 352: 345-347.
13. Shaw, P., Bovey, R., Tardy, S., Sahli, R., Sordat, B., Costa, J. (1992) Induction of apoptosis by wild-type p53 in a human colon tumor-derived cell line. *Proc Natl Acad Sci USA* 89:4495-4499.
14. Lane, D. P.(1992) p53:guardian of the genome. *Nature* 358: 15-16.
15. Lowe, S.W., Bodis, S., McClatchey, A., Remington, L., Ruley, H.E., Fisher, D.E., Housman, D.E., Jacks, T. (1994) p53 status and the efficacy of cancer therapy *in vivo*. *Science* 266: 807-810.
16. Gjerset, R.A., Turla, S.T., Sobol, R.E., Scalise, J.J., Mercola, D., Collins, H., Hopkins, P.J. (1995) Use of wild-type p53 to achieve complete treatment sensitization of tumor cells expressing endogenous mutant p53. *Molecular Carcinogenesis* 14: 275-285.
17. Gjerset, R.A., Lebedeva, S., Haghghi, A., Turla, S.T., Mercola, D., (1999) Inhibition of the Jun kinase pathway blocks DNA repair, enhances p53-mediated apoptosis and promotes gene amplification. *Cell Growth and Differentiation* 10: 545-554.
18. Price, J.E., Polyzos, A., Zhang, R.D., and Daniels, L.M. (1990) Tumorigenicity and metastasis of human breast carcinoma cell lines in nude mice. *Cancer Res.* 50: 717-721.

APPENDIX COVER PAGE

1. Gjerset, R.A., Lebedeva, S., Haghghi, A., Turla, S.T., and Mercola, D. (1999) Inhibition of the Jun Kinase pathway blocks DNA repair, enhances p53-mediated apoptosis and promotes gene amplification. *Cell Growth and Differentiation* 10:545-554.
2. Haghghi, A., Lebedeva, S., and Gjerset, R.A. (1999) Preferential platination of an activated cellular promoter by cis-diamminedichloroplatinum. *Biochemistry* 38:12432-12438.
3. Gjerset, R.A., and Mercola, D. (2000) Sensitization of tumors to chemotherapy through gene therapy, In: "Cancer Gene Therapy: Past Achievements and Future Challenges", N. Habib, ed., Plenum Publishing Corporation, New York, London, Moscow. pp. 273-291.
4. Gjerset, R.A., Haghghi, A., Lebedeva, S., Mercola, D. Gene Therapy Approaches to sensitization of human prostate carcinoma to cisplatin, In: "Methods in Molecular Biology: Genomics Protocols", M. Starkey and R. Elaswarapu, eds. The Humana Press, Inc., Totowa, N.J. (*in press*).
5. Haghghi, A., Lebedeva, S., Mercola, D., Saadatmandi, N., and Gjerset, R. "T98G glioblastoma cells defective in DNA repair show enhanced p53-mediated growth suppression and apoptosis." (Abstract) Presented at the AACR Special Conference on DNA Repair Defects, San Diego, CA, January 14-18, 2000.

Inhibition of the Jun Kinase Pathway Blocks DNA Repair, Enhances p53-mediated Apoptosis and Promotes Gene Amplification¹

Ruth A. Gjerset,² Svetlana Lebedeva, Ali Haghghi, Sally T. Turla, and Dan Mercola

Sidney Kimmel Cancer Center, San Diego, California 92121

Abstract

We have previously shown, by expression of a nonphosphorylatable dominant inhibitor mutant of c-Jun [cJun(S63A,S73A)], that activation of the NH₂-terminal Jun kinase/stress-activated protein kinase by genotoxic damage is required for DNA repair. Here, we examine the consequences of inhibition of DNA repair on p53-induced apoptosis in T98G cells, which are devoid of endogenous wild-type p53. Relative to parental or wild-type c-Jun-expressing control cells, mutant Jun-expressing T98G clones show similar growth rates and plating efficiencies. However, these cells are unable to repair DNA (PCR-stop assays) and exhibit up to an 80-fold increased methotrexate-induced colony formation due to amplification of the dihydrofolate reductase gene. Moreover, the mutant c-Jun clones exhibit increased apoptosis and elevated bax:bcl₂ ratios on expression of wild-type p53. These results indicate that inhibition of DNA repair leads to accumulation of DNA damage in tumor cells with unstable genomes and this, in turn, enhances p53-mediated apoptosis.

Introduction

Tumor progression involves the rapid accumulation of genetic alterations, some of which promote cell proliferation and enable cell survival in changing environments. Genomic instability, one of the unique features of cancer, may provide the driving force for progression by facilitating these rapid genetic alterations (see Ref. 1). Nevertheless, this instability generates strand breaks and other forms of DNA damage that could be deleterious to cell survival. There is, therefore, selective pressure on the cancer cell to modulate its DNA

damage response to insure survival while accommodating this increased genetic instability.

One way in which a cancer cell may modulate its DNA damage response is loss of the tumor suppressor p53. p53 mediates apoptosis in response to DNA damage, possibly as a result of its ability to recognize and bind to damaged DNA, including DNA containing single-stranded ends (2) and DNA in abnormal structures known as insertion-deletion loops (3). Stabilization of p53 protein occurs after DNA damage in a process that involves DNA-PK³/ATM as a key mechanism (4, 5). Numerous studies correlate loss of p53 with increased genome instability (6–9), aneuploidy (10, 11), and tumor progression (12), suggesting that loss of p53 renders cells permissive for further genome destabilizing events that accompany and promote tumor progression, such as gene amplification and deletion. Restoration of p53 function in tumor cells that no longer express wild-type p53 restores the DNA damage recognition pathways and leads to G₁ arrest or apoptosis (see Ref. 13, review).

DNA damage also leads to activation of the JNK/stress-activated PK (14). JNK phosphorylates the c-Jun component of the AP-1 complex and related transcription complexes on serines 63 and 73 in the NH₂-terminal domain, thereby greatly activating transcriptional transactivation by AP-1 and related c-Jun-containing complexes, such as the c-Jun/ATF2 heterodimer. JNK activity is strongly induced in response to a variety of DNA damaging treatments, such as UV irradiation (15), cisplatin (15, 16), camptothecin (17), and etoposide (18). We have previously shown that activation of the JNK pathway that follows DNA damage is required for DNA repair, suggesting an essential role of JNK in regulating the DNA repair process (16). Phosphorylation of c-Jun is also induced by certain oncogenes (19) and is required for c-Jun plus Ha-ras cotransformation of rat embryo fibroblasts (19, 20). Complete loss of c-Jun in transgenic mouse embryo fibroblasts results in proliferation defects leading to prolonged passage through crisis and delay of spontaneous immortalization (21).

To more fully understand the role of the JNK pathway and c-Jun phosphorylation in cellular transformation, tumorigenesis, and DNA repair, we have recently selected T98G glioblastoma cells modified to express a mutant Jun that acts as a dominant-negative inhibitor of wild-type c-Jun downstream targets. T98G cells express only mutant p53 (22) and, unlike many other cell types, including normal lung epithelial cells (23), they express elevated, easily detectable levels of

Received 12/29/98; revised 4/30/99; accepted 6/24/99.

The costs of publication of this article were defrayed in part by the payment of page charges. This article must therefore be hereby marked advertisement in accordance with 18 U.S.C. Section 1734 solely to indicate this fact.

¹ Supported in part by National Cancer Institute Grants CA69546 (to R. A. G.), CA63783-05 (to D. A. M.), and CA76173-01 (to D. A. M.); Grant DAMD17-96-1-6038 from the Department of Defense (to R. A. G.); a grant from Introgen Therapeutics, Inc. (Houston, TX; to R. A. G.); and Grant 3CB-0246 from the Breast Cancer Research Program of the University of California (to D. A. M.).

² To whom requests for reprints should be addressed, at Sidney Kimmel Cancer Center, 10835 Altman Row, San Diego, CA 92121. Phone: (619) 450-5990; Fax: (619) 450-3251; E-mail: rgjerset@skcc.org.

³ The abbreviations used are: PK, protein kinase; JNK, Jun kinase; AP, activator protein; ATF, activating transcription factor; DHFR, dihydrofolate reductase; EGF, epidermal growth factor; ES, embryonal stem; HPRT, hypoxanthine phosphoribosyltransferase.

JNK activity, which can be activated an additional 5–10-fold by treatment with the DNA cross-linking agent cisplatin (16). The Jun mutant construct used to modify T98G cells was originally derived by Binétruy *et al.* (19) and Smeal *et al.* (20) and has alanine substitutions at serine positions 63 and 73. Mutant Jun, therefore, cannot be phosphorylated by JNK. Expression of mutant Jun does not alter the basal or induced levels of JNK activity in these cells, indicating that mutant Jun has no direct effect on the JNK enzyme.⁴ However, it does strongly inhibit transactivation of AP-1 reporter plasmids in rodent fibroblasts (19, 20) and T98G cells,⁴ indicating that mutant Jun acts as a competitive inhibitor in the formation of an active AP-1 complex and, therefore, greatly impedes phosphorylation-dependent transactivation functions of c-Jun (19, 20). Furthermore, in A549 human lung carcinoma cells, in which the JNK pathway is known to be required for the EGF-stimulated cell growth (23), inhibition of the JNK pathway by the application of high affinity JNK oligonucleotides leads to inhibition of EGF-dependent growth in a manner indistinguishable from that caused by stable expression of mutant Jun (23). Thus, stable expression of mutant Jun seems to be a potent and specific inhibitor of phosphorylation-dependent effects of endogenous c-Jun that are usually promoted by the action of JNK.

T98G cells that express mutant Jun have a marked increase in sensitivity to the DNA damaging drug cisplatin and to UV radiation, and this increased sensitivity to DNA damage correlates with an inability to repair DNA (16). This suggests that phosphorylation of the wild-type c-Jun subunit of transcription factors, such as AP-1 and the c-Jun/ATF2 heterodimer, may contribute to DNA repair and survival after DNA damage through induction of DNA synthesis and repair genes such as topoisomerase I and DNA polymerase β , both of which have functional AP-1 and ATF2/cAMP-responsive element binding protein sites (which bind to c-Jun/ATF2) in their promoters (24–27). Phosphorylation of c-Jun may also contribute to cell survival during the crisis phase of tumorigenic transformation by promoting repair of DNA strand breaks generated by the mechanisms that destabilize the genome during tumor progression.

Restoration of p53 function in T98G glioblastoma cells by exposure to p53 adenovirus promotes low levels of apoptosis at gene transfer efficiencies of 50–80% (28). We have found that levels of apoptosis can be significantly increased in these cells when they are treated with p53 adenovirus in combination with DNA damaging agents, such as cisplatin and radiation. This is consistent with a model in which the level of DNA damage sustained by the cell is a strong determinant of p53-mediated apoptosis, as suggested by Chen *et al.* (29). In this study, we hypothesized that inhibition of DNA repair by expression of mutant Jun, would also enhance p53-mediated apoptosis. It is known that various forms of genetic instability characteristic of cancer cells, including gene amplification, gene deletion, and broken chromosomes are related in origin through the involvement of strand breaks (see Ref. 30, review). By blocking DNA repair, mutant Jun is

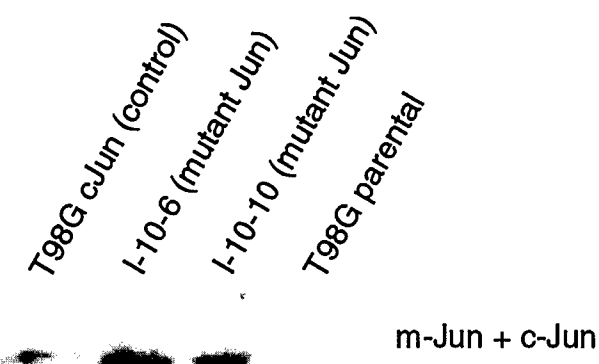


Fig. 1. Increased expression of immunoreactive Jun in stable transfectants. Western blot analysis of total c-Jun plus mutant Jun in lysates of control c-Jun-modified clone T98GcJun (Lane 1), T98G mutant Jun-expressing clones I-10-6 (Lane 2) and I-10-10 (Lane 3), and parental T98G cells (Lane 4). Each lane represents the electrophoresis of 40 μ g of total protein.

predicted to promote elevated levels of strand breaks, which then serve as signals for p53-mediated apoptosis. The elevated level of strand breaks could also stimulate further gene amplification. In the studies reported here, we extend and confirm our earlier observations that mutant Jun expression leads to inhibition of DNA repair. Moreover, we show that mutant Jun expression predisposes cells to gene amplification as judged by the amplification of the *DHFR* gene. We further show that expression of mutant Jun greatly enhances p53-mediated apoptosis. These observations provide support for the hypothesis that inhibition of DNA repair in cancer cells with unstable genomes enhances sensitivity to DNA damaging chemotherapy and p53-dependent apoptosis.

Results

T98G Mutant Jun-expressing Cells Resemble Parental T98G Cells with Respect to Growth Rate and Plating Efficiency. We have previously shown that mutant Jun-expressing T98G clone I-10-10 has decreased viability after treatment with cisplatin and other DNA-damaging agents, likely due to a defect in DNA repair (16). Here, we examine this and a second mutant Jun-expressing clone, I-10-6, as well as a control c-Jun-expressing clone (T98GcJun) and parental T98G cells for the expression levels of total immunoreactive Jun, for proliferation rates, and for plating efficiencies. Fig. 1 shows a Western blot of lysates from each of these four cell lines using an antibody that recognizes both mutant Jun and c-Jun. Equivalent loading was confirmed by stripping the blots and reprobing them with an anti- β -actin antibody (data not shown). As shown in the figure, mutant Jun-modified clones I-10-10 and I-10-6, as well as control c-Jun-modified clone T98GcJun, overexpress total Jun, consistent with expression of the exogenous constructs. The mutant Jun-expressing clones, as well as the control c-Jun-modified clone, show little difference from parental T98G cells with respect to proliferation rate or plating efficiency (Table 1). Only slight growth alterations were observed, but these did not correlate with expression of mutant Jun be-

⁴ O. Potopova and D. Mercola, unpublished observations.

Table 1 Culture characteristics of T98G clones

Clone	Relative doubling time ^a	Plating efficiency ^b
T98G	1	47% ± 3%
T98GcJun (control)	1.0 ± 0.14	52% ± 17%
I-10-10	0.83 ± 0.10	42% ± 13%
I-10-6	1.2 ± 0.04	45% ± 2%

^a Average of two experiments on different occasions, each in triplicate.

^b Average of three experiments on different occasions, each in triplicate.

cause clone I-10-10 proliferates about 20% faster than parental cells or c-Jun-modified cells and clone I-10-6 proliferates about 20% slower. Therefore, expression of mutant Jun in T98G glioblastoma cells inhibits their ability to repair DNA damage (see below), but it is not growth suppressive in itself.

T98G Mutant Jun-expressing Cells Are Defective in Repair of Cisplatin Adducts. Cisplatin adduct formation and repair was analyzed by a PCR-based assay (PCR-stop assay), as described in "Materials and Methods." Because cisplatin adducts block PCR amplification by Taq polymerase, the intensity of the PCR signal derived from a given amplified region (in our case, the *HPRT* gene) is inversely proportional to the platination level and can be used as a quantitative measure of the number of cisplatin-DNA adducts on that region (31). Platination levels determined by PCR amplification of a given housekeeping gene have been shown to correspond to determinations of platination levels on genomic DNA by atomic absorption, demonstrating that the PCR method reflects global DNA platination levels (31). We have also observed in a variety of tumor cell lines that cells shown to be DNA repair deficient by the PCR assay were also defective in repairing a cisplatin-damaged reporter plasmid, as assayed by expression of the reporter gene 2 days after transfection.⁵ The PCR assay was chosen for these studies because it measures repair of an endogenous genomic sequence. Fig. 2 shows the results of a PCR-stop assay performed on genomic DNA isolated from parental T98G cells, mutant Jun-expressing I-10-10 and I-10-6 cells, and control c-Jun-expressing T98GcJun cells after treatment with cisplatin, with and without a subsequent 16-h recovery period. The bars represent the relative amounts of PCR product resulting from PCR amplification of a 2.7-kb region of the *HPRT* gene of genomic DNA from cisplatin-treated versus untreated cells. In all cases, the results have been corrected for sample to sample fluctuations in PCR efficiency by normalizing the results to a 170-base PCR product of the same gene (i.e., a fragment too small to register significant levels of platination and where fluctuation from sample to sample varied by <5%). The data show that treatment with 100 µM cisplatin results in an immediate decrease in the PCR signal intensity to about 85% of control signals obtained from DNA from untreated cells. On the basis of a Poisson relationship, this corresponds to an adduct density of about 0.16 adducts/2.7 kb. By 16 h after treatment, both T98G cells and c-Jun-expressing control cells (T98GcJun) have efficiently repaired the adducts, and the PCR signal strengths are equal to

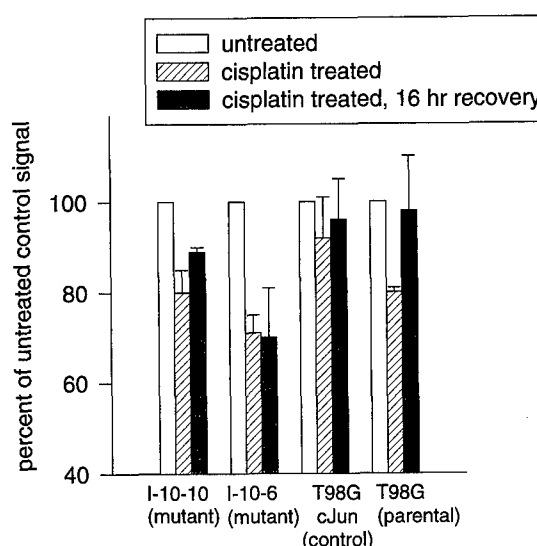


Fig. 2. PCR-stop assays of cisplatin adduct formation and repair. A 2.7-kb region of the *HPRT* gene was PCR amplified from genomic DNA from untreated cells or from cells treated 1 h, 15 min with 100 µM cisplatin and harvested either immediately or 16 h after treatment. Bars, the relative amounts of PCR product obtained from damaged versus undamaged templates. The results represent the averages of triplicate PCR reactions performed on two independent occasions.

controls (i.e., no detectable adducts at 16 h). In contrast, mutant Jun-expressing clones I-10-10 and I-10-6 failed to repair the adducts, and PCR signal strengths remain unchanged after the 16-h recovery period (Fig. 2). These observations confirm and extend our earlier results (16) and strongly indicate that inhibition of the JNK pathway effectively blocks DNA repair.

T98G Mutant Jun-expressing Cells Give Rise to Methotrexate-resistant Clones with Higher Frequency Than Do Parental T98G Cells or c-Jun-expressing Cells. Certain types of DNA repair defects contribute to tumorigenesis (32, 33) and increased genome instability (34, 35). We examined the T98G clones described above for *DHFR* gene amplification, one measure of genome instability known to correlate with increased tumorigenicity after *in vivo* implantation of cells (36–38). T98G cells were plated in the presence of concentrations of methotrexate five times the LD₅₀ and nine times the LD₅₀ determined for these cells (i.e., concentrations at which gene amplification of DHFR is known to be the predominant mechanism of resistance to the cytotoxic effects of methotrexate; Refs. 39 and 40). Thus, the frequencies of appearance of methotrexate-resistant clones is a measure of genome instability. As shown in Table 2, T98G I-10-10 cells produce methotrexate-resistant colonies at about 20 times the frequency of the parental T98G cells, and T98G I-10-6 cells produce methotrexate-resistant colonies at about 80 times the frequency of parental T98G cells ($P = 0.006$). In contrast, stable expression of wild-type c-Jun had no effect on the frequency of resistance, indicating strongly that interference with a phosphorylation-dependent function of JNK predisposed cells to form resistant colonies.

To verify the occurrence of gene amplification in methotrexate-resistant colonies, several colonies were picked from

⁵ R. A. Gjerset and A. Haghghi, unpublished results.

Table 2 Frequency of methotrexate-resistant colonies arising from T98G, T98GcJun, and T98G mutant Jun clones I-10-10 and I-10-6

Cells were plated at a density of 10^5 cells/10-cm culture dish and incubated 4 weeks in the presence of methotrexate at the indicated concentrations. Plates were then stained with 70% methylene blue in methanol, and colonies were counted. For analysis of *DHFR* gene amplification, and colonies were counted. For analysis of *DHFR* gene amplification, several colonies were picked before staining and expanded, and cellular DNA was prepared and subjected to quantitative PCR analysis.

Clone	Methotrexate dose ^a	Frequency of colonies/ 10^5 cells (average of three experiments)	<i>DHFR</i> gene dosage relative to parental in representative colonies
T98G parental	5 \times LD ₅₀	2.3 \pm 2.5	1
	9 \times LD ₅₀	0.3 \pm 0.6	
T98GcJun (control)	5 \times LD ₅₀	2 ^b	N/T
	9 \times LD ₅₀	0	
I-10-10	5 \times LD ₅₀	38 \pm 19	3-4
	9 \times LD ₅₀	6 \pm 5	
I-10-6	5 \times LD ₅₀	174 \pm 21	2
	9 \times LD ₅₀	16 \pm 12	

^a LD₅₀, 0.1 μ M (T98G and T98GcJun) or 0.04 μ M (I-10-10 and I-10-6).

^b One experiment.

each selection condition and expanded. Genomic DNA was prepared and subjected to quantitative PCR analysis using ³²P-labeled primers that define a 270-base fragment of the *DHFR* gene, which includes parts of exon 1 and intron A. PCR products were analyzed by agarose gel electrophoresis and quantitated by radioanalytic imaging, as described in "Material and Methods." The relative increase in PCR product from cellular DNA of methotrexate-resistant cells compared with unselected parental T98G cells was taken as a measure of the increased copy number of the *DHFR* gene and is indicated in Table 2. The methotrexate-resistant clones derived from T98G mutant Jun-expressing clones have from two to four times the gene dosage of the *DHFR* gene, relative to parental T98G cells, indicating that the observed methotrexate resistance reflected an increased *DHFR* gene copy number. We conclude, therefore, that inhibition of DNA repair by mutant Jun in T98G glioblastoma cells leads to accumulated DNA damage that can promote gene amplification.

T98G Mutant Jun Cells Are More Susceptible Than Are Parental Cells to p53-mediated Growth Suppression. T98G cells lack wild-type p53 function as a result of a methionine to isoleucine replacement in p53 at codon 237 (41). Restoration of wild-type p53 in T98G cells through gene transfer results in partial G₁ arrest (41) or apoptosis (28). Furthermore, agents that promote DNA strand breaks and other forms of DNA damage enhance p53-mediated apoptosis (28). On the basis of the observations above, indicating that mutant Jun-expressing cells are inhibited in DNA damage repair and predisposed to gene amplification, we predicted that strand breaks would accumulate in mutant Jun-expressing cells, thereby leading to increased p53-dependent growth inhibition and apoptosis. Fig. 3 compares the growth inhibition of Ad-p53-transduced cells relative to Ad- β -gal transduced cells 6 days after infection. The results represent the average of two experiments performed on

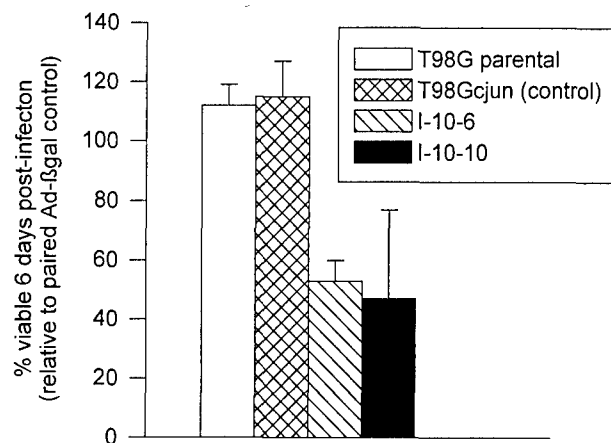


Fig. 3. Six-day viability assay of T98G subclones after treatment with Ad-p53, 100 pfu/cell for 3 h. Viability of Ad-p53-treated cultures is represented as a percentage of the same culture treated under identical conditions with Ad- β gal.

separate occasions, with each experiment being performed in triplicate. The infection efficiency, determined by X-gal staining of parallel cultures with Ad- β gal, was about 50% in all cases, low enough to cause incomplete growth suppression of parental T98G cells and control cells modified to stably express wild-type c-Jun, as shown in Fig. 3. Growth studies revealed that T98G I-10-10 and I-10-6 cells were considerably more growth suppressed upon expression of p53 under these conditions. Western blot analysis (Fig. 4) of the p53-responsive gene product p21^{waf1/cip1} in cell lysates 48 h after infection shows induction of p21^{waf1/cip1} in all cases. The data, thus, show that p21^{waf1/cip1} is not a crucial player in this setting. Equivalent loading was confirmed by stripping the blots and reprobing them with an anti- β -actin antibody (data not shown).

T98G Mutant Jun-expressing Cells Are More Susceptible to p53-mediated Apoptosis. To determine whether the p53-mediated growth inhibition of T98G mutant Jun-expressing cells observed in Fig. 3 could be accounted for by the induction of apoptosis, we assayed the cytoplasmic fractions of Ad-p53 or Ad- β -gal-infected cells 48 h after infection for the presence of oligonucleosomal fragments (Fig. 5). These fragments are released from the nuclei of cells undergoing apoptosis and can be detected by an ELISA assay using antihistone antibodies and anti-DNA peroxidase antibodies. We assayed for apoptosis 48 h after exposure to p53 adenovirus or β -gal adenovirus because this is the point at which we have observed maximal transgene expression in Ad- β -gal-infected cells.⁶ Fig. 5A shows the results of the ELISA assay on the various T98G cell clones. Low levels of oligonucleosomal fragment release similar to levels observed in uninfected cells were observed in Ad- β -gal-infected cells. Treatment of parental T98G cells and control wild-type c-Jun-expressing T98GcJun cells with Ad-p53 (100 pfu/cell, 3 h) resulted in virtually no induction of apoptosis under our

⁶ Unpublished observations.

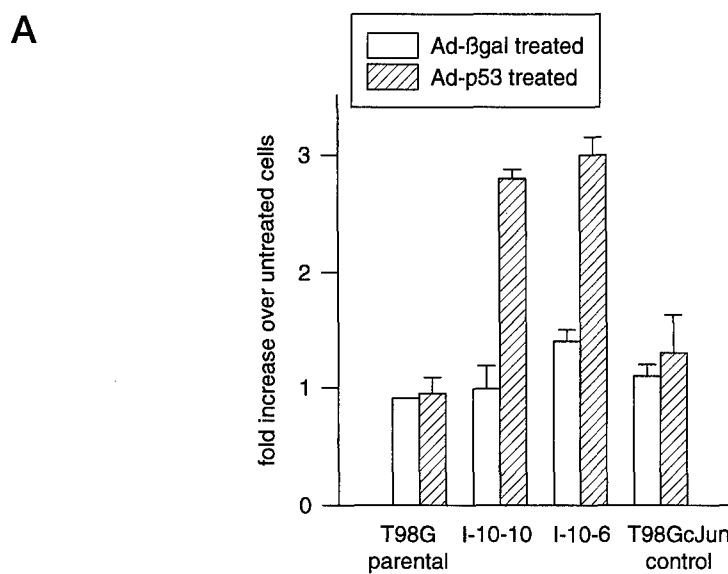
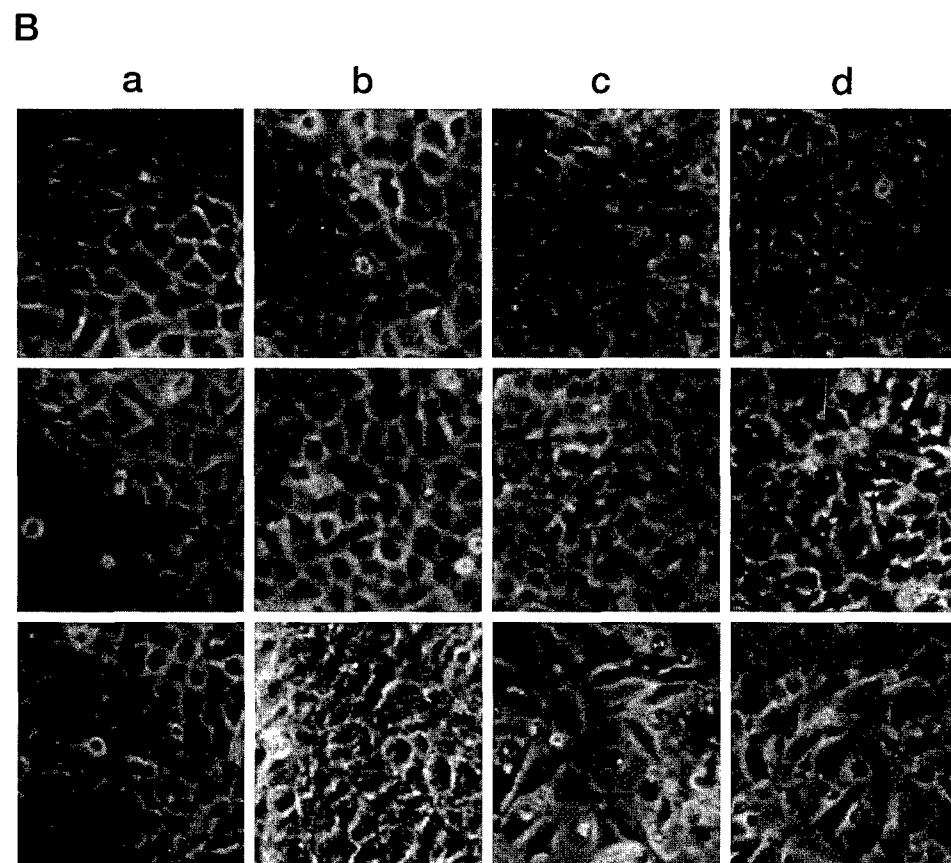


Fig. 5. *A*, ELISA apoptosis assay of cytoplasmic nucleosomes in untreated cells or in cells 48 h after being treated with 100 pfu/cell of Ad- β gal or Ad-p53 for 3 h. *B*, light microscopy ($\times 40$) of untreated cells (top row), or cells 72 h after treatment with Ad- β gal (middle row) or Ad-p53 (bottom row). *a*, T98G parental cells; *b*, c-Jun-modified clone T98GcJun; *c*, mutant Jun-modified clone I-10-6; *d*, mutant Jun-modified clone I-10-10.



induced stabilization of transduced wild-type p53, leading to apoptosis. Our results directly demonstrate both gene amplification and significantly increased p53-dependent apoptosis in mutant Jun-expressing cells in support of this hypothesis.

One possible explanation for our observations is that one or more downstream targets of wild-type c-Jun promotes

repair of endogenous strand breaks. Candidate targets include DNA polymerase β , PCNA, topoisomerase I, topoisomerase II, and GADD153, all of which have potential AP-1 or c-Jun/ATF2 binding sequences in their promoter regions (see Refs. 24–27 and Ref. 46, review). In the cases of DNA polymerase β and topoisomerase I, these c-Jun/ATF2 binding sites are known to be functional and stress activated (46).



Fig. 4. Western blot analysis of p21^{Waf1} protein in lysates from T98G parental cells, mutant Jun-expressing clones I-10-10 and I-10-6, and control c-Jun-expressing clone T98GcJun 48 h after treatment with Ad- β gal or Ad-p53, 100 pfu/cell for 3 h. Each lane represents 40 μ g of protein: Lane 1, T98G parental-Ad β gal; Lane 2, T98G parental-Adp53; Lane 3, mutant Jun clone I-10-10-Ad β gal; Lane 4, mutant Jun clone I-10-10-Adp53; Lane 5, mutant Jun clone I-10-6-Ad β gal; Lane 6, mutant Jun clone I-10-6-Adp53; Lane 7, control T98GcJun-Ad- β gal; Lane 8, control T98GcJun-Adp53.

conditions, consistent with growth assays showing no suppression of overall growth after treatment of these cell lines with Ad-p53. However, readily detectable and significantly increased levels of apoptosis were observed in mutant Jun-expressing clones I-10-10 and I-10-6. These results are consistent with the appearance of Ad-p53-treated cultures as shown in Fig. 5B. Ad-p53-treated I-10-10 and I-10-6 cells lose contact with neighbors, become large, and contain cytoplasmic vacuoles. Thus, p53-mediated apoptosis is markedly enhanced in mutant Jun-expressing cells, possibly as a consequence of being triggered by endogenous strand breaks that fail to be repaired.

To confirm a p53-dependent mechanism of apoptosis, we carried out a Western blot analysis of the apoptosis regulatory proteins bax and bcl₂ in cells treated with Ad-p53 or Ad- β gal (Fig. 6). The levels of the proapoptotic effector bax, the gene of which is induced by p53 (42), increase after treatment with Ad-p53, as expected, whereas levels of the antiapoptotic protein bcl₂ remain largely unchanged. A comparison of the bax to bcl₂ protein is indicated by the ratios under the lanes in Fig. 6. The bax:bcl₂ ratio after treatment with Adp53 is significantly higher in mutant Jun-expressing cells I-10-10 and I-10-6 (ratios of 10 and 2.5, respectively) than in parental cells (ratio of 1.7) and c-Jun control cells (ratio of 0.8). Furthermore, a comparison of these ratios in uninduced versus induced cells (Ad β gal-treated versus Adp53-treated) reveals a 3–4-fold increase for the Adp53-treated parental and cJun-expressing control cells compared with the same cells treated with Ad β gal, whereas Adp53-treated mutant Jun-expressing cells I-10-10 and I-10-6 show an increase of some 8–25-fold, respectively, compared with the same cells treated with Ad β gal. In accordance with other data suggesting that the bax:bcl₂ ratio is a critical determinant of apoptosis (see Ref. 43, review), these data support a role for bax in the increased apoptosis observed after Adp53 treatment of mutant Jun-expressing cells.

Discussion

In this study, we have examined how a dominant-negative inhibitor of phosphorylated wild-type c-Jun downstream targets affects cell proliferation, DNA repair, susceptibility to p53-mediated apoptosis, and DHFR gene amplification in T98G glioblastoma cells. The JNK/stress-activated PK pathway is a cellular DNA damage and stress-response pathway that is activated by a variety of signals, including mitogens

such as EGF (23), oncogenes (19), and numerous DNA-damaging agents such as UV radiation and cisplatin (15–17). Phosphorylation of c-Jun by JNK activates the transcriptional potential of AP-1 and related transcription factors such as c-Jun/ATF2, which use c-Jun as a heterodimeric partner in the transcription complex. The nonphosphorylatable mutant Jun construct used in these and earlier studies resembles normal cellular c-Jun, except for two alanine replacements at positions 63 and 73. This change has been shown to abrogate the cotransformation properties of c-Jun with H-ras in rat embryo fibroblasts (19, 20), and to block EGF-induced proliferation of lung carcinoma cells (23). T98G glioblastoma cells expressing this mutant Jun have reduced viability after treatment with the DNA-damaging drug cisplatin (16), and this result is due to an inability to repair cisplatin adducts, as we show here and in an earlier study (16). Thus, the JNK pathway may promote cell survival during transformation and in response to DNA damage.

In this study, we extend the analysis of the T98G mutant Jun clones analyzed previously. We observe that they grow with similar doubling times and have similar plating efficiencies as parental T98G cells or c-Jun-modified control cells, indicating that stable expression of mutant Jun does not substantially alter DNA synthesis. However, methotrexate-resistant clones arising in the presence of $\geq 5 \times LD_{50}$ are generated at a 20–80-fold higher frequency in mutant Jun-expressing clones compared with parental T98G cells and the wild-type c-Jun-expressing clone T98GcJun. Under these conditions, resistance to methotrexate is known to be primarily due to amplification of the DHFR gene (39, 40). We confirmed a low, but detectable increase in DHFR gene copy number of about 2–4-fold compared with parental T98G cells by quantitative PCR analysis of genomic DNA isolated from several representative clones of methotrexate-selected T98G I-10-10 and I-10-6 cells. Although low, such an increase in copy number could explain the increase in methotrexate resistance observed in these cells and is supported by previous studies that showed that a low level of DHFR gene amplification was sufficient to confer resistance to methotrexate (44). Furthermore, mutant Jun-expressing T98G cells, which do not express endogenous wild-type p53, exhibited increased growth suppression and apoptosis after exposure to p53 adenovirus and restoration of wild-type p53 function. Therefore, mutant Jun alone had little effect on the growth properties of T98G cells but manifested a negative effect on growth in the presence of wild-type p53.

Our results demonstrate that expression of a nonphosphorylatable mutant Jun, but not c-Jun, leads to a defect in DNA repair and contributes to increased gene amplification, one manifestation of genomic instability in mammalian cells. These observations are consistent with other examples in which DNA repair defects are seen to underlie a genome instability phenotype (34, 35). The results suggest that the DNA repair defect associated with expression of mutant Jun may generate elevated levels of strand breaks in T98G cells compared with T98G parental cells and c-Jun-modified cells, both of which have an intact JNK pathway. The elevated level of breaks may, in turn, serve as initiation events for increased gene amplification (45), as well as triggers for DNA damage-

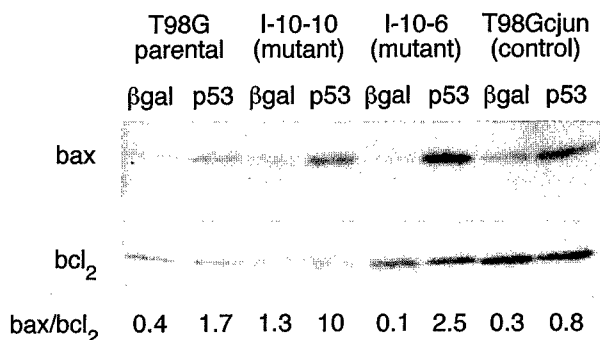


Fig. 6. Western blot analysis of bax and bcl_2 protein in lysates from T98G parental cells, mutant Jun-expressing clones I-10-10 and I-10-6, and control c-Jun-expressing clone T98GcJun 48 h after treatment with Ad-p53 or Adp53, 100 pfu/cell for 3 h. Each lane represents 15 μg of protein for the bax analysis and 30 μg of protein for the bcl_2 analysis. After immunostaining and band detection with enhanced chemiluminescence Western reagent, bands were quantitated using Kodak digital software. Ratios of bax to bcl_2 are indicated below the lanes. Experiment was carried out twice with similar results.

Moreover, all of these gene products have been implicated in the repair of cisplatin-DNA adducts (47). Thus, although an intact JNK pathway in T98G parental cells and in c-Jun-modified control cells would not directly prevent DNA damage-induced p53 stabilization, the pathway would act indirectly to attenuate p53-mediated apoptosis by efficiently promoting repair of endogenous strand breaks that would trigger p53 stabilization.

An additional mechanism also may play a role in cells expressing endogenous wild-type p53. Shreiber *et al.* (21) have recently shown that c-Jun directly down-regulates p53 expression through binding to a variant AP-1 site in the endogenous cellular p53 promoter. In their study, negative regulation of p53 by c-Jun seemed to be crucial to cellular transformation in that transgenic mouse embryo fibroblasts lacking c-Jun displayed proliferation defects, elevated p53 expression, and prolonged transit through crisis before spontaneous immortalization. Thus, c-Jun may attenuate p53-mediated apoptosis both by down-regulating expression of p53 and by promoting repair of endogenous DNA damage that could trigger p53 stabilization and apoptosis.

Two independently derived mutant Jun-expressing clones show similar properties, whereas a third clone expressing wild-type c-Jun and maintained in culture for a similar period did not share any of these properties. These observations strengthen the argument that down-regulation of DNA repair as a consequence of mutant Jun expression underlies the elevation in DHFR gene amplification and enhanced predisposition to p53-mediated apoptosis. Our results suggest, in addition, that increased expression of the p53-regulated pro-apoptotic effector bax leads to an increased bax: bcl_2 ratio that contributes to enhanced apoptosis in mutant Jun-expressing cells after exposure to p53 adenovirus. This is consistent with a variety of observations in other systems showing the importance of the bax: bcl_2 ratio in determining apoptosis (see Ref. 43, review). Thus, an elevated level of endogenous DNA strand breaks in mutant Jun-expressing cells may result in increased stabilization and activation of p53 and increased induction of bax.

The recent identification of p53 as a physiological substrate for JNK (48) indicates that the JNK response extends to other targets besides c-Jun, and these could mediate the various aspects of the stress response. Although inhibited in c-Jun phosphorylation, T98G cells modified with mutant Jun express constitutively active JNK at levels similar to the parental T98G cells.⁷ They would, therefore, be expected to carry out phosphorylation of other JNK substrates similarly to parental cells. The ability of T98G mutant Jun cells to carry out apoptosis after restoration of p53 activity suggests that any JNK-related apoptotic functions are not disrupted by the mutant Jun modification.

Consistent with our observations that the mutant Jun modification has no significant effect on cell growth or plating efficiency of T98G cells is a study demonstrating that ES cells lacking c-Jun had similar viability and growth rate as parental ES cells and were able to efficiently transactivate AP-1 reporter constructs (49). Thus, most of the functions of c-Jun in ES cells seemed to be complemented by other Jun proteins. In our case, mutant Jun itself may be able to carry out the c-Jun functions required for basal growth. However, phosphorylation of c-Jun seems to be critical in the cellular response to DNA damage.

Our results can be understood in light of a growing body of evidence supporting a role for p53 in modulating apoptosis in response to DNA damage (see review, Ref. 50) and in proportion to the extent of damage (29). p53 is a DNA damage recognition protein known to bind to a variety of types of DNA damage, including single-strand ends (2), and insertion-deletion loops (3). These types of damage, which could serve as triggers for p53-mediated apoptosis, are likely to be generated in tumor cells by the mechanisms that promote spontaneous gene rearrangements, deletions, and amplifications. As such, a failure of DNA repair in mutant Jun-expressing cells would promote the accumulation of strand breaks, which would, on the one hand, favor gene amplification and other manifestations of genome instability and, on the other hand, promote DNA damage-induced stabilization of p53 and apoptosis.

As depicted in the scheme in Fig. 7, we hypothesize that activation of JNK and loss of p53 represent independent mechanisms by which tumor cells undergoing progression accommodate increased levels of genomic instability and insure survival while sustaining potentially lethal genome destabilizing events. By promoting DNA repair, the JNK pathway may limit damage to levels compatible with survival. Loss of p53 would further enhance survival owing to a down-regulated apoptotic response to unrepaired damage.

Materials and Methods

Cell Lines. T98G glioblastoma cells were obtained from Dr. Hoi U (University of California, San Diego, CA) and cultured at 37°C in 10% CO₂ in DMEM supplemented with 10% newborn calf serum. The T98G clones that had been modified to express mutant Jun, termed T98G-dnJun-I-10-10 and I-10-6 (see Ref. 16), or simply T98G I-10-10 and T98G I-10-6, were cultured in the same way as were T98G cells, except that 100 $\mu\text{g}/\text{ml}$ hygromycin was added to the culture medium. The pLHCmjun vector

⁷ O. Potopova, unpublished observations.

Responses to DNA damage in tumor cells

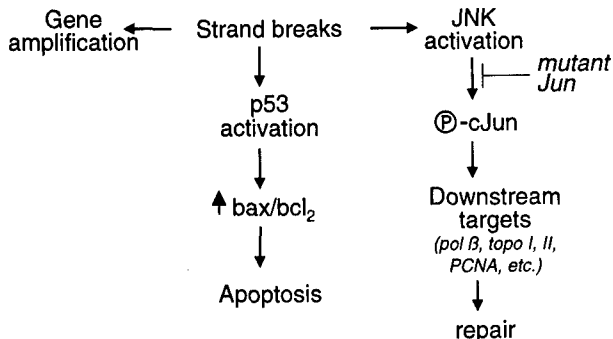


Fig. 7. Model explaining how, through inhibition of potential c-Jun downstream targets leading to DNA repair (e.g., DNA polymerase β , topoisomerase I, II, PCNA), mutant Jun promotes the accumulation of endogenous DNA strand breaks in genetically unstable tumor cells and, thus, collaborates with p53 to promote p53-mediated induction of bax and apoptosis.

encodes a dominant negative mutant of c-Jun and was prepared, as described previously (51), by insertion of DNA encoding mutant Jun [obtained by site-directed mutagenesis by Smeal *et al.* (20)] into the retroviral vector pLHGX. Mutant Jun has ser \rightarrow ala substitutions at positions 63 and 73, two sites of DNA damage-induced phosphorylation in wild-type c-Jun, and cannot be phosphorylated at these sites. As a control, T98G cells modified to overexpress wild-type c-Jun (T98GcJun) were obtained by cotransfection with a c-jun expression vector, pSV2cjun and with pSV2neo, and were cultured similarly, with the addition of 100 μ g/ml G418.

Western Blot Analysis. Levels of total cellular Jun protein (c-Jun + mutant Jun), as well as levels of the gene products of the p53-regulated genes *p21^{waif1}*, *bax*, and *bcl₂* were determined by Western blot analysis. Cell lysates (20–40 μ g) were electrophoresed on a 12% acrylamide gel and blotted onto nylon membranes. Membranes were then treated with rabbit polyclonal anti c-Jun (1:200), or with mouse monoclonal anti *p21^{waif1}* (1:200), or with rabbit polyclonal anti-bax (1:200), or with mouse monoclonal anti-*bcl₂* (1:100), followed by an appropriate antirabbit or antimouse secondary antibody conjugated with horseradish peroxidase. All antibodies were purchased from Santa Cruz Biotechnology, Inc. (Santa Cruz, CA) and used according to the protocol recommended by the manufacturer. Antibody reactive bands were revealed using the enhanced chemiluminescence Western detection system (Amersham Life Sciences, United Kingdom). For quantitation of bands, we used Kodak digital camera and analysis software.

Analysis of Repair of Cisplatin-DNA adducts. Cisplatin (*cis*-diamminedichloroplatinum) adduct formation and repair was analyzed by a PCR-based DNA damage assay (PCR-stop assay; Ref. 31). The assay is based on observations that Taq polymerase is blocked at cisplatin adducts, was used to analyze cisplatin adduct formation and repair. Because DNA fragments are platinated randomly, the distribution of damage fits a Poisson distribution, where a mean level of one adduct/fragment (*i.e.*, the portion of the genome defined by the forward and reverse PCR primers) will leave 37% of the fragments undamaged and these will be amplified to produce a PCR signal 37% of that from control DNA. For cisplatin treatments, cells were plated at 50% confluence in three wells of a 6-well plates in standard medium described above. After attachment, duplicate wells were treated with 100 μ M cisplatin (Platinol, aqueous solution at 1 mg/ml, purchased from local pharmacies) for one h, 15 min, and one well was left untreated. After treatment, the untreated cells and one well of 100 μ M cisplatin-treated cells were harvested, and genomic DNA was prepared. The remaining treated well was incubated an additional 16 h in the absence of cisplatin before harvesting. DNA was prepared using the QIAamp blood kit essentially following the manufacturer's

protocol, except that cells were lysed directly on the plate in the presence of PBS, Qiagen protease, and lysis buffer supplied in the kit. After purification, DNA was adjusted to 0.5 mg/ml in sterile water and stored at -20°C. Quantitative PCR was used to compare cisplatin adduct formation on a 2.7-kb region of the *HPRT* gene. As an internal control for PCR efficiency, we PCR-amplified from the same templates a 170-base non-overlapping region of the same gene. The smaller region represents a target too small to register significant levels of damage under our conditions. We found that both the 2.7-kb and 170-base products increased linearly with input template over the range 0.1–0.5 μ g DNA/25 μ l reaction and we, therefore, routinely used 0.125–0.25 μ g template/reaction. Reactions were performed in 25 μ l using 0.125–0.25 μ g DNA, 25 pmol each of forward and reverse primer, 250 μ M dNTPs (Pharmacia), 1.25 units of Taq polymerase (Qiagen), 1 \times buffer (Qiagen), and solution Q (Qiagen). Bands were quantitated using a Kodak digital camera and analysis software. The amplification program was as follows: 1 cycle (94°C, 1 min, 30 s); 25 cycles (94°C, 1 min; 57°C, 1 min; 70°C, 2 min, 30 s); 1 cycle (94°C, 1 min; 57°C, 1 min; 70°C, 7 min). All assays were performed in triplicate on two separate occasions.

Virus. Replication-defective adenoviruses (Ad-p53 and Ad- β gal), in which the human p53 coding sequence or the bacterial β -galactosidase gene, respectively, replaced the viral early region *E1A* and *E1B* genes, were provided by Introgen Therapeutics, Inc. (Houston, TX).

Virus Treatments. Cells at 80% confluence were placed in DMEM supplemented with 2% heat-inactivated fetal bovine serum and infected for 3 h at a multiplicity of 100 pfu/cell. The efficiency of infection was determined by X-gal (5-bromo-4-chloro-3-indolyl- β -D-galactopyranoside) staining a sample of the β -gal virus-infected cells (see Ref. 28) and was usually $\geq 50\%$.

Viability and Growth Assays. After infection, triplicate aliquots of cells were replated in 96-well plates at a density of 1000 cells/well. Plates were incubated for 5–7 days, and surviving cells were determined by adding a solution containing MTS [3-(4,5'-dimethylthiazol-2-yl)-5-(3-carboxymethoxyphenyl)-2-(4-sulfophenyl)-2H-tetrazolium inner salt] and PMS (phenazine methosulfate; both purchased from Promega, Madison, WI.) for 1 h and determining A590 nm of the resulting formazan product, following procedures provided by the manufacturer. For growth assays, cells were plated at 1000 per well in 96-well plates. On successive days from day 1 through day 8, triplicate samples were stained with MTS, as described above.

Generation of Methotrexate-resistant Clones. LD₅₀ values for methotrexate were determined for the cell lines to be tested. Cells were seeded at a starting density of 10³ cells/cm² and allowed to attach for 16 h. Methotrexate (Sigma Chemical Co., St. Louis, MO) was then added to a concentration of 5 \times LD₅₀ or 9 \times LD₅₀, concentrations known to select for DHFR gene amplification (39, 40). Medium with fresh methotrexate was replaced weekly. When colonies developed and reached a size of about 100–200 cells (about 5 weeks), plates were washed in PBS and stained with 1% methylene blue in 70% methanol.

Analysis of DHFR Gene Copy Number. To verify DHFR gene amplification after selection in methotrexate, as described above, several clones were picked and expanded. Genomic DNA from these clones, as well as from parental unselected cells was prepared from about 10⁶ cells in each case using the QIAamp Blood Kit (Qiagen, Inc., Chatsworth, CA) and resuspended at 0.5 mg/ml in sterile H₂O. Quantitative PCR was performed in 50- μ l aliquots containing 0.2 μ g of DNA, 50 pmol each of forward and reverse primers defining a 270-bp region of exon 1 and intron A of the DHFR gene (see below), 50 mM of KCL, 10 mM of Tris (pH 8.3), 1.5 mM of MgCl₂, 250 mM dNTPs, 0.5 μ l of Tac polymerase (Qiagen, Inc.), 10 μ l of Q buffer (Qiagen, Inc.), and 1 pmol of radioactively end-labeled reverse primer (labeled with γ -³²P-dATP). PCR conditions were as follows: 1 cycle, 94°C (1 min, 30 s); 25 cycles, 94°C (1 min), 57°C (1 min), and 70°C (2 min, 30 s); 1 cycle, 94°C (1 min), 57°C (1 min), and 70°C (7 min). After PCR, 10 μ l aliquots were electrophoresed on a 1% agarose gel. The gel was vacuum-dried for 2 h onto filter paper, and the PCR-amplified 270-bp band was quantitated using an Ambis4000 Radioanalytic Imaging system (Ambis, Inc., San Diego, CA). Quantitative conditions were established by demonstrating in control reactions with known amounts of DNA in 2-fold dilutions that product formation was directly proportional to input template. Primer sequences for the DHFR gene were: forward primer, 5'-GGTCGCTAAACTGCATCGTCGC-3', and reverse primer, 5'-CAGAAAT-CAGCAACTGGGCCTCC-3'. An increase in DHFR gene copy number was

then equal to the fold increase in the PCR product from cellular DNA of methotrexate-resistant clones compared with that of unselected parental cells.

Apoptosis Assay. Apoptosis was assayed using the Cell Death Detection ELISA (Boehringer Mannheim, Indianapolis, IN), a quantitative photometric peroxidase immunoassay that detects cytoplasmic histone-associated DNA fragments (mono- and oligonucleosomes) that are released from the nuclei of cells undergoing apoptosis. Cells (2×10^5) were plated in 24-well plates and infected the next day (when the cells were about 80% confluent) with Ad-p53 or Ad- β gal, as described above. Forty-eight h after infection, cells were collected and cytoplasmic fractions were prepared and assayed for the presence of mono- and oligonucleosomes by following the manufacturer's protocol.

Acknowledgments

We thank M. Karin for providing the mutant Jun expression vectors and Dr. Hoi U for providing the T98G cells.

References

- Nowell, P. C. The clonal evolution of tumor cell populations. *Science (Washington DC)*, 194: 23–28, 1976.
- Bakalkin, G., Selivanova, G., Yakovleva, T., Kiseleva, E., Kashuba, E., Magnusson, K. P., Szekely, L., Klein, G., Terenius, L., and Wiman, K. G. p53 binds single stranded DNA ends through the C-terminal domain and internal DNA segments via the middle domain. *Nucleic Acids Res.*, 23: 362–369, 1995.
- Lee, S., Elenbas, B., Levine, A., and Griffith, J. p53 and its 14-kDa C-terminal domain recognize primary DNA damage in the form of insertion/deletion mismatches. *Cell*, 81: 1013–1021, 1995.
- Shieh, S.-Y., Ikeda, M., Taya, Y., and Prives, C. DNA damage-induced phosphorylation of p53 alleviates inhibition by MDM2. *Cell*, 91: 325–334, 1997.
- Woo, R. A., McLure, K. G., Lees-Miller, S. P., Rancourt, D. E., and Lee, P. W. DNA-dependent protein kinase acts upstream of p53 in response to DNA damage. *Nature (Lond.)*, 394: 700–704.
- Tainsky, M. A., Bischoff, F. Z., and Strong, L. C. Genomic instability due to germline p53 mutations drives preneoplastic progression toward cancer in human cells. *Cancer Metastasis Rev.*, 14: 43–48, 1995.
- Agapova, L. S., Ilyinskaya, G. V., Turovets, N. A., Ivanov, A. V., Chumakov, P. M., and Kopnin, B. P. Chromosome changes caused by alterations of p53 expression. *Mutat. Res.*, 354: 129–138, 1996.
- Bertrand, P., Rouillard, D., Boulet, A., Levalois, C., Soussi, T., and Lopez, B. S. Increase of spontaneous intrachromosomal homologous recombination in mammalian cells expressing a mutant p53 protein. *Oncogene*, 14: 1117–1122, 1997.
- Bouffler, S. D., Kemp, C. J., Balmain, A., and Cox, R. Spontaneous and ionizing radiation-induced chromosomal abnormalities in p53-deficient mice. *Cancer Res.*, 55: 3883–3889, 1995.
- Donehower, L. A., Godley, L. A., Aldaz, C. M., Pyle, R., Shi, Y.-P., Pinkel, D., Gray, J., Bradley, A., Medina, D., and Varmus, H. E. Deficiency of p53 accelerates mammary tumorigenesis in wnt-1 transgenic mice and promotes chromosomal instability. *Genes Dev.*, 9: 882–895, 1995.
- Lanza, G., Jr., Maestri, I., Dubini, A., Gafa, R., Santini, A., Ferretti, S., and Cavazzini, L. p53 expression in colorectal cancer: relation to tumor type, DNA ploidy pattern and short-term survival. *Am. J. Clin. Pathol.*, 105: 604–612, 1996.
- Gryfe, R., Swallow, C., Bapat, B., Redston, M., Gallinger, S., and Couture, J. Molecular biology of colorectal cancer. *Curr. Probl. Cancer*, 21: 233–300, 1997.
- Levine, A. J. p53, the cellular gatekeeper for growth and division. *Cell*, 88: 323–331, 1997.
- Derijard, B., Hibi, M., Wu, I. H., Barrett, T., Su, B., Deng, T., Karin, M., and Davis, R. J. JNK1: a protein kinase stimulated by UV light and Ha-ras that binds and phosphorylates the c-Jun activation domain. *Cell*, 76: 1025–1037, 1994.
- Adler, V., Fuchs, S. Y., Kim, J., Kraft, A., King, M. P., Pelling, J., and Ronai, Z. Jun-NH₂-terminal kinase activation mediated by UV-induced DNA lesions in melanoma and fibroblast cells. *Cell Growth Differ.*, 6: 1437–1446, 1995.
- Potapova, O., Haghghi, A., Bost, F., Liu, C., Birrer, M. J., Gjerset, R., and Mercola, D. The JNK/stress-activated protein kinase pathway functions to regulate DNA repair and inhibition of the pathway sensitizes tumor cells to cisplatin. *J. Biol. Chem.*, 272: 14041–14044, 1997.
- Saleem, A., Datta, R., Yuan, Z. M., Kharbanda, S., and Kufe, D. Involvement of stress-activated protein kinase in the cellular response to 1- β -D-arabinofuranosylcytosine and other DNA damaging agents. *Cell Growth Differ.*, 6: 1651–1658, 1995.
- Osborne, M. T., and Chambers, T. C. Role of stress-activated/c-Jun NH₂-terminal protein kinase pathway in the cellular response to adriamycin and other chemotherapeutic drugs. *J. Biol. Chem.*, 271: 30950–30955, 1996.
- Binétruy, B., Smeal, T., and Karin, M. Ha-ras augments c-Jun activity and stimulates phosphorylation of its activation domain. *Nature (Lond.)*, 351: 122–127, 1991.
- Smeal, T., Binétruy, B., Mercola, D. A., Birrer, M., and Karin, M. Oncogenic and transcriptional cooperation with Ha-ras requires phosphorylation of c-Jun on serines 63 and 73. *Nature (Lond.)*, 354: 494–496, 1991.
- Schreiber, M., Kolbus, A., Piu, F., Szabowski, A., Mohle-Steinlein, U., Tian, J., Karin, M., Angel, P., and Wagner, E. F. Control of cell cycle progression by c-Jun is p53 dependent. *Genes Dev.*, 13: 607–619, 1999.
- Takahashi, J. A., Fukumoto, M., Koza, Y., Ito, N., Oda, Y., Kikuchi, H., and Hatanaka, M. Inhibition of cell growth and tumorigenesis of human glioblastoma cells by neutralizing antibody against human basic fibroblast growth factor. *FEBS Lett.*, 288: 65–71, 1991.
- Bost, F., McKay, R., Dean, N., and Mercola, D. The Jun kinase/stress-activated protein kinase pathway is required for epidermal growth factor stimulation of growth of human A549 lung carcinoma cells. *J. Biol. Chem.*, 272: 33422–33429, 1997.
- Srivastava, D. K., Rawson, T. Y., Showalter, S. D., and Wilson, S. H. Phorbol ester abrogates up-regulation of DNA polymerase β by DNA-alkylating agents in Chinese hamster ovary cell. *J. Biol. Chem.*, 270: 16402–16408, 1995.
- Kedar, P. S., Widen, S. G., Englander, E. W., Fornace, A. J., Jr., and Wilson, S. H. The ATF/CREB transcription factor-binding site in the polymerase β promoter mediates the positive effect of N-methyl-N-nitro-N-nitrosoguanidine on transcription. *Proc. Natl. Acad. Sci. USA*, 88: 3729–3733, 1991.
- Baumgartner, B., Heiland, S., Kunze, N., Richter, A., and Knippers, R. Conserved regulatory elements in the type I DNA topoisomerase gene promoters of mouse and man. *Biochim. Biophys. Acta*, 1218: 123–127, 1994.
- Heiland, S., Knippers, R., and Kunze, N. The promoter region of the human type-I-DNA-topoisomerase gene. Protein-binding sites and sequences involved in transcriptional regulation. *Eur. J. Biochem.*, 217: 813–822, 1993.
- Gjerset, R. A., Turla, S. T., Sobol, R. E., Scalise, J. J., Mercola, D., Collins, H., and Hopkins, P. J. Use of wild-type p53 to achieve complete treatment sensitization of tumor cells expressing endogenous mutant p53. *Mol. Carcinog.*, 14: 275–285, 1997.
- Chen, X., Ko, L. J., Jayaraman, L., and Prives, C. p53 levels, functional domains, and DNA damage determine the extent of the apoptotic response of tumor cells. *Genes Dev.*, 10: 2438–2451, 1996.
- Stark, G. R. Regulation and mechanisms of mammalian gene amplification. *Adv. Cancer Res.*, 61: 87–113, 1993.
- Jennerwein, M. M., and Eastman, A. A polymerase chain reaction-based method to detect cisplatin adducts in specific genes. *Nucleic Acids Res.*, 19: 6209–6214, 1991.
- Robbins, J. H., and Burk, P. G. Relationship of DNA repair to carcinogenesis in xeroderma pigmentosum. *Cancer Res.*, 33: 929–935, 1973.
- Nacht, M., Strasser, A., Chan, Y. R., Harris, A. W., Schlissel, M., Bronson, R. T., and Jacks, T. Mutations in the p53 and SCID genes cooperate in tumorigenesis. *Genes Dev.*, 10: 2055–2066, 1996.
- Melton, D., Ketchen, A. M., Nuñez, F., Bonatti-Abbondandolo, S., Abbondandolo, A., Squires, S., and Johnson, R. Cells from ERCC1-

deficient mice show increased genome instability and a reduced frequency of homologous recombination. *J. Cell. Sci.*, **111**: 395–404, 1998.

35. Lengauer, C., Kinzler, K. W., and Vogelstein, B. Genetic instability in colorectal cancers. *Nature (Lond.)*, **386**: 623–627, 1997.
36. Sager, R., Gadi, I. K., Stephens, L., and Grabowy, C. T. Gene amplification: an example of accelerated evolution in tumorigenic cells. *Proc. Natl. Acad. Sci. USA*, **82**: 7015–7019, 1985.
37. Otto, E., McCord, S., and Tlsty, T. D. Increased incidence of *CAD* gene amplification in tumorigenic rat lines as an indicator of genomic instability of neoplastic cells. *J. Biol. Chem.*, **264**: 3390–3396, 1989.
38. Tlsty, T. D. Normal diploid human and rodent cells lack a detectable frequency of gene amplification. *Proc. Natl. Acad. Sci. USA*, **87**: 3132–3136, 1990.
39. Brown, P. C., Tlsty, T. D., and Schimke, R. T. Enhancement of methotrexate resistance and dihydrofolate reductase gene amplification by treatment of mouse 3T6 cells with hydroxyurea. *Mol. Cell. Biol.*, **3**: 1097–1107, 1983.
40. Tlsty, T. D., Brown, P. C., and Schimke, R. T. UV-radiation facilitates methotrexate resistance and amplification of the dihydrofolate reductase gene in cultured 3T6 mouse cells. *Mol. Cell. Biol.*, **4**: 1050–1056, 1984.
41. Mercer, W. E., Shields, M. T., Amin, M., Sauve, G. J., Appela, E., Roman, J. W., and Ullrich, S. J. Negative growth regulation in a glioblastoma tumor line that conditionally expresses human wild-type p53. *Proc. Natl. Acad. Sci. USA*, **87**: 6166–6170, 1990.
42. Miyashita, T., and Reed, J. C. Tumor suppressor p53 is a direct transcriptional activator of the human *bax* gene. *Cell*, **80**: 293–299, 1995.
43. Basu, A., and Haldar, S. The relationship between *Bcl₂*, *Bax* and p53: consequences for cell cycle progression and cell death. *Mol. Hum. Reprod.*, **4**: 1099–1109, 1998.
44. Windle, B., Draper, B. W., Yin, Y. X., O'Gorman, S., and Wahl, G. M. A central role for chromosome breakage in gene amplification, deletion formation, and amplicon integration. *Genes Dev.*, **5**: 160–174, 1991.
45. Smith, K. A., Agarwal, M. L., Chernov, M. V., Chernova, O. B., Deguchi, Y., Ishizaka, Y., Patterson, T. E., Poupon, M. F., and Stark, G. R. Regulation and mechanisms of gene amplification. *Philos. Trans. R. Soc. Lond. B. Biol. Sci.*, **347**: 49–56, 1995.
46. Gjerset, R. A., and Mercola, D. Sensitization of tumors to chemotherapy through gene therapy. In: N. Nagy (ed.), *Cancer Gene Therapy: Past Achievements and Future Challenges*. New York, London, and Moscow: Plenum Publishing Corporation, in press, 1999.
47. Zamble, D. B., and Lippard, S. J. Cisplatin, and DNA repair in cancer chemotherapy. *Trends Biochem. Sci.*, **20**: 435–439, 1995.
48. Milne, D. M., Campbell, L. E., Campbell, D. G., and Meek, D. W. P53 is phosphorylated *in vitro* and *in vivo* by an ultraviolet radiation-induced protein kinase characteristic of the c-Jun kinase, JNK1. *J. Biol. Chem.*, **270**: 5511–5518, 1995.
49. Hilberg, F., and Wagner, E. F. Embryonic stem (ES) cells lacking functional c-Jun: consequences for growth and differentiation, AP-1 activity and tumorigenicity. *Oncogene* **7**: 2371–2380, 1992.
50. Harris, C. C. Structure and function of the p53 tumor suppressor gene: clues for rational cancer therapeutic strategies. *J. Natl. Cancer Inst.*, **88**: 1442–1445, 1996.
51. Potapova, O., Fahkrai, H., Baird, S., and Mercola, D. Platelet-derived growth factor-B/v-sis confers a tumorigenic and metastatic phenotype to human T98G glioblastoma cells. *Cancer Res.*, **56**: 280–286, 1996.

Preferential Platination of an Activated Cellular Promoter by *cis*- Diamminedichloroplatinum

Ali Haghghi, Svetlana Lebedeva, and Ruth A. Gjerset

Sidney Kimmel Cancer Center, 10835 Altman Row,
San Diego, California 92121

Biochemistry®

Reprinted from
Volume 38, Number 38, Pages 12432–12438

Preferential Platination of an Activated Cellular Promoter by *cis*-Diamminedichloroplatinum[†]

Ali Haghghi, Svetlana Lebedeva, and Ruth A. Gjerset*

Sidney Kimmel Cancer Center, 10835 Altman Row, San Diego, California 92121

Received May 11, 1999; Revised Manuscript Received July 6, 1999

ABSTRACT: This study examines how accessibility to cisplatin on various genomic regions in T47D breast cancer cells, including the retinoic acid receptor β gene promoter and coding region and the dihydrofolate reductase gene promoter and coding region, is affected by treatment of the cells with 9-*cis* retinoic acid, a treatment that activates the retinoic acid receptor β gene promoter in these cells. A PCR-based assay was used to measure cisplatin adduct density based on the inhibition of PCR amplification of templates from cisplatin treated versus untreated cells. Treatment of cells with 9-*cis* retinoic acid enhanced accessibility to cisplatin on the retinoic acid receptor β gene promoter region, but not on the coding regions of that gene nor on the dihydrofolate reductase gene promoter or coding regions, where accessibilities to cisplatin remained 2–4 times lower than on the activated retinoic acid receptor β gene promoter. Examination of smaller regions within this promoter region showed a repression of platination in the 500 bp region surrounding the TATA box in cells prior to 9-*cis* retinoic acid treatment, which was abolished following promoter activation. Differences in sequence composition between the various regions could not fully account for differences in platination, suggesting that structural features such as bends in retinoic acid receptor β gene promoter DNA following gene activation, create energetically favorable sites for platination, and contribute to the cytotoxicity of the drug.

cis-Diamminedichloroplatinum (cisplatin) is a highly effective chemotherapeutic agent used in the treatment of a variety of human tumors (1). Its cytotoxicity derives from its ability to damage DNA, forming primarily bifunctional 1,2-intrastrand cross-links between adjacent guanines or adenine-guanine dinucleotides, as well as other minor adducts including interstrand cross-links (2). Adduct formation impedes DNA polymerase progression, inhibits DNA synthesis, and triggers apoptosis (3–5). While inhibition of DNA synthesis is believed to be a critical step in cisplatin's cytotoxicity, it does not by itself account for the marked antitumor efficacy of cisplatin. For example, adducts formed by the geometric isomer of cisplatin, *trans*-diamminedichloroplatinum (transplatin), also impede DNA polymerase progression and inhibit DNA synthesis (6). Yet transplatin does not induce apoptosis and has little antitumor activity. Furthermore, while cisplatin causes slowing of DNA synthesis, cells treated with cisplatin do not arrest in S phase, but progress and block in G2 (7). In addition, the extent to which DNA synthesis is slowed by cisplatin in sensitive versus resistant cells does not correlate with its relative toxicity to those cells (8). Several studies have pointed to transcription as a key target for cisplatin and have suggested that cisplatin's ability to target certain genetic regulatory elements and inhibit specific gene expression may contribute greatly to its toxicity (9–12).

A structural distortion in DNA occurs upon cisplatin binding that has been proposed to underlie the biological toxicity of cisplatin. Crystallographic studies reveal that the 1,2-cisplatin cross-link induces a bend of about 45° toward the major groove of the DNA helix accompanied by thermal destabilization (13). Such a bend appears to generate a structural motif with biological specificity, as certain chromosomal proteins bind with high affinity to these sites. These proteins include histone H1 (14), HMG1 (15), HMG2 (16), the human structure-specific recognition protein SSRP1 (17, 18), and the human transcription factor hUBF (18), all of which are proteins known to bend DNA and whose binding to DNA might be facilitated by the bends generated by cisplatin. In contrast, the structural effects of transplatin appear to be of greater variability (19), and transplatin adducts do not constitute high affinity binding sites for the above-mentioned chromosomal proteins (see ref 20 for review). Cisplatin's toxicity may therefore be related to the structural consequences of adduct formation, which could involve a disruption of normal binding of chromosomal proteins, or an impediment to conformational changes that are necessary for biological regulation.

In the studies reported here we have addressed the possibility that cisplatin may actually target chromosomal regions such as transcriptional promoters, where DNA bends or partial unwinding of DNA may occur following transcription factor recruitment to an activated promoter. If so, such a structural motif may provide a preferential target for cisplatin and contribute to the cytotoxicity of this drug. We have examined cisplatin adduct formation on promoter and

* This work was supported in part by grants (to R.A.G.) from the National Cancer Institute CA69546 and from the U.S. Army Breast Cancer Research Program DAMD17-96-1-6038.

† To whom correspondence should be addressed. Phone: (858) 450-5990. Fax: (858) 450-3251. E-mail: rgjerset@skcc.org.

downstream regions of the retinoic acid receptor β (RAR β)¹ gene in T47D breast cancer cells, where this gene undergoes retinoic-acid-dependent activation. Adduct formation as determined by a quantitative PCR-based assay was observed to be significantly higher on the activated RAR β promoter than on a downstream region of the same gene, as well as on the coding and promoter regions of the constitutively expressed housekeeping gene, dihydrofolate reductase (DHFR). Adduct formation on the DHFR promoter, which does not undergo retinoic-acid-dependent activation, did not increase following retinoic acid treatment of cells. Cisplatin's cytotoxicity may therefore derive in part from its ability to target and disrupt the function of certain genetic regulatory loci such as the RAR β promoter.

EXPERIMENTAL PROCEDURES

Cell Culture. T47D breast cancer cells were purchased from ATCC and maintained in RPMI medium supplemented with 10% heat-inactivated fetal bovine serum, 1 mM sodium pyruvate, 2 mM L-glutamine, 0.1 mM nonessential amino acids, and 50 μ g/mL gentamycin. Cell culture reagents were purchased from Irvine Scientific, Santa Ana, CA. All experiments were performed using charcoal-treated serum (600 mg of activated charcoal/50 mL of serum for 10 min at 4 °C, followed by filtration).

Analysis of RAR β and DHFR Gene Expression. About 5 \times 10⁵ T47D cells (at about 70% confluence) were treated as indicated and total cellular RNA was prepared using the Rneasy kit from Qiagen and following the manufacturer's procedure. One microgram of RNA was reverse transcribed into cDNA in a 20 μ L reaction containing 0.5 mM dNTPs (Pharmacia), 100 μ g/mL oligo dT (Promega), 2 units of RNAsin (Promega), 10 units of Moloney Murine leukemia virus reverse transcriptase (Promega), and reverse transcriptase buffer (Promega). This cDNA was then used as a template for quantitative PCR. Primers were chosen so as to amplify a 178 base region of the RAR β coding sequence encompassing parts of exons 4 and 5, as well as a 246 base region of the coding sequence of the dihydrofolate reductase from exons 1–4. The sequences are as follows: RAR β message (forward), 5'-GTGTACAAACCTGCTTCGTCT-GC-3'; (reverse) 5'-CTGGAGTCGACAGTATTGGCATCG-3'; DHFR message (forward), 5'-GGTCGCTAAACTGCATCGTCG-3'; (reverse) 5'-GTGGAGGTTCTTGAG-TTCTCTG - 3'.

Amplification conditions were as described below for the PCR-stop assay. Quantitative conditions were verified by preparing cDNA with 100 and 10 ng of RNA (in addition to 1 μ g of RNA) and amplifying serial 2-fold dilutions of the cDNA from 2 to 0.25 μ L of template to show that product formation was proportional to input template under our conditions. Following amplification, products were analyzed by agarose gel electrophoresis followed by band quantitation using a Kodak digital camera.

Cell Viability. Following treatments, cell viability was monitored by adding 10% Trypan blue and determining the fraction of cells that excluded the dye.

Cisplatin Treatments. Cells were plated at 50% confluence in six-well plates in medium supplemented with 10% charcoal-treated FBS in addition to the other standard additives described above. Following attachment, cultures were pretreated 24 h in the presence or absence of 1 μ M 9-cis retinoic acid (Sigma, St. Louis, MO), followed by a 2 h incubation in the presence or absence of 1 mM cisplatin (Platinol, aqueous solution at 1 mg/mL, purchased from local pharmacies). The preincubation medium was then replaced, and genomic DNA was prepared 24 h later as described below. Although DNA repair has been observed to occur over 24 h in cells treated with lower doses of cisplatin (21–22), at the high levels used in our studies we observed an overall increase in adduct formation over 24 h, so that adduct densities approached 1–4 adducts/10 Kb and were therefore readily detectable in our assay. The increase in adduct formation over time suggests that residual cisplatin continued to cause DNA damage and that repair did not keep pace with adduct formation under our conditions.

Preparation of Genomic DNA. DNA was prepared from treated cultures using the QIAamp blood kit essentially following the manufacturer's protocol, except that cells were lysed directly on the plate in the presence of PBS, Qiagen protease, and lysis buffer supplied in the kit. Following purification, DNA was adjusted to 0.25 mg/mL in sterile water and stored at –20 °C until use.

Analyses of DNA Damage by PCR Stop Assay. Quantitative PCR was used to compare cisplatin adduct formation on specific regions of DNA. The assay, known as the PCR stop assay, has been described (23). Because Taq polymerase is blocked at cisplatin adducts, the relative efficiency of PCR amplification of genomic DNA from cisplatin-treated versus control cells decreases in proportion to platination levels. The relative PCR efficiency is equivalent to the frequency (P) of undamaged strands within a population. P is related to the average number (n) of cisplatin adducts per fragment, by the Poisson formula: $P = e^{-n}$, or $-(\ln P) = n$. Adducts per Kb would then be equal to $-(\ln P)/(size\ of\ fragment\ in\ Kbs)$. We found that fragment sizes of around 1 Kb provided a sufficiently large target size to enable measurement of adduct densities in the range 0.1–0.4 adducts/Kb observed here. A drop in the PCR signal of damaged DNA to 0.67 of the control signal would therefore reflect an average cisplatin adduct density of $-(\ln 0.67) = 0.4$ adducts/fragment. Standard deviations among triplicate PCRs were in the range of $\pm 5\%$, meaning that adduct densities of less than about 0.05 adducts/fragment were undetectable. For each primer pair, we verified that product formation was directly proportional to input template DNA by performing a pilot experiment with serial 2-fold dilutions of template, followed by electrophoresis on a 1% agarose gel containing 0.5 μ g/mL ethidium bromide. Bands were quantitated using Kodak digital camera and analysis software. Depending on the primer set, the amount of template used in the PCR reaction ranged 0.03–0.25 μ g/25 μ L reaction. Reactions were performed in 25 μ L containing template DNA, 25 pmol each of forward and reverse primer, 250 μ M dNTPs (Pharmacia), 1.25 units of Taq polymerase (Qiagen), 1 \times buffer (Qiagen), and solution Q (Qiagen). The amplification program was as follows: 1 cycle (94 °C, 1 min 30 s); 25 cycles (94 °C, 1 min; 57 °C, 1 min; 70 °C, 2 min, 30 s); 1 cycle (94 °C, 1 min; 57 °C, 1 min; 70 °C, 7 min). Two independent templates

¹ Abbreviations: RAR β , retinoic acid receptor β ; RARE, retinoic acid response element; PCR, polymerase chain reaction; DHFR, dihydrofolate reductase; ATCC, American type culture collection; PBS, phosphate-buffered saline; Kb, kilobase; bp, base pair; CDS, coding sequence.

Table 1: Primers Used for PCR-stop Assay of Genomic DNA

gene	region amplified	primer sequences (5' → 3')	product size (base pairs)
RAR β	RAR β Promoter (includes A,B,C below) (A) promoter, upstream and including TATA and RARE (B) promoter region of TATA and RARE (C) promoter, downstream and including TATA and RARE	1: CGAGTGCAGTCATTCAAGGCCAGG (for) 2: GCTTATCCTCTAGGTGTGGAGGC (rev) 1: see above (for) 3: CTTCCCTACTACTTCTGTACACAG (rev) 4: GGGAGAGAAGTTGGTGCTAACG (for) 5: CCTTCCGAATGCGTCCGGATC (rev) 6: GCTTTTGAGGGCTGCTGGGAG (for) 2: see above (rev)	1043 624 483 592
	RAR β CDS (1036 bp) (exon 10)	7: GGTGCAGAGCGTGTAAATTACCTTG (for) 8: CTGCCTTGGAGGCTATCATTACTG (rev)	1036
	RAR β CDS (483 bp) (exon 10)	7: see above (for) 9: GGTCTTGGCCATGCATCTGAGTG (rev)	483
	DHFR	10: CAGAATGGGAGTCAGGAGACCTG (for)	1000
	11: GCAGAAATCAGCAACTGGGCCTC (rev)	12: CCGTAGACTGGAAGAATCGGCTC (for)	1062
	DHFR CDS (1062 bp) (exons 1,2,adjacent introns)	13: CAGTTGCCAATTCTGCCCATGC (rev)	
	DHFR CDS (472 bp) (exon 1 and adjacent introns)	14: CAATTCGCGCAAACCTTGACCG (for)	472
	DHFR CDS (272 bp) (exon 1 and adjacent introns)	15: GAGCTCTAAGGCACCTGACAAAC (rev)	
	(internal control)	16: GGTCGCTAAACTGCATCGTCGC (for)	272
		17: CAGAAATCAGCAACTGGGCCTC (rev)	

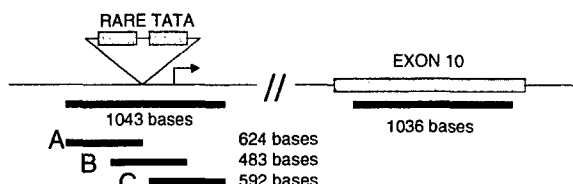


FIGURE 1: Location and sizes of PCR amplification products from the RAR β gene of T47D cells (see also Table 1). For the analysis in Figure 3, PCR primers were chosen so as to amplify a 1043 bp region of the RAR β promoter, including the retinoic acid response element (RARE) and TATA box, and a 1036 bp region of the RAR β coding sequence (CDS). For the analysis in Figure 4, PCR primers were chosen so as to amplify the subregions A, B, and C.

were prepared for each treatment condition, and each one was analyzed in triplicate. As an internal PCR control for each template, a 270 bp fragment of the dihydrofolate reductase gene was amplified. This fragment is too small to register significant levels of damage under the conditions we used, and its amplification product was seen to vary by less than 5% among the various templates. The primers 1–17 used for PCR amplification of various regions of genomic DNA are summarized in Table 1. Figure 1 shows a schematic representation of regions amplified from the RAR β gene.

RESULTS

Transcriptional Response of the RAR β Gene to 9-cis Retinoic Acid and Cisplatin. Figure 2 shows the results of an RT-PCR assay demonstrating retinoic-acid-dependent activation of the RAR β gene (lane 2 compared to lane 1) and cisplatin-mediated inhibition of this activation (lane 3). Under the same conditions, we observed little change in DHFR expression (lanes 4–6), indicating that expression of this gene is not retinoic acid dependent and that cisplatin has little immediate effect on its expression. This is consistent with another study in which treatment with cisplatin did not alter levels of DHFR message (24), although long term in vitro selection for cisplatin-resistant ovarian carcinoma cell lines by repeated exposure to cisplatin has been reported to generate variants that overexpress DHFR (25). Genomic DNA from cells before and after treatment with 9-cis retinoic

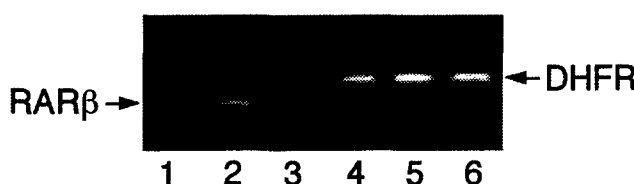


FIGURE 2: Quantitative RT-PCR analysis of RAR β gene expression (lanes 1–3) and DHFR gene expression (lanes 4–6) in T47D cells under various conditions. Lanes 1 and 4: untreated T47D cells. Lanes 2 and 5: T47D cells treated 24 h with 1 μ M 9-cis retinoic acid. Lanes 3 and 6: cells treated 24 h with 9-cis retinoic acid, followed by 2 h with 200 μ M cisplatin. Quantitative conditions for cDNA synthesis and PCR amplification were verified as described in the Experimental Procedures. A total of 10 and 2 μ L, respectively, of the RAR β and DHFR PCR reactions were analyzed.

acid was then used to analyze platination of the RAR β gene in its active and inactive state.

Preferential Cisplatin Adduct Formation on the Activated RAR β Gene Promoter. We performed a PCR stop assay to examine cisplatin adduct density on genomic DNA templates from 9-cis-retinoic-acid-treated (RA+) or -untreated (RA-) cells. Regions spanning about 1 Kb in length of the RAR β promoter (1043 bp), the RAR β coding sequence (1036 bp), the DHFR promoter (1000 bp), and the DHFR coding sequence (1062 bp) were examined as defined by primers listed in Table 1. PCR products were analyzed on agarose gels (Figure 3A) and bands were quantitated in order to determine the relative PCR efficiencies from platinated versus unplatinated templates. Using templates from (RA-) cells (Figure 3A, lanes 1 and 2), the relative PCR efficiencies from platinated versus unplatinated templates (lane 2 versus lane 1) were as follows: RAR β promoter (0.88), RAR β coding sequence (0.85), DHFR promoter (0.85), DHFR coding sequence (0.87). Using templates from (RA+) cells (lanes 3 and 4), the relative PCR efficiencies from platinated versus unplatinated templates (lane 4 versus lane 3) were as follows: RAR β promoter (0.65), RAR β coding sequence (0.88), DHFR promoter (0.9), DHFR coding sequence (0.88). On the basis of the PCR results, the cisplatin adduct densities were calculated by the Poisson equation described above. The results plotted in Figure 3B represent the averages

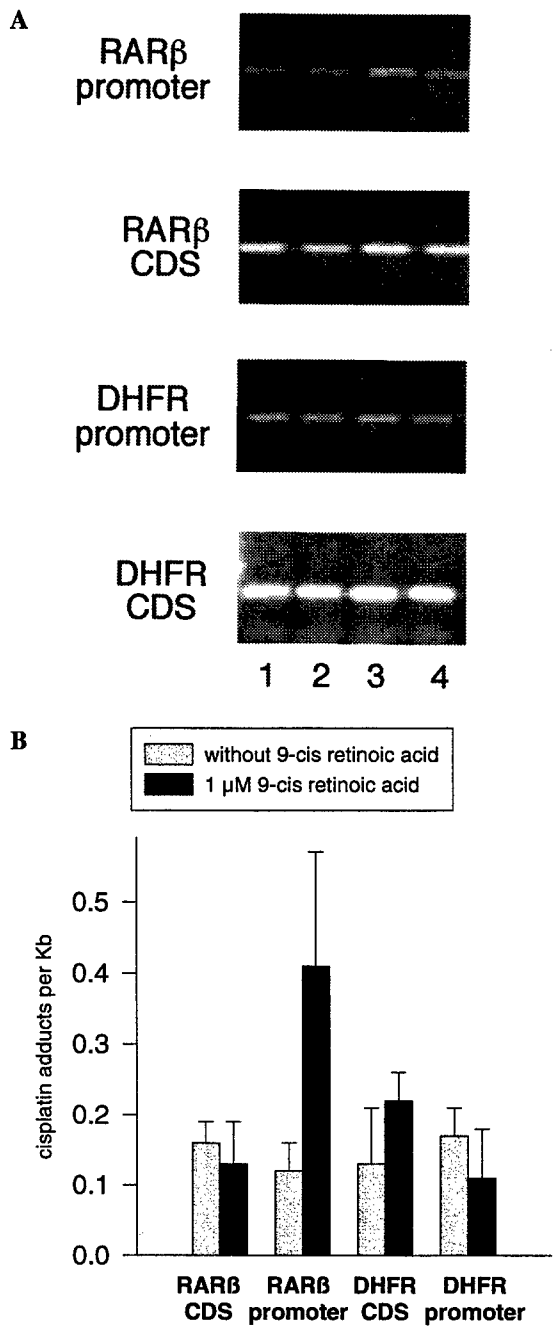


FIGURE 3: Cisplatin adduct formation on various regions of T47D cell genomic DNA as determined by the PCR stop assay. Regions analyzed were the RAR β CDS (1036 bp), the RAR β promoter (1043 bp), the DHFR CDS (1062 bp), and the DHFR promoter (1000 bp). Genomic DNA was prepared from cells pretreated in the presence (RA+) or absence (RA-) of 9-cis retinoic acid for 24 h followed by 2 h in the presence or absence of 1 mM cisplatin. (A) Agarose gel analysis of PCR products from one experiment. Lanes 1 and 2 (RA- cells). Lanes 3 and 4 (RA+ cells). Lanes 1 and 3 (no cisplatin). Lanes 2 and 4 (plus cisplatin). (B) Bar graph showing cisplatin adducts per Kb as calculated from the PCR results as described in the Experimental Procedures. The results represent the averages and standard deviations of two separate experiments with independently prepared templates, with each experiment being performed in triplicate. For each experiment, results were corrected for variations in the 270 bp PCR product of the DHFR gene.

and standard deviations of two separate experiments with independently prepared templates, with each experiment being performed in triplicate and corrected for variations in the 270 bp PCR product of the DHFR gene.

As shown in Figure 3B, in the case of the RAR β CDS (1036 bp), the DHFR CDS (1062 bp), and the DHFR promoter (1000 bp), treatment of cells with 9-cis retinoic acid has little effect on cisplatin adduct density. Thus, adduct densities (in adducts per Kb) on these regions in untreated cells (RA-) are observed to be 0.16 ± 0.03 , 0.13 ± 0.08 , and 0.17 ± 0.04 , respectively. Adduct densities on these same regions in 9-cis-retinoic-acid-treated cells (RA+) are observed to be 0.13 ± 0.06 , 0.2 ± 0.04 , and 0.11 ± 0.07 , respectively.

In contrast, cisplatin adduct density on the RAR β promoter (1043 bp) is enhanced in cells following treatment of cells with 9-cis retinoic acid (Figure 3B). For this region, adduct densities increase from 0.12 ± 0.04 adducts/Kb in untreated cells (RA-) to 0.4 ± 0.16 adducts/Kb in treated cells (RA+). Cisplatin adduct density measured on the active RAR β promoter region in RA+ cells is therefore about 2 times as high as on the DHFR CDS (1062 bp) or DHFR promoter regions in RA+ cells, and nearly 3.5 times as high as on the inactive RAR β promoter in RA- cells. Cisplatin adduct density on the constitutively expressed DHFR promoter does not increase following 9-cis retinoic acid treatment (Figure 3B).

To determine the extent to which differences in sequence composition might account for differences in adduct density, we examined the number of GG and AG dinucleotide pairs (the major sites of adduct formation in DNA) in the various DNA regions studied, as summarized in Table 2 (column 2). Clusters of three or four Gs were scored as one site. The number of potential sites for adduct formation was in turn used to estimate the relative frequencies of cisplatin targets per Kb compared to the DHFR CDS (1062 bp) region (Table 2, column 5), given that AG is targeted by cisplatin only about 40% as frequently as GG dinucleotides (2). We find that cisplatin adducts form on the RAR β promoter (1043 bp) about two times as frequently as we would anticipate on the basis of sequence composition alone. That is, the estimated frequency of targets is about the same for the RAR β promoter (1043 bp) region and the DHFR CDS (1062 bp) region, yet the observed adduct frequency on the promoter region is about two times what it is on the DHFR CDS (1062 bp) region (0.4 ± 0.16 versus 0.2 ± 0.04 adducts/Kb). Similarly, the estimated frequency of targets on the RAR β promoter (1043 bp) is about two times the estimated frequency on RAR β CDS (1036 bp), yet the observed adduct frequency is three times greater on the promoter compared to the CDS (0.4 ± 0.16 versus 0.13 ± 0.06 adducts/Kb). This suggests that other factors also contribute to the preferential targeting of cisplatin to the induced RAR β promoter.

Location of Cisplatin Adducts within the Promoter Region. To further localize adduct formation within the promoter, we subdivided the RAR β promoter (1043 bp) region into three overlapping regions A (624 bp), B (483 bp), and C (592 bp) shown schematically in Figure 1, and defined by primers listed in Table 1. As shown in Figure 4, in the absence of promoter activation with 9-cis retinoic acid, adduct formation is virtually undetectable in the central region (B) encompassing the TATA box and RARE (retinoic acid response element) and approximately equivalent in regions A and C in adducts per Kb to what we observe on the larger 1043 base region of the promoter (0.17 adducts/

Table 2: Comparison of Expected versus Observed Adduct Density in Various Gene Fragments from Cells Treated with 9-cis Retinoic Acid and 1 mM Cisplatin

gene fragment	no. of GG and AG sites	3		4	5	6	7
		cisplatin targets per fragment ^a	(a) (b) sum				
DHFR CDS	GG 77	GG 77	88	83	1.0	0.2	0.2 ± 0.04
1062 bases	AG 26	AG 11					
RAR β CDS (1036 bp)	GG 25	GG 25	47	45	0.54	0.11	0.13 ± 0.06
	AG 56	AG 22					
RAR β promoter (1043 bp)	GG 72	GG 72	92	88	1.1	0.21	0.40 ± 0.16
	AG 50	AG 20					
DHFR promoter (1000 bp)	GG 84	GG 84	106	106	1.3	0.26	0.11 ± 0.07
	AG 55	AG 22					

^a AG adducts are about 40% as likely to form as GG adducts (16); therefore, AG targets (column 3a) = AG sites (column 2) × 0.4. ^b From column 7. ^c Calculated from PCR data in Table 2 using Poisson equation relating adducts per fragment to PCR signal, and correcting for fragment size.

Kb on each of regions A, C versus 0.12 adducts/Kb on the larger fragment overall). This suggests that some portion of the central region of the promoter included in fragment B is protected from platinination in the uninduced state.

Following promoter activation, all three regions A, B, and C sustain elevated levels of damage, (0.34 ± 0.07, 0.43 ± 0.07, and 0.27 ± 0.11 adducts/Kb, respectively), which is on the average what we observe on the larger 1043 base region of the activated promoter (0.4 ± 0.16 adducts/Kb). This confirms the measurement of adduct density on the larger 1043 base region (Figure 3 and Table 2) and supports the conclusion drawn from the comparison of sequence composition that the activated RAR β promoter sustains levels of cisplatin damage greater than would be expected on the basis of base composition alone. Because regions A, B, and C do not differ significantly between themselves in GG and AG sequence compositions, the result here suggests that cisplatin adducts are distributed evenly over the activated promoter and that protection from platinination in region B is abolished by promoter activation.

DISCUSSION

In these studies, we have used a PCR-based assay to detect platinination on genomic regions encompassing about 1 Kb of the RAR β promoter, the RAR β coding sequence (CDS), the DHFR promoter, and the DHFR CDS in T47D breast cancer cells. We see that treatment of these cells with 9-cis retinoic acid, a treatment that activates the RAR β promoter but not the DHFR promoter, results in a 3-fold increase in accessibility of the RAR β promoter region to cisplatin (0.4 ± 0.16 versus 0.12 ± 0.04 adducts/Kb). In contrast, the accessibilities to cisplatin of the DHFR promoter, DHFR CDS, and RAR β CDS are not significantly altered by treatment of cells with 9-cis retinoic acid, and observed adduct densities remain about 2–4-fold lower than on the activated RAR β promoter (0.11 ± 0.07, 0.2 ± 0.04, and 0.13 ± 0.06 adducts/Kb, respectively). The activated RAR β promoter appears therefore to be hypersensitive to cisplatin adduct formation. Preferential platinination of the RAR β promoter relative to the other regions examined could be attributed only in part to differences in sequence composition, suggesting that structural factors also play a role in directing adduct formation to certain sites.

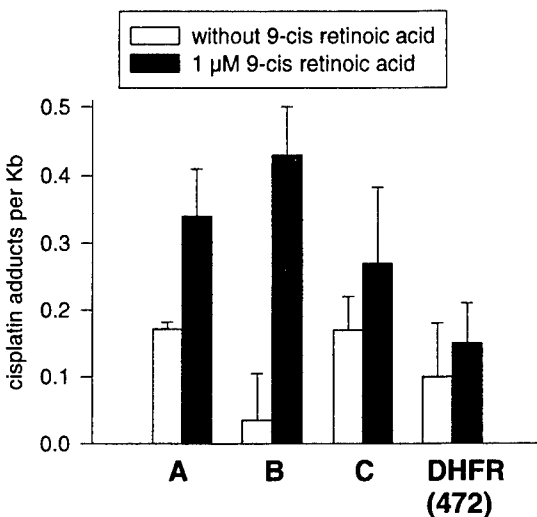


FIGURE 4: Cisplatin adduct formation on three overlapping regions A (624 bp), B (483 bp), and C (592 bp) of the RAR β promoter 1043 bp region shown schematically in Figure 1. Primers used are listed in Table 1. Cells were treated as in Figure 3. Results represent the average of triplicate assays.

The possibility that promoter-specific structural changes influence reactivity with cisplatin is further supported by the analysis of subregions of the larger RAR β promoter fragment, where we see that accessibility to cisplatin increases over the entire promoter region following activation of the promoter. Furthermore, the accessibility to cisplatin of the central region of the promoter, including the TATA box and RARE appears to be suppressed in the inactive state, and this suppression is relieved upon promoter activation. In this case, inhibition of accessibility to cisplatin might be due to steric hindrance due to the possible positioning of a nucleosome at or near the start site of transcription. A recent analysis of a large set of unrelated RNA polymerase II promoters, both TATA-containing and TATA-less, has revealed a common bendability profile of DNA just downstream of the start site of transcription, suggesting that the DNA could wrap around protein in a nucleosome (26). In addition, the complementary triplet pair, CAG/CTG, shown to correlate with nucleosome positioning (27, 28) is overrepresented in the region just downstream of the transcription start site (26). Complexation with nucleosomes near the transcription start site of the inactive promoter might

therefore impede adduct formation by cisplatin, and displacement or destabilization of nucleosomes by the transcription initiation complex might remove this impediment.

Following transcriptional activation, the RAR β promoter not only becomes more accessible to cisplatin than it was prior to transcriptional activation but also appears to bind more cisplatin than would be expected based on sequence composition alone. This suggests that some structural feature of the DNA of the activated promoter might make it an energetically favorable site for cisplatin adduct formation. One such feature might be an induced bend in the promoter DNA generated as a result of protein–protein interactions between transcription factors bound to distant sites (see ref 29 for review). Such a bend might provide the stored energy required for strand separation and initiation of transcription, and this process could be blocked by the formation of a cisplatin adduct.

The retinoids *all-trans*-retinoic acid (ATRA) and *9-cis* retinoic acid (*9-cis* RA), as well as several synthetic analogues of these natural retinoids, have attracted considerable attention as potential chemotherapeutic agents for the treatment of promyelocytic leukemia (30) and other cancers (31–33). As ligands for nuclear retinoic acid receptors (RAR α , β , or γ) and retinoid X receptors (RXR α , β , or γ), retinoids regulate the expression of sets of overlapping genes involved in the regulation of cell proliferation, differentiation, and apoptosis (34–36). *all-trans*-Retinoic acid, binding to RAR α , β , or γ , and *9-cis* retinoic acid, binding to either RAR α , β , or γ or RXR α , β , or γ , promote the heterodimerization of these receptors and facilitate the binding of the heterodimeric complex to specific response elements (RAREs) in the promoter regions of retinoic-acid-responsive genes. This binding is believed to facilitate the recruitment of the components of the basal transcription complex to the promoter and promote chromatin remodeling required for the onset of transcription. While these events may by themselves lead to partial suppression of some solid tumors, in most examples studied, retinoids showed more potential when used in combination with DNA-damaging chemotherapies such as cisplatin, etoposide, and 5-fluorouracil (37–39). A synergistic activity between retinoids and cisplatin has been observed only when retinoid treatment preceded cisplatin treatment, and this correlated with a 1.5-fold increase in cisplatin adduct content of DNA without a change in cisplatin uptake (39). These data suggest that retinoid treatment induces an event or events that directly enhance cisplatin cytotoxicity and are consistent with the possibility suggested by our data that retinoids may generate cisplatin-hypersensitive structures that contribute to an enhanced response to cisplatin.

These data implicate chromatin organization as a component influencing the toxicity of cisplatin and add further support to a growing body of evidence pointing to the transcription process as a target for cisplatin mediated cytotoxicity. Cisplatin adduct formation may disrupt transcription through several mechanisms, including the following. (a) Cisplatin adducts may generate inappropriate binding sites for transcription factors and chromosomal proteins with HMG domains, titrating them away from their natural sites (18). A variety of HMG-box chromosomal proteins involved in the transcription complex bind to cisplatin adducts (14–18). (b) Cisplatin may inhibit transcription factor binding to

certain promoters, as has been shown for a stably integrated mouse mammary tumor virus promoter-driven reporter gene (40). In this case, cisplatin treatment prior to hormonal induction prevented activation of the reporter gene and blocked recruitment of the transcription complex to the promoter. (c) By targeting GG dinucleotides, cisplatin may inhibit certain regulatory elements rich in strings of guanosines, leading to selective inhibition of such promoters (9, 10). (d) As suggested by our results, cisplatin may target a DNA structure generated in the active promoters of certain genes, such as the RAR β gene. Assembled on activated promoters may be some of the factors needed to trigger apoptosis, including the transcription factor p53. Of interest is the recent identification of HMG-1, which is known to bind to cisplatin adducts, as a specific activator of p53 (41).

The differential toxicities of various platinum drugs may therefore be related to their respective abilities to mimic or disrupt chromatin structures critical to transcription. Further studies will be required to determine to what extent the observations made in this study extend to other promoters and to other DNA damaging agents.

REFERENCES

- Loehr, P. J., and Einhorn, L. H. (1984) *Ann. Intern. Med.* **100**, 704–713.
- Eastman, A. (1986) *Biochemistry* **25**, 3912–3915.
- Pinto, A. L., and Lippard, S. J. (1985) *Proc. Natl. Acad. Sci. U.S.A.* **82**, 4616–4619.
- Howle, J. A., and Gale, G. R. (1970) *Biochem. Pharmacol.* **19**, 2757–2762.
- Chu, G. (1994) *J. Biol. Chem.* **269**, 787–790.
- Heiger-Bernays, W. J., Essigmann, J. M., and Lippard, S. J. (1990) *Biochemistry* **29**, 8461–8466.
- Sorenson, C. M., and Eastman, A. (1988) *Cancer Res.* **48**, 4484–4488.
- Sorenson, C. M., and Eastman, A. (1988) *Cancer Res.* **48**, 6703–6707.
- Gralla, J. D., Sasse-Dwight, S., Poljak, L. G. (1987) *Cancer Res.* **47**, 5092–5096.
- Buchanan, R. L., and Gralla, J. D. (1990) *Biochemistry* **29**, 3436–3442.
- Evans, G. L., and Gralla, J. D. (1992) *Biochem. Biophys. Res. Commun.* **184**, 1–8.
- Evans, G. L., and Gralla, J. D. (1992) *Biochem. Pharmacol.* **44**, 107–119.
- Takahara, P. M., Rosenzweig, A. C., Frederick, C. A., and Lippard, S. J. (1995) *Nature* **377**, 649–652.
- Yaneva, J., Leuba, S. H., van Holde, K., and Zlatanova, J. (1997) *Proc. Natl. Acad. Sci. U.S.A.* **94**, 13448–13451.
- Pil, P. M., and Lippard, S. J. (1992) *Science* **256**, 234–237.
- Billings, P. C., Davis, R. J., Engelsberg, B. N., Skov, K. A., Hughes, E. N. (1992) *Biochem. Biophys. Res. Commun.* **188**, 1286–1294.
- Bruhn, S. L., Pil, P. M., Essigmann, J. M., Housman, D. E., and Lippard, S. J. (1992) *Proc. Natl. Acad. Sci. U.S.A.* **89**, 2307–2311.
- Treibler, D. K., Zhai, X., Jantzen, H.-M., and Essigman, J. M. (1994) *Proc. Natl. Acad. Sci. U.S.A.* **91**, 5672–5676.
- Bellon, S. F., Coleman, J. H., and Lippard, S. J. (1991) *Biochemistry* **30**, 8026–8035.
- Zlatanova, J., Yaneva, J., and Leuba, S. H. (1998) *FASEB J.* **12**, 791–799.
- Bohr, V. A. (1991) *Carcinogenesis* **12**, 1983–1992.
- Rampino, N. J., and Bohr, V. A. (1994) *Proc. Natl. Acad. Sci. U.S.A.* **91**, 10977–10981.
- Jennerwein, M. M., and Eastman, A. (1991) *Nucleic Acids Res.* **19**, 6209–6214.
- Sheibani, N., and Eastman, A. (1990) *Cancer Lett.* **52**, 179–185.

25. Scanlon, K. J., and Kashani-Sabet, M. (1988) *Proc. Natl. Acad. Sci. U.S.A.* **85**, 650–653.
26. Pedersen, A. G., Baldi, P., and Chauvin, Y. (1998) *J. Mol. Biol.* **281**, 663–673.
27. Baldi, P., Brunak, S., Cauvin, Y., and Krogh, A. (1996) *J. Mol. Biol.* **263**, 503–510.
28. Liu, K., and Stein, A. (1997) *J. Mol. Biol.* **270**, 559–573.
29. Van der Vliet, P. C., and Verrijzer, C. P. (1993) *Bioessays* **15**, 25–32.
30. Huang, M. E., Ye, Y. C., and Chen, S. R. (1988) *Blood* **72**, 567–572.
31. Redfern, C. P., Lovat, P. E., Malcolm, A. J., and Person, A. D. (1995) *Eur. J. Cancer* **31A**, 486–494.
32. Anzano, M. A., Byers, S. W., Smith, J. M., Peer, C. W., Mullen, L. T., Brown, C. C., Roberts, A. B., and Sporn, M. B. (1994) *Cancer Res.* **54**, 4614–4617.
33. Gottardis, M. M., Lamph, W. W., Shalinsky, D. R., Wellstein, A., and Heyman, R. A. (1996) *Breast Cancer Res. Treat.* **38**, 85–96.
34. Breitman, T., Selonic, S., and Collins, S. (1980) *Proc. Natl. Acad. Sci. U.S.A.* **77**, 2936–2940.
35. Sporn, M., and Robert, A. (1984) *J. Natl. Cancer Inst.* **73**, 1382–1387.
36. Martin, S., Bradley, J., and Cotter, T. (1990) *Clin. Exp. Immunol.* **79**, 448–453.
37. Sacks, P. G., Harris, D., and Chou, T.-C. (1995) *Int. J. Cancer* **61**, 409–415.
38. Guchelaar, H. J., Timmer-Bosscha, H., Dam-Meiring, A., Uges, D. R., Oosterhuis, J. W., de Vries, E. G., and Mulder, N. H. (1993) *Int. J. Cancer* **55**, 442–447.
39. Caliaro, M. J., Vitaux, P., Lafon, C., Lochon, I., Nehme, A., Valette, A., Canal, P., Bugat, R., and Jozan, S. (1997) *Br. J. Cancer* **75**, 333–340.
40. Mymryk, J. S., Zaniewski, E., and Archer, T. K. (1995) *Proc. Natl. Acad. Sci. U.S.A.* **92**, 2076–2080.
41. Jayaraman, L., Moorthy, N. C., Murthy, K. G., Manley, J. L., Bustin, M., and Prives, C. (1998) *Genes Dev.* **12**, 462–472.

BI991079R

SENSITIZATION OF TUMORS TO CHEMOTHERAPY THROUGH GENE THERAPY

Ruth A. Gjerset and Dan Mercola

Sidney Kimmel Cancer Center
10835 Altman Row
San Diego, California 92121

1. INTRODUCTION

The cellular response to DNA damage plays a critical role not only in tumor progression but also in the process of acquired drug resistance, a problem that affects about half of all cancer cases overall and remains one of the major obstacles to successful therapy of cancer. Modulation of these DNA damage response pathways may therefore provide us with a means to reverse acquired drug resistance and improve the outcome of therapy for a large fraction of cancer patients. In this article we will focus on two major pathways involved in the cellular response to DNA damage: The Jun kinase stress activated pathway, and the p53-mediated DNA damage response pathway leading to apoptosis. Through independent mechanisms, each of these pathways modulates the cellular response to DNA damaging chemotherapies and radiation. Therapeutic approaches based on inhibiting the Jun kinase pathway and/or restoring the p53 pathway may, therefore, provide us with new biological strategies for reversing acquired drug resistance, thus improving the outcome of therapy for most cancers.

2. THE p53 TUMOR SUPPRESSOR AND THE DNA DAMAGE RESPONSE

Over half of all cancers suffer loss of function of the p53 tumor suppressor (Levine, 1993), a key player in the induction of apoptosis in response to DNA damage (Clarke *et al.*, 1993; Gjerset *et al.*, 1995; Lotem *et al.*, 1993; Lowe *et al.*, 1993), in addition to its roles in cell cycle regulation and DNA repair (Levine, 1997). Its involvement in DNA damage-induced apoptosis may derive from its ability to bind, alone or possibly in combination with other DNA damage recognition proteins, to sites of damaged DNA, including single stranded ends and insertion-deletion loops (Bakalkin *et al.*, 1995; Lee *et al.*, 1995; Levine 1997 (review)). p53 might also bind to DNA adducts and strand breaks induced by various therapies. The frequent loss of p53 function in

cancer, often associated with disease progression and increased genomic instability, may reflect at least in part the role of p53 in DNA damage recognition and apoptosis. Most genome destabilizing events, including gene amplification, gene deletion and gene translocation, involve DNA strand breaks (Stark, 1993). These breaks could serve as triggers for p53-mediated apoptosis and provide the driving force for loss of p53.

The same process that underlies the progression of cancer, that is, genomic instability accompanied by loss of p53-mediated apoptosis, can also lead to therapy resistance. Support for the idea that loss of p53 could desensitize a cell to the damaging effects of drugs and radiation comes from studies of p53-null transgenic mice. In these studies it was observed that normal transgenic hematopoietic cells (Lotem and Sachs, 1993), E1A-expressing transgenic fibroblasts (Lowe *et al.*, 1993), and transformed transgenic fibroblasts (Lowe *et al.*, 1994) were all more resistant to apoptosis following treatment with any of a wide variety of anti-cancer agents including radiation, than were the comparable cells from the parental strain of mice that express wild-type p53. Cell killing was therefore enhanced in cells that expressed wild-type p53 and were able to trigger their own cell death program.

The possibility that p53 status is a factor in therapy responsiveness finds further support from a recent anti-cancer drug screening of human tumor cell lines expressing mutant or wild-type p53 (O'Connor *et al.*, 1997). In that study the growth inhibitory properties of some 123 anti-cancer agents were tested in 60 human tumor lines of known p53 status. It was found that cells expressing mutant p53 showed less growth inhibition than did wild-type p53-expressing cell lines following treatment with the majority of clinically used anti-cancer agents, including DNA cross-linking agents such as cisplatin, antimetabolites such as 5-fluorouracil, and topoisomerase I and II inhibitors. Since these agents are known to cause DNA damage, either directly or indirectly, these results are consistent with a role of p53 in mediating the cellular apoptotic response to DNA damage. One class of agents, the antimitotic agents, appeared to suppress growth in a p53-independent manner, consistent with the primary target for these agents being the mitotic apparatus rather than DNA.

Taken together, these studies suggest that p53 gene transfer could have clinical application in suppressing cancer and enhancing the responsiveness of tumors to a wide variety of DNA damaging therapies, a possibility that greatly expands the clinical application of p53-based approaches. Numerous *in vitro* studies in a variety of tumor cell systems support the use of p53 gene transfer to sensitize tumors to such therapy, including, 5-fluorouracil, cisplatin, topoisomerase I inhibitors and gamma radiation (see below).

2.1. *In Vitro* Sensitization of Tumor Cells to Chemotherapeutic Drugs by p53

In Figs. 1 and 2 we have summarized the results of screening tumor cells for sensitivity to various chemotherapeutic agents following exposure of cells to a replication-defective adenovirus encoding wild-type p53 (Ad-p53, Ad- β gal, and Ad-Luc (luciferase) vectors provided by Dr. Deborah R. Wilson, Introgen Therapeutics, Inc.). The cells were treated with virus under conditions which achieve about 70–80% infection efficiency, as judged by infection of parallel cultures with a β -galactosidase adenovirus. Following infection, cells were replated at low density in 96-well plates and treated with varying levels of chemotherapeutic agent, followed by an additional 5–7 days of incubation and measurement of cell viability.

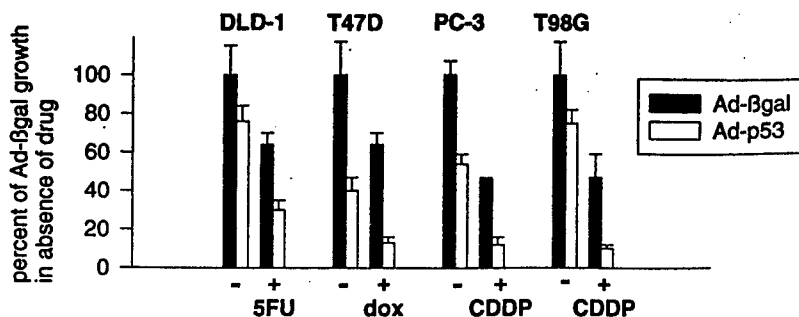


Figure 1. Viability assay showing that Ad-p53 suppresses growth and enhances sensitivity to DNA damaging chemotherapeutic drugs in p53-mutant-expressing cells (DLD-1 colon cancer, T47D breast cancer, PC-3 prostate cancer, and T98G glioblastoma). Infection efficiencies were 60–70% and drug treatments 1 day post-infection were as follows: 5-fluorouracil (5FU) 10 μM 1 hour; doxorubicin (dox) 3.7 μM 1 hour; cisplatin (CDDP) 30 μM 1 hour for PC-3 and 20 μM 1 hour for T98G. Viability was assayed 6 days post drug treatment in all cases except PC-3 which was 4 days post drug treatment, and expressed as a percent of control cells treated with Ad-βgal.

In numerous examples from a variety of cancer types, we have observed suppression of mutant-p53-expressing tumor cells *in vitro* following treatment with Ad-p53. As shown in Fig. 1, restoration of wild-type p53 in mutant p53-expressing cells (DLD-1, T47D, PC-3, T98G) results in marked enhancement of sensitivity to a variety of DNA damaging treatments (5-fluorouracil, doxorubicin, cisplatin), consistent with possibility that we have restored the p53-mediated pathway of DNA damage recognition and apoptosis. Apoptosis was confirmed by (a) propidium iodide staining of fixed cells followed by FACS analysis to reveal a sub G1 peak of apoptotic cells, and (b) an ELISA assay (Boehringer Mannheim Corp, Indianapolis, IN) to detect oligonucleosomal fragments released from the nuclei of cells in the early phases of apoptosis (see Gjerset *et al.*, 1995).

In contrast, this enhancement of sensitivity is not observed in two wild-type p53-expressing cell lines, MCF7 and LS174T (Fig. 2). This suggests that wild-type p53 gene transfer may be effective in therapy sensitization only in the case of tumors that have lost wild-type p53 function.

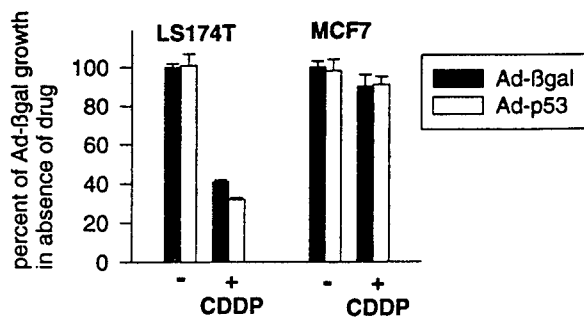


Figure 2. Viability assay showing that Ad-p53 neither suppresses growth nor enhances sensitivity to DNA damaging chemotherapeutic drugs in wild-type p53-expressing cells (LS174T colon cancer cells and MCF7 breast cancer cells). Infection efficiencies were 60–70%, and drug treatments 1 day post-infection were 30 μM cisplatin (CDDP) 1 hour for LS174T and 20 μM 1 hour for MCF7. Viability was assayed 6 days post drug treatment.

2.2. *In Vivo* Sensitization of Tumors to Chemotherapeutic Drugs by p53

We have extended our *in vitro* observations on tumor suppression and therapy sensitization to *in vivo* models for human head and neck cancer and colon cancer (Gjerset *et al.*, 1997) and prostate cancer (Fig. 3) in nude mice, where established tumors were treated *in vivo* with replication-defective p53 adenovirus, and chemotherapy. We have also studied chemosensitization by p53 using *ex vivo* modified cells in an orthotopic model of glioblastoma in Fisher rats (Dorigo *et al.*, 1998). The results are consistent with other *in vivo* studies in animal models showing a combined benefit of p53 and chemotherapy (Badie *et al.*, 1998; Fujiwara *et al.*, 1994; Miyake *et al.*, 1998; Nielsen *et al.*, 1998; Nguyen *et al.*, 1996). Together with the *in vitro* data, these results support the clinical application of adenovirus p53 combination approaches to tumors expressing mutant p53. In the experiment shown in Fig. 3, PC-3 prostate cancer cells which express mutant p53, were implanted in 20 nude mice (5×10^6 cells/animal) where they form rapidly growing subcutaneous tumors. At 5 days post-implantation, when tumor sizes had obtained a volume of about 50 mm^3 , animals were randomized by tumor size and treatment was initiated. The first day of treatment was then designated day 1 and consisted of intraperitoneal injection of cisplatin (PlatinolTM, Bristol Laboratories, obtained through local pharmacies), at 4 mg/kg (LD10) on days 1 and 8. Vector (Ad-p53 or Ad-luc control) was administered intratumorally (10^8 pfu per tumor) of days 1, 3, 5, 8, and 10. In both cases, some suppression was observed with Ad-p53 alone, with a significant enhancement of suppression when Ad-p53 was combined with chemotherapy. The vector doses used here

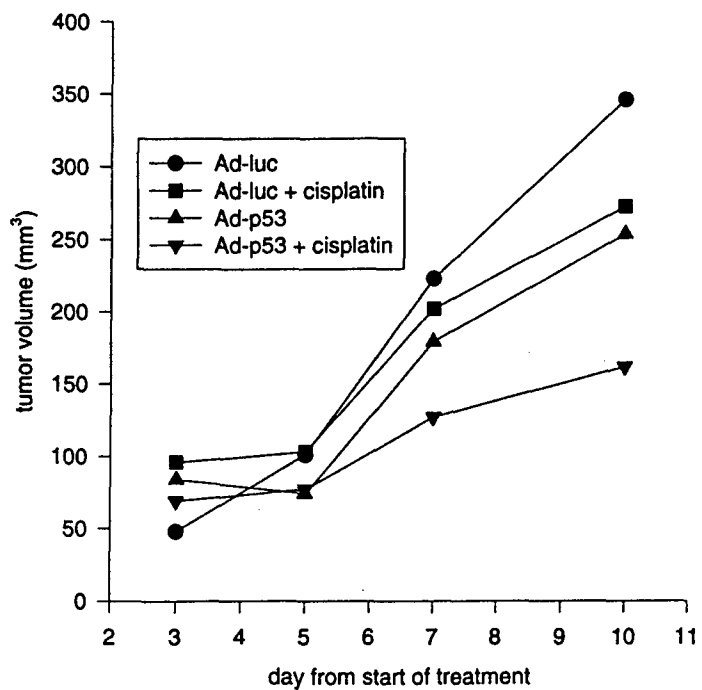


Figure 3. Suppression of PC-3 prostate tumor growth in nude mice by Ad-p53 plus cisplatin. Vector (10^8 pfu per tumor) was administered on days 1, 3, 5, 8, 10, and cisplatin was administered on days 1, 8.

were relatively low (10–30 pfu per tumor cell) and completely without side effects (as judged by periodic weight measurements on the animals and histological examination). We observe little or no toxicity in nude mice of vector doses as high as 10⁹ pfu per animal (Gjerset *et al.*, 1997). Phase I clinical trials employing p53 adenovirus also demonstrate that this vector is well tolerated in patients (Roth *et al.*, 1998). Thus restoration of wild-type p53 function through gene therapy may provide a significant benefit for patients with advanced cancers, when used in combination with conventional therapies.

3. THE JUN KINASE/STRESS-ACTIVATED PROTEIN KINASE PATHWAY AND THE DNA DAMAGE RESPONSE

Another important cellular pathway is also triggered in response to DNA damage: the Jun Kinase/Stress-activated protein kinase pathway (JNK/SAPK), one of several distinct Mitogen-Activated Protein Kinase (MAPK) Pathways involved in signal transduction. Besides its role in the DNA damage response (discussed below), the JNK/SAPK pathway is also induced by growth factors such as EGF-1(Bost *et al.*, 1999), by oncogene expression (Binétruy *et al.*, 1991), and is essential for transformation of rat embryo fibroblasts (Smeal *et al.*, 1991). As we show below, inhibition of this pathway enhances sensitivity to DNA damaging therapies in both p53 mutant and p53 wild-type tumors, as T98G glioblastoma cells, PC-3 prostate cancer cells, and U87 glioblastoma cells which express mutant p53, and MCF7 breast cancer cells which express wild-type p53, are all sensitized to various DNA damaging treatments by expression of a dominant-negative inhibitor of the pathway. Thus it may be possible to modulate this pathway by itself or in combination with p53 gene replacement to enhance tumor cell responsiveness to DNA damaging chemotherapies.

The Mitogen Activated Protein Kinase (MAPK) pathways play roles in several cellular processes, including cellular transformation, proliferation, differentiation, and the DNA damage response. Through these pathways extracellular growth and stress stimuli transmit signals through a cascade of kinases and phosphorylation events that result in the phosphorylation and activation of transcription factors such as c-Jun (a heterodimeric component of the AP-1 complex and related transcription complexes), ATF-2 and Elk-1 (Bost *et al.*, 1997; Cavigelli *et al.*, 1995; Dérijard *et al.*, 1994; Gupta *et al.*, 1995; Hibi *et al.*, 1993; Livingstone *et al.*, 1995; Potapova *et al.*, 1997; Smeal *et al.*, 1991, 1992). This phosphorylation activates the transcriptional transactivation properties of AP-1 and related factors and leads to the subsequent induction of specific response genes. The cascade of events begins with the activation of the Mitogen Activated Protein Kinase Kinase Kinases (MAPKKK), followed by activation of the Mitogen Activated Protein Kinase Kinases (MAPKK), and finally activation of the Mitogen Activated Protein Kinases (MAPK), of which the Jun Kinase family of enzymes (including JNK 1,2,3) is one example.

3.1. *In Vitro* Sensitization to Chemotherapeutic Drugs Through Inhibition of the JNK/SAPK Pathway

T98G glioblastoma cells activate the JNK/SAPK pathway in response to treatment with the chemotherapeutic agent, cisplatin (Potapova *et al.*, 1997), which forms bifunctional DNA cross links between adjacent guanines or adenine-guanine dinucleotides. This

is consistent with numerous other reports in which activation of the JNK/SAPK pathway has been observed in response to genotoxic DNA treatments, including UV irradiation (Dérijard *et al.*, 1994, Adler *et al.*, 1995a, 1995b, 1996), ionizing radiation (Kharbanda *et al.*, 1995), the mutagens methylmethane sulfate (MMS), N-nitro-N'-nitroso-guanidine (MNNG) and numerous genotoxic chemotherapeutic agents such as Ara-C (1- β -D-Arabinofuranosylcytosine) (van Dam *et al.*, 1995; Kharbanda *et al.*, 1995). For several of these agents such as a UV-irradiation, the activation of the JNK/SAPK pathway is directly proportional to the number of DNA damaging events (Adler *et al.*, 1995a). Activation is often rapid, detectable within a few minutes. These characteristics have given rise to the hypothesis that the role of the JNK/SAPK pathway may be to mediate DNA repair (Potapova *et al.*, 1997).

To evaluate the role of JNK/SAPK activation in the cellular DNA damage response we selected clones of T98G cells modified to express a non-phosphorylatable mutant of c-Jun (T98G mJun), in which serines 63 and 73, the targets of Jun Kinase-mediated phosphorylation, have been replaced by alanines (Smeal *et al.*, 1991, 1992). These cells are therefore suppressed in JNK-mediated functions. We found that unlike control vector-modified cells (T98GLHCX) or wild-type c-Jun-modified cells (T98GcJun), both of which are highly resistant to cisplatin, the modified clones expressing mJun (T98GdnJun) showed a significant loss of viability following treatment with cisplatin (Fig. 4). Furthermore, the increase in cisplatin sensitivity correlated with the level of expression of mJun in several different clones (Fig. 5). We observed a similar increase in sensitivity to cisplatin in MCF7 breast cancer cells, in PC-3 prostate cancer cells, and in U87

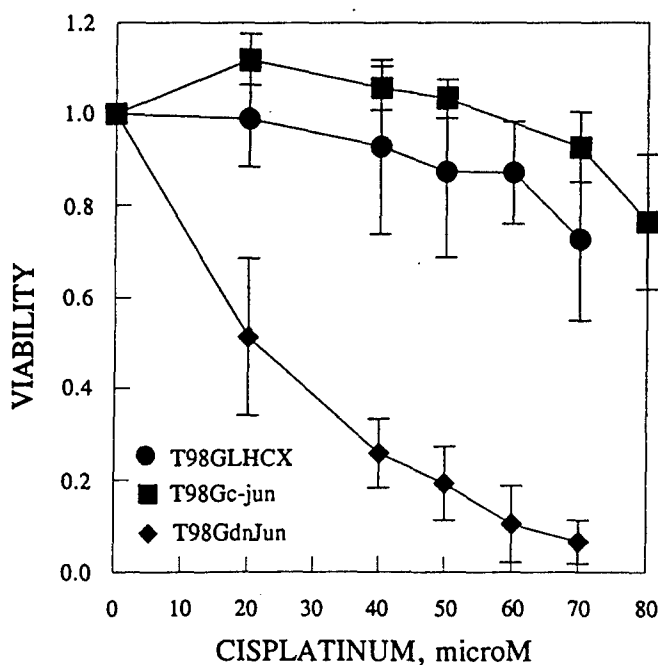


Figure 4. Viability assay showing that mutant Jun sensitizes T98G cells to cisplatin. Viability was assayed 5 days following a 1 hour treatment with cisplatin. Empty vector control cells (●); wild-type c-Jun-expressing cells (■); and mutant Jun-expressing cells (◆).

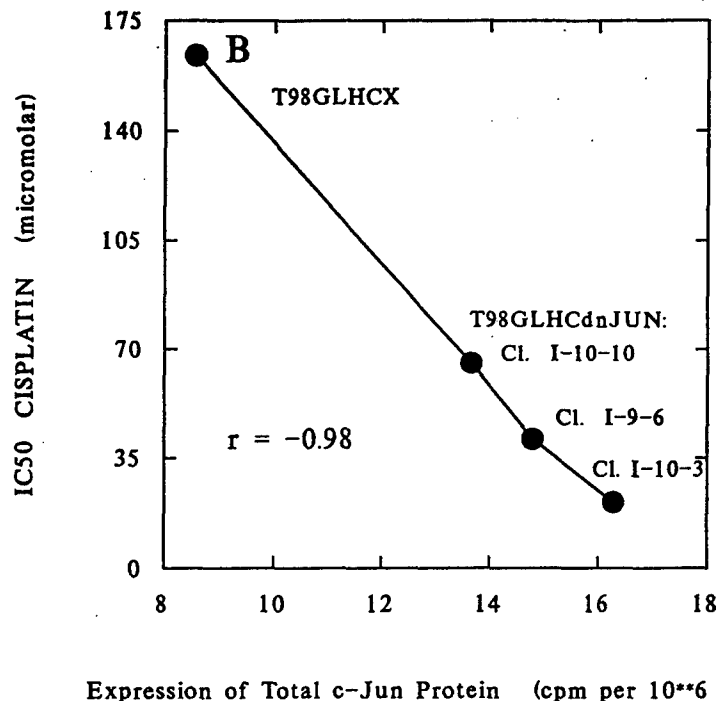


Figure 5. Dose response curve of the IC_{50} (cisplatin) versus total immunoreactive Jun (c-Jun + mutant Jun). Total immunoreactive Jun was determined by sequential immunoprecipitation of ^{35}S -labeled cells using specific Jun B, Jun D, followed by pan-Jun antiserum.

glioblastoma cells that were modified with the non-phosphorylatable mJun (not shown). We also observed enhanced sensitivity to cisplatin in cells modified with the TAM67 mutant of c-Jun (not shown). Tam67 has a truncated N-terminal domain and is known to be a dominant negative inhibitor of c-Jun phosphorylation (Grant *et al.*, 1996). However, we did not observe in mJun modified T98G cells nor in mJun modified PC-3 cells an increase in sensitivity to the anti-mitotic agent, taxotere™ (kindly provided by Dr. Pierre Potier, Centre Nationale de la Recherche Scientifique, Paris), whose primary target is the mitotic spindle rather than DNA (Fig. 6). Taken together these results argue that the JNK/SAPK pathway plays a role in resistance to DNA damaging agents but not to agents that do not damage DNA, and that inhibition of this pathway could be a means to reverse resistance to DNA damaging therapies used in cancer treatment.

3.1.1. Inhibition of DNA Repair by Inhibition of the JNK/SAPK Pathway. T98G clones modified to express mutant Jun are compromised in repair of cisplatin-DNA adducts (Potapova *et al.*, 1997), an observation that further supports the rationale for enhancing sensitivity to DNA damage through inhibition of the JNK/SAPK pathway. DNA repair is known to play a role in acquired resistance to DNA damaging chemotherapies (Barret and Hill, 1998; Crul *et al.*, 1997; Reed, 1998; Fink, Aebi and Howell, 1998; Saves and Masson, 1998; Scanlon, 1989). Furthermore, as summarized in Table 1, a number of the genes involved in DNA synthesis and repair are potentially regulated by the AP-1 transcription factor and related transcription factors targeted by the

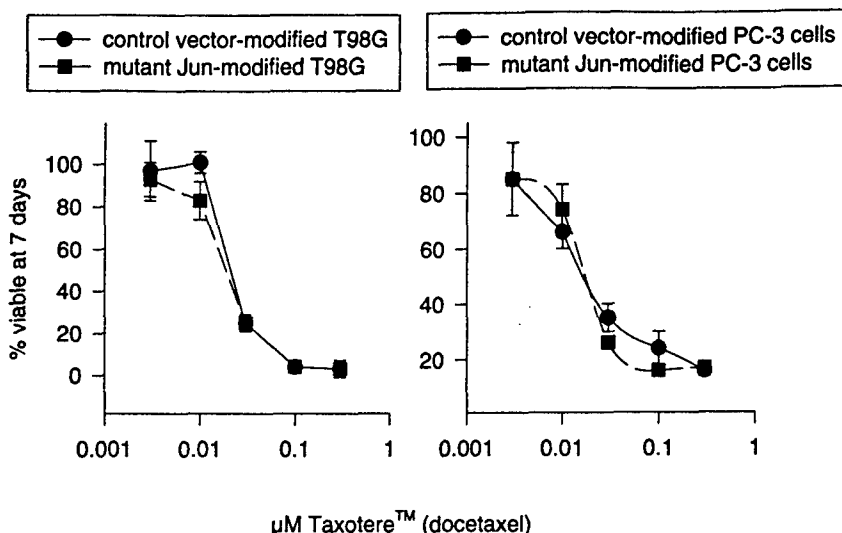


Figure 6. Viability assay showing that mutant Jun does not sensitize T98G cells to Taxotere™. Viability was assayed 7 days following a 1 hour treatment with Taxotere™.

JNK/SAPK pathway (i.e., c-Jun and ATF2, components of AP-1 and c-Jun-ATF2 heterodimeric transcription activating complexes, respectively). Furthermore, down regulation of AP-1 by treatment of cells with a c-fos antisense ribozyme, has previously been shown to correlate with down regulation of expression of certain of these enzymes (thymidylate synthetase, DNA polymerase β) and enhanced sensitivity to cisplatin (Scanlon *et al.*, 1991).

We analyzed DNA repair using a PCR-based assay developed by Jennerwein and Eastman (1991) based on their observations that DNA-cisplatin adducts block the progression of the Taq polymerase and lead to a decrease the yield of PCR product obtained from any given PCR amplicon in proportion to the extent of platination. The authors demonstrated that the relationship between the relative PCR signal strength (P) for a given amplicon from damaged versus undamaged templates, and overall platination level fits a Poisson distribution predicted from a random platination, so that $P = e^{-n}$, where $n = \text{adducts per amplicon-sized fragment}$.

We have used primers described by Oshita and Saijo (1994) to amplify a 2.7 Kb fragment of the human hypoxanthine phosphoribosyl transferase (HPRT) gene, a fragment large enough to sustain readily detectable levels of damage following cisplatin treatment of cells. As an internal control for the efficiency of the PCR reaction, we used a nested 5' primer which amplified a 150 base fragment of the same gene. At levels of cisplatin used to treat cells, damage to the smaller fragment was undetectable. PCR reactions were performed under quantitative conditions such that the extent of reaction remained directly proportional to amount of template. Figure 7 shows an example of PCR amplification of the 2.7 Kb fragment and the 150 base fragment from DNA prepared from T98G glioblastoma cells treated with 0, 100, and 200 μM cisplatin for 1 hour. Quantitation of band intensities was accomplished using Kodak digital camera and analysis software, and relative band intensity measurements were then used to calculate adducts per Kb based on the Poisson relationship described above.

Table 1. DNA REPAIR ASSOCIATED GENES WHICH CONTAIN POTENTIAL JNK-REGULATED SEQUENCES¹

Repair-associated gene	Element	Sequence (consensus sequence) ²	Position ³	LLG score	Reference for function
DNA Polymerase β	AP-1/TRE	CTGACTCA (tt g a c t c a)	337	2.0	Known to be functional and TPA-activated classic TRE (1).
	ATF/CREB	TTACGTAA (tt a c g t c a)	282	2.0	
DNA Polymerase α (26)	ATF/CREB	CACGTCA (t/g a c g t c a)	-82		Known to be genotoxic-activated (1, 9). Function of ATF/CREB (26) unknown.
		GGGGTCA (t g a g t c a)	-149		
Topoisomerase I	AP-1	GGGGGG (t g a g t c a)	753	2.0	(2-3)
	AP-1	TGACCCA (t g a c t c a)	217	2.0	
ATF/CREB		TGACGTCA (t g a c g t c a)	792	2.0	known to be functional & stress-activated (2-3).
		TGACGCCG (t g a c g t c a)	286	2.0	
Topoisomerase II α	ATF/CREB	TGATTTGG (t g a g t c a)	337	2.0	(10-11); Topo II is UV-inducible and functions early in UV-induced DNA damage repair.
	AP-1	TGACTCA (t g a c t c a)	3	2.0	
Topoisomerase II β	AP-1	AGAGTCA (t g a g t c a)	65	1.6	(12)
	AP-1	TGAGTAA (t g a c g t c a)	-1,600		
ATF-3	AP-1	ATAGTCA (t g a c g t c a)	-1,353		(13) ATF-3 is stress-induced, anisomycin (JNK activator) induced, and induced by ATF-2/c-Jun coexpression suggesting functional role for the ATF/CREB site. ATF-3/c-Jun heterodimers bind ATF/CREB sites and activate transcription (14-15) and ATF-3/c-Jun and ATF-3/JunD heterodimers have been shown to bind TTACGTAC, a ATF/CREB sequence, which mediates EGF/ras/raf-stimulated transcription (28), however, a role in induction of DNA repair genes is not known.
	AP-1	AGACTAA (t g a c g t c a)	-605		
ATF/CRE	AP-1	GAGTCA (t g a c g t c a)	-380		(28), however, a role in induction of DNA repair genes is not known.
		TTACGTCA-92 (t t a c g t c a)			

(continued)

Table 1. *Continued*

Repair-associated gene	Element	Sequence (consensus sequence) ²	Position ³	LLG score	Reference for function
<i>c-Jun</i>	ATF/CREB	TGACCTCA (t t a c g t c a)	141	2.0	(4-5); the "functional" association with DNA repair is strong induction of <i>c-Jun</i> by genotoxins known to activate JNK/SAPK
Uracil Glycosylase	AP-1	TGGGTCA (t g a c t c a)	489	2.0	DNA polymerase- α accessory protein function;
PCNA	AP-1	TGACTCA (t g a c t c a)	209	1.64	(7-8); IL-2, a potent JNK/SAPK activator, induces PCNA expression via ATF/CREB promoter sites which is blocked by rapamycin.
Proliferating Cell Nuclear Antigen	ATF/CREB	TGAGGTCAAGGG (t g a c g t c a - - -)	1,253	1.60	
ATF/CREB	ATF/CREB	GTGACGTCA C (- t t a c g t c a - - -)			
GADD153 (19)	ATF/CREB	ACTCCCTGACTT (t g/t a c g t c a - - -)	207	1.63	Induction requires phosphorylation-dependent event that is <i>not</i> PKA, PKC (16), or p38 (25) mediated consistent with a role for JNK/SAPK (16). Moreover GADD153 is induced by MMS (16) & cisplatin (17-18). The role of the ATF/CREB site is unknown. GADD153 is phosphorylated and activated by p38 in response to stress (25).
Growth Arrest and DNA-damage ⁴ , Inducible Gene	AP-1	TGACTCA (t g a c t c a)	710	2.0	
XRCCL (20)	ATF/CREB	ACGTCA (a c g t c a)	1,815	2.0	The site at 466 is consistent with c-Jun/ATF-3 vs. ATF-2 (TESS).
X-ray Damage Repair Cross Completing Gene Product.	ATF/CREB	GGACGTCAA (t g a c g t c a)	1,814	2.0	
	ATF/CREB	CCTGACCTCA (- t g a c g t c a)	2,029	1.64	Functional roles of these ATF/CREB and AP-1 sites are not known <i>zzzz</i> .
	ATF/CREB	GCTGACGTCA G (- t g a c g t c a -)	466	1.60	
		CCAATCA (t g/t a c g t c a)	93	2.0	

MGMT (22)	ATF/CREB	TGGGTCA (t g a c g t c a) GTGACATCAT (t g a c t c a -)	1,661	2.0
O6-Methylguanine-DNA-Methyl-transferase	ATF/CREB	TGAGTCA (t g a g t c a) TTACTCA (t t a c t c a)	1,195	
	AP-1		734	2.0
	AP-1		285	1.73
MSH2 (23)	ATF/CREB	TGGCGTCA (t g a c t c a) TGAAATCA (t g a c g t c a) TGATGAAA (t g a c g t c a)	108	1.62
	AP-1		569	2.0
	AP-1		884	1.62
Metallothionein IIA	AP-1	GAGCCGCAAGT (g a g t c a - - - t) GACTTCTAGCG g a c t c a a g t c CGGGCGTG a - - - - t g)	188	2.0
				(6); TPA and UV-light activated

¹Repair associated protein for which only partial promoter sequences are known (i.e. in Genbank) without recognizable AP-1 regulated sites include ADP ribose polymerase, tif2/refl, SSRP, Ercel and thymidylate synthetase.

²AP-1 consensus: TG/TAC/GTC; CREB/ATF-2 consensus: TG/TACGTCA.

³Positions are based on TESS numbering of promoter sequences unless preceded by (-).
 References: 1. Srivastava *et al.* J. Biol. Chem., 1995;270:16408. 2. Baumgärtner *et al.*, Biochim. Biophys. Acta, 1994;1218:123. 3. Heiland *et al.*, Eur. J. Biochem., 1993;217:813. 4. Kharbanda *et al.*, Canc. Res., 1991;51:6636. 5. Kharbanda *et al.*, J. Clin. Inv., 1990;86:1517. 6. Lee *et al.*, Nature, 1987;325:358. 7. Feuerstein N, *et al.*, J. Biol. Chem., 1995;270:9454. 8. Huang D, *et al.*, Molec. Cell. Biol., 1994;14:4233; 9. Kedar *et al.*, PNAS USA, 88:3729. 10. Hochhauser D, *et al.*, J. Biol. Chem., 1992;26:187961-187965. 11. Popanda O, Thielmann H, W, Carcinogenesis, 1992;13:2321. 12. Unpublished: Genebank Acc. #T29334, Inst. Genomics Res., 1995. 13. Liang *et al.*, J. Biol. Chem., 1996;271:1695. 14. Hsu, J.-C, *et al.*, Mol. Cell. Biol., 1992;12:4654. 15. Chu, H.-M, *et al.*, Mol. Endocrinol., 1994;8:59. 16. Luehy, J, and Holbrook, N, Cancer Res., 1994;54:19025. 17. Gately, D, *et al.*, Br. J. Cancer, 1994;70:1102. 18. Delmastro, D, *et al.*, Canc. Chemother. Pharmacol., 1997;39:245. 19. Park, J, *et al.*, Genes, 1992;16:259 (Acc. #S840707). 20. Lamerdin, J, *et al.*, Genomics, 1995;25:547 (Acc. #L34079). 21. Lefebvre, P, *et al.*, *Dna Cell Biol.*, 1993;12:233. 22. Iwakuma, T, *et al.*, DNA Cell Biol., 1996;15:863. 23. Seib, T, *et al.*, Gene Bank direct submission Acc. #U232824. 24. Leach, F, *et al.*, Cell, 1993;75:1215. 24. Kolodner, R, *et al.*, Genomics, 1994;24:515. 24. Mello, J, *et al.*, Chem. Biol., 1996;3:579. 25. XiaoZhong, W, and Ron, D, Science, 1997;272:1347-1349. 26. Pearson, B, *et al.*, Molec. Cell. Biol., 1991;11:2081. 27. Scanlon, K, *et al.*, PNAS USA, 1994;91:11123. 28. Nilsson *et al.*, *Cell Growth & Diff.*, 1997;8:913.

Abbreviations: L.I.G. Log likelihood score which is 2 for a perfect match of the candidate response element with the consensus sequence (TESS criteria) and all ambiguous matches yield a score of 0; AP-1, activator protein-1 complex, a Jun and a Fos family member; CREB/ATF, cAMP response element binding proteins, N-terminal phosphorylated c-Jun and N-terminal phosphorylated ATF-2 for a cAMP-independent complex which bind the CRE-like sequence TTACGTCA. XRCC, MMS, methyl methanesulfonate.

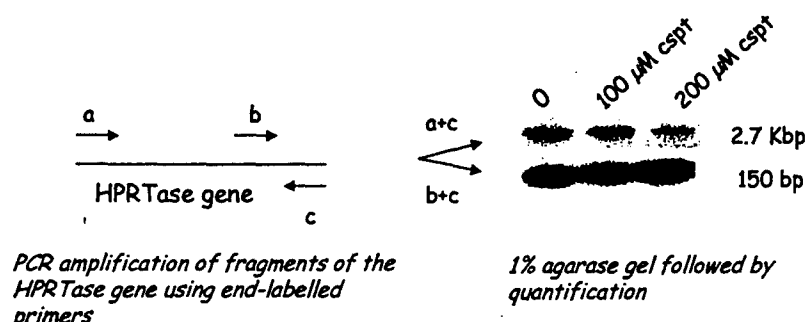


Figure 7. PCR amplification of DNA from T98G cells that had been incubated 1 hour with 0, 100 μM , and 200 μM cisplatin. Products were analyzed on an agarose gel and stained with ethidium bromide, followed by quantitation of band intensities using the Electrophoresis Documentation and analysis System 120 (Kodak Digital ScienceTM).

Table 2 summarizes the cisplatin adducts per Kb observed on DNA from T98G glioblastoma cells treated for 1 hour with 200 μM cisplatin and then harvested either immediately or after a 6 hour recovery period. As shown in the table, cisplatin adducts occur at greater frequency in DNA from T98G mutant Jun expressing cells than in DNA from parental T98G cells. Furthermore, parental T98G cells repair more than half of the adducts during the 6 hour recovery period, whereas little repair occurs in T98G mJun cells during that period of time. Thus the increase in cisplatin sensitivity observed in T98G mJun cells can be accounted for at least in part by a defect in their ability to repair damaged DNA.

3.2. Mechanism of Action of JNK/SAPK in DNA Repair

How might the activation of JNK by genotoxic stress affect DNA repair? The answer to this question is not known in any detail, but a number of observations point to several testable hypotheses. It was noted that the promoters of certain genes known to be involved in carrying out cisplatin-DNA adduct repair contain AP-1-like or ATF2/CREB regulatory elements (section 3.1.1). The repair of DNA-cisplatin adducts is believed to require the nucleotide-excision repair process (Reed, 1998). In addition, a number of enzymes utilized for DNA synthesis are reported to be involved (reviewed in Zamble and Lippard, 1995). These included DNA polymerase β , topoisomerase I, topoisomerase II, uracyl glycosylase, PCNA, metallothioneine and others (Table 1, and references therein). In each case the promoter regions contains one or more AP-1

Table 2. Cisplatin-DNA adducts per 2.7 KBASE

Treatment	T98G parental cells	T98G mutant jun cells
200 μM cisplatin 1 hour	0.48 \pm 0.08	0.63 \pm 0.2
200 μM cisplatin 1 hour, 6 hour recovery	0.20 \pm 0.05	0.55 \pm 0.2

or ATF2/CREB regulatory sequences. In several cases such as DNA polymerase beta, genotoxic stress in the form of UV-irradiation is known to induce the gene and that the ATF2/CREB sites are required for this event (Table 1 and references therein). Moreover, the N-terminal phosphorylation of c-Jun and ATF2 by the action of Jun Kinase leads to increased DNA binding and transactivation potential of heterodimeric complex formed by phosphorylated c-Jun and ATF2. Indeed, the c-Jun promoter itself is one of the better studied example of a gene that is up-regulated upon binding of the c-Jun-ATF2 heterodimer (van Dam *et al.*, 1995; Wilhelm *et al.*, 1995). N-terminal phosphorylation of both c-Jun and ATF2 is required for the activation of the c-jun gene (van Dam *et al.*, 1995; Wilhelm *et al.*, 1995). Other examples of gene that are up-regulated upon formation of c-Jun-ATF2 heterodimers include the ELAN promoter (De Luca, *et al.*, 1994) and the TNF-alpha promoter (Newell *et al.*, 1994). Thus, there is circumstantial evidence supporting the hypothesis that activation of the Jun Kinase pathway by genotoxic stress leading to the phosphorylation of both ATF2 and c-Jun and thereby causing preferential formation of ATF2-c-Jun heterodimers. These complexes preferentially bind promoters containing octomeric ATF2/CREB regulatory elements. This hypothesis predicts that several of the genes known to be involved in cisplatin-DNA adduct repair may be coordinately upregulated upon activation of the JNK pathway following damage to DNA by cisplatin. If verified, such an explanation suggests that the JNK pathway is a potentially useful target for intervention and that agents that inhibit JNK activity or formation may be useful in achieving enhanced sensitivity of tumor cells to cisplatin.

3.3. JNK/SAPK Pathway with Antisense Approaches

The above observations argue that targeting the JNK/SAPK pathway could have potential as a sensitizer to a variety of DNA damaging chemotherapies, a possibility that we have investigated directly using antisense oligonucleotides to either JNK 1 or 2 family of JNK isoforms.

Antisense mechanisms result most likely from oligonucleotide-target mRNA hybrid formation in the nucleus which stimulates the cleavage of the mRNA at one or more sites near the terminus of the hybrid complex by ribonuclease H (Crooke, 1992, 1998; Dean *et al.*, 1996), as well as from cytoplasmic complexes which may lead to translation arrest (Crooke, 1992, 1998; Dean *et al.*, 1996). Because steady state mRNA levels do not always predict steady state gene product levels, we monitor the effects antisense by the fractional reduction of the gene product. An enzymatic assay that discriminates among the various isoforms of Jun Kinase can be used (Hibi *et al.*, 1993), as well as Western analysis or PAGE analysis following immunoprecipitation.

The appropriate oligonucleotide controls for antisense efficacy have been described in detail (Stein and Kreig, 1994), and include a sense sequence, scrambled sequence or random control oligonucleotides, and antisense sequences bearing one or a small number of mismatched bases, i.e. mismatched with respect to the complementary target sequence.

For our studies we have used antisense oligonucleotides complementary to the JNK1 or JNK 2 families of JNK isoforms by selecting target sequences common to the major isoforms of human JNK1 and JNK2. Phosphorothioate backbone chemistry has been used as this formulation is nuclease resistant, readily available and a common element of second generation compounds (Crooke, 1992, 1998; Dean *et al.*, 1996; McKay *et al.*, 1999).

In collaboration with ISIS Pharmaceuticals, Inc. (Carlsbad, CA) we have identified effective antisense oligonucleotides capable of entering and inhibiting specifically JNK1

or JNK2 mRNA expression in A549 lung cancer cells (Bost *et al.*, 1997, 1999). As an example of a screening for JNK1 and JNK2, Fig. 8 is included. As shown, most candidate oligonucleotides had only a small effect on the steady state level of JNK1 or JNK2 mRNA (Fig. 8). However, their degree of activity greatly varied depending on the targeted region (Fig. 8). Among the most potent oligonucleotides of the array complementary to JNK1 is ISIS 12539 (JNK1ASISIS12539) (5'-CTCTCTGTAGGCC-CGCTTGG-3') located in the 3' end of the coding region. Treatment with this oligonucleotide leads to a reduction of steady state mRNA level by 95% (Fig. 8A) as observed 24 hours after a 4 hour exposure of the cells to 0.4 μM antisense oligonucleotides. ISIS 12560 (JNK2ASISIS12560) (5'-GTCCGGGCCAGGCCAAAGTC-3'), located in the 5' end of the coding region of JNK2 genes, was the most efficient oligonucleotide in reducing JNK2 steady state mRNA levels. Lipofection with this oligonucleotide lead to a decrease in the steady-state JNK2 message level by 92% compared to the control JNK2 steady state mRNA level. The oligonucleotides targeted to the regions flanking either side of the sequences for JNK1ASISIS12539 and JNK2ASISIS12560 also inhibited JNK1 and JNK2 steady state mRNA but in a manner that decreased with increasing distance from the optimum sequence (Fig. 8A and B) suggesting that discrete regions of the target mRNA are accessible and sensitive to the antisense-mediated elimination of steady-state mRNA as previously described (Crooke, 1992, 1998).

Cross inhibition tests demonstrated isoform class specificity. As shown in Fig. 9, JNK1ASISIS12539 eliminates JNK1 mRNA and protein but does not affect JNK2 mRNA and protein and, conversely, JNK2ASISIS12560 has no effect on JNK1 mRNA and protein but abolishes JNK2 mRNA and protein. In the northern analysis we describe an example where two other antisense oligonucleotides from the initial gene screening are less efficient in reducing mRNA steady-state levels of their respective target gene (Fig. 9). Similarly, western analysis shows that lipofections with the antisense oligonucleotides leads to complete elimination of their respective target steady state protein levels, whereas the scrambled sequence versions of the candidate oligonucleotides, JNK1Scr or JNK2Scr have no effect (Fig. 10). Thus effective and specific reagents can be obtained.

These reagents have been used to examine the growth promoting roles of the Jun Kinase pathway in human T98G glioblastoma cells (Potapova *et al.*, 1998), human A549 NSCLC cells (Bost *et al.*, 1997, 1999), and human PC3 prostate carcinoma cells (Yang *et al.*, 1998) and shown to specifically inhibit growth and, in the case of A549 cells, anchorage independent growth. Moreover, these reagents have been used in systemic treatment of established PC3 xenografts and shown to block growth and promote regression of the established tumors in high frequency (Bost *et al.*, 1998). In this case, growth inhibition by antisense treatment of 78% was superior to that of cisplatin treatment alone (47%), however the effects of combined antisense JNK-cisplatin of 89% inhibition was greater than either alone suggesting that, indeed, it may be possible to sensitize solid tumors to cisplatin by elimination of Jun Kinase. It will be of interest, therefore, to determine whether JNK is involved in a general mechanism utilized in other tumor cell lines and/or mediates DNA damage repair of other DNA-damaging agents.

4. CONCLUSIONS

These results have clinical implications with regard to the application of therapies designed to alleviate drug resistance. As tumors progress, particularly if they have been exposed to DNA damaging therapies, they may upregulate their DNA repair response

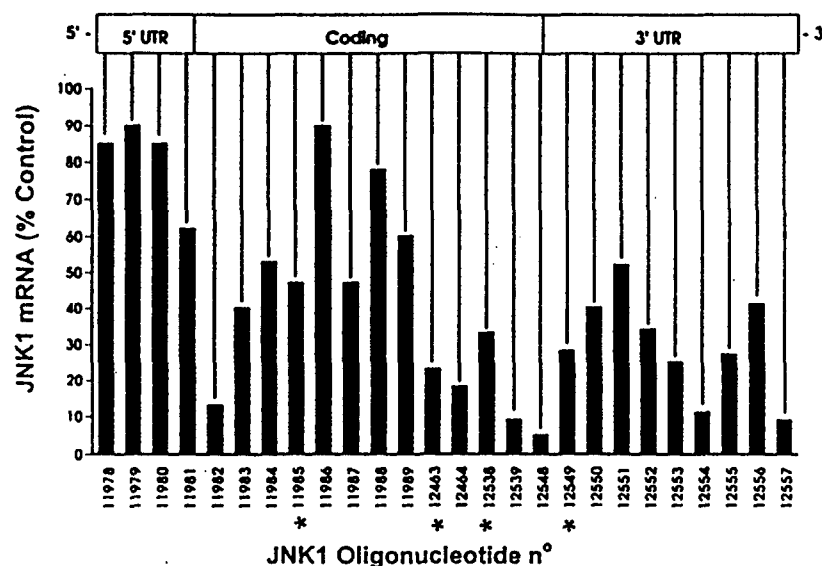
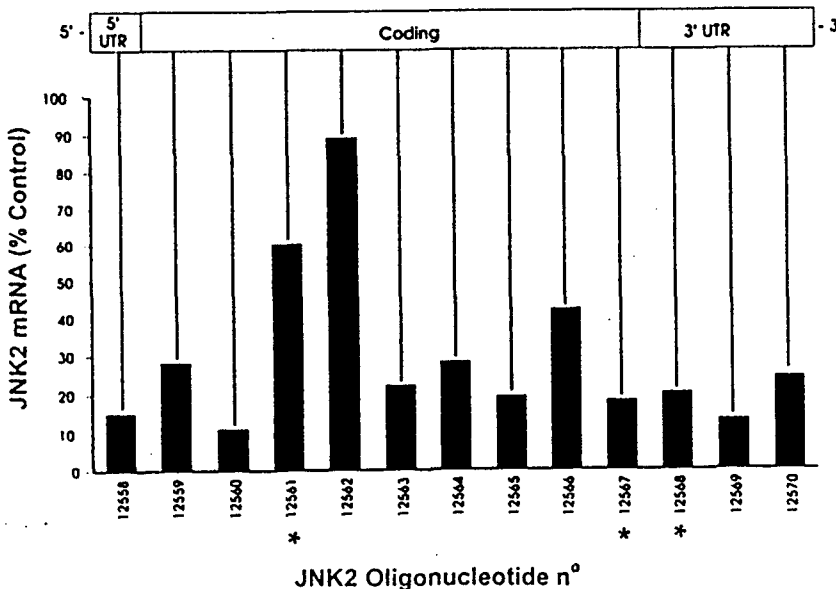
A**B**

Figure 8. "Messenger walk" survey for the elimination of JNK1 and JNK2 mRNA levels following treatment with phosphorothioate antisense oligonucleotides targeted to JNK1 or JNK2 mRNA. A, JNK1 mRNA steady state levels in A549 cells following treatment with 26 different phosphorothioate antisense oligonucleotides targeted to JNK1 mRNA. JNK1AS^{11979/12559} gave the most consistent results for the elimination of JNK1 mRNA steady state levels. B, Similar experiment to the previous one (Fig. 1A) was performed with 13 phosphorothioate antisense oligonucleotides complementary to the indicated regions of the JNK2 mRNA. JNK2AS^{12561/12560} yielded the most consistent results for the elimination of JNK2 mRNA steady state levels. All oligonucleotides are arrayed relative to their complementary sequence along the JNK transcript. The asterisks indicate the oligonucleotides having a very similar nucleotide composition (2–4 bases) to the leading compound. These screenings have been repeated two times with similar results.

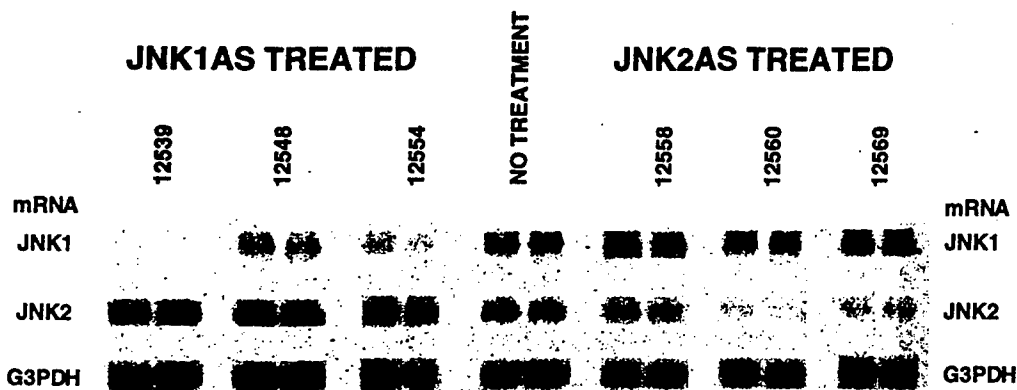


Figure 9. A549 cells were treated with 3 different antisense oligonucleotides complementary to JNK1 mRNA (including the active antisense oligonucleotide JNK1AS^{SIS12339}) and 3 different antisense oligonucleotides complementary to JNK2 mRNA (including the active antisense oligonucleotide JNK2AS^{SIS12560}). 24 hours after a 4 hours transfection with 0.4 μM antisense oligonucleotide, mRNA was prepared and examined by northern analysis, the same membrane was hybridized successively with JNK1 probe, JNK2 probe and the G3PDH probe.

(see Reed, 1998 for review), which may in part involve AP-1 regulated DNA synthesis and repair genes. Elevated c-fos expression, one component of the AP-1 transcription factor, correlates with cisplatin resistance (Scanlon *et al.*, 1991; Funato *et al.*, 1992) and may directly affect the synthesis of AP-1 regulated DNA synthesis and repair genes, such as polymerase β, topoisomerase I and thymidylate synthetase (Scanlon and Kashini-Sabet, 1998). Loss of DNA damage-induced apoptosis through loss of wild-type p53 expression also correlates with drug resistance (O'Connor *et al.*, 1997) and represents an independent mechanism through which tumors acquire resistance to therapy. Because the success or failure of DNA repair could be critical in determining how a cancer cell responds to expression of p53, it may be necessary, in optimizing the benefits of

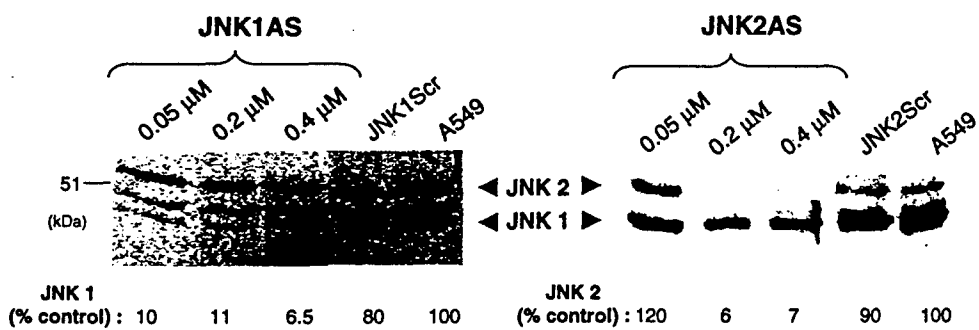


Figure 10. A549 cells were treated with the indicated concentration of phosphorothioate 2'-O-methoxyethyl-modified antisense oligonucleotides JNK1AS^{SIS15346} or JNK2AS^{SIS15353} and 0.4 μM of their respective control oligonucleotides JNK1Scr^{SIS18076} and JNK2Scr^{SIS18078}. Cell extracts were prepared 36 hours after the transfection and examined by western analysis using anti-JNK1 antibodies (SC-571). Protein level (below) was determined by comparison to respective protein level in untreated cells using the Electrophoresis Documentation and Analysis System 120 (Kodak Digital Science™).

p53-based approaches, to concurrently down-regulate the cellular stress and DNA damage response pathways such as the Jun Kinase pathway. Combination approaches targeting independently these two cellular responses to DNA damage can be foreseen today, and may provide an optimal strategy for reversing or alleviating drug resistance in advanced cancers.

ACKNOWLEDGMENTS

The authors would like to acknowledge financial support from the following grants CA69546 (RAG), CA56834 (DM), CA76173 (DM) from the National Cancer Institute, grant DAMD17-96-1-6038 from the U.S. Army Breast Cancer Research Program (RAG), grant 1PF0140 from the California Cancer Research Program (RAG), grant 83401 from the California Breast Cancer Research Program (DM), and Introgen Therapeutics, Inc. (RAG). The authors would also like to thank Drs. Fred Bost and Olga Potapova for making available to us manuscripts prior to publication. We thank Deborah Wilson, Ph.D. of Introgen Therapeutics, Inc. for providing us with replication recombinant adenoviruses (Ad-p53, Ad- β gal, Ad-Luc). We also thank R. McKay, Ph.D. and N. Dean, Ph.D. of ISIS Pharmaceuticals for their support and materials for the studies reviewed here.

REFERENCES

Badie, B., Kramar, M.H., Lau, R., Boothman, D.A., Economou, J.S., and Black, K.L., 1998, Adenovirus-mediated p53 gene delivery potentiates the radiation-induced growth inhibition of experimental brain tumors, *J. Neurooncol.* 37:217-222.

Bakalkin, G., Selivanova, G., Yakovleva, T., Kiseleva, E., Kashuba, E., Magnusson, K.P., Szekely, L., Klein, G., Terenus, L., and Wiman, K.G., 1995, p53 binds single stranded DNA ends through the C-terminal domain and internal DNA segments via the middle domain, *Nucl. Acids Res.* 23:362-269.

Barret, J.M., and Hill, B.T., 1998, DNA repair mechanisms associated with cellular resistance to antitumor drugs: potential novel targets, *Anticancer Drugs* 9:105-123.

Binetruy, B., Smeal, T., and Karin, M., 1991, Ha-ras augments c-Jun activity and stimulates phosphorylation of its activation domain, *Nature* 351:122-127.

Cavigelli, M., Dolfi, F., Claret, F.X., and Karin, M., 1995, Induction of c-fos expression through JNK-mediated TCF/Elk-1 phosphorylation, *EMBO J.* 14:5957-5964.

Chelliah, J., and Jarvis, W.D., 1996, Effect of 1-beta-D-arabinofuranosylcytosine on apoptosis and differentiation in human monocytic leukemia cells (U937) expressing a c-Jun dominant-negative mutant protein (TAM67), *Cell Growth Differ.* 7:603-613.

Clarke, A.R., Purdie, C.A., and Harrison, D.J., et al., 1993, Thymocyte apoptosis induced by p53-dependent and independent pathways, *Nature* 362:849-852.

Crooke, S.T., 1992, Therapeutic applications of oligonucleotides, *Annu. Rev. Pharmacol. Toxicol.* 32:329-376.

Crooke, S.T., 1998, Molecular mechanisms of antisense drugs: Rnase H, *Antisense Nucleic Acid Drug Dev.* 8:133-134.

Crul, M., Scheelens, J.H., Beijnen, J.H., and Maliepaard, M., 1997, Cisplatin resistance and DNA repair, *Cancer Treat Rev.* 23:341-366.

Dean, N.M., McKay, R., Miraglia, L., Geiger, T., Muller, M., Fabbro, D., and Bennett, C.F., 1996, Antisense oligonucleotides as inhibitors of signal transduction: development from research tools to therapeutic agents, *Biochem. Soc. Trans.* 24:623-629.

De Luca, L.G., Johnson, D.R., Whitley, M.Z., Collins, T., and Pober, J.S., 1994, cAMP and tumor necrosis factor competitively regulated transcriptional activation through a nuclear factor binding to the cAMP-responsive element/activating transcription factor element of the endothelial leukocyte adhesion molecule-1 (E-selectin) promoter, *J. Biol. Chem.* 269:19193-19196.

Derijard, B., Hibi, M., Wu, I.H., Barrett, T., Su, B., Deng, T., Karin, M., and Davis, R.J., 1994, JNK1: a protein kinase stimulated by UV light and Ha-Ras that binds and phosphorylates the c-Jun activation domain, *Cell* 76:1025-1037.

Dorigo, O., Turla, S.T., Lebedeva, S., and Gjerset, R.A., 1998, Sensitization of rat glioblastoma multiforme to cisplatin *in vivo* following restoration of wild-type p53 function, *J. Neurosurg.* 88:535-540.

Fink, D., Aebi, S., Howell, S.B., 1998, The role of DNA mismatch repair in drug resistance, *Clin. Cancer Res.* 4:1-6.

Fujiwara, T., Grimm, E.A., Mukhopadhyay, T., Zhang, W.W., Owen-Schaub, L.B., and Roth, J.A., 1994, Induction of chemosensitivity in human lung cancer cells *in vivo* by adenovirus-mediated transfer of the wild-type p53 gene, *Cancer Res.* 54:2287-2291.

Funato, T., Yoshida, E., Jiao, L., Tone, T., Kashani-Sabet, M., and Scanlon, K.J., 1992, The utility of an antisense ribozyme in reversing cisplatin resistance in human carcinomas, *Adv. Enzyme Regul.* 32:195-209.

Gjerset, R.A., Turla, S.T., Sobol, R.E., Scalise, J.J., Mercola, D., Collins, H., Hopkins, and P.J., 1995, Use of wild-type p53 to achieve complete treatment sensitization of tumor cells expressing endogenous mutant p53. *Molec. Carcinog.* 14:275-285.

Gjerset, R.A., Dorigo, O., and Maung, V., et al., 1997, Tumor regression *in vivo* following p53 combination therapy, *Cancer Gene Therapy* 4:0-2.

Grant, S., Freemerman, A.J., Birrer, M.J., Martin, H.A., Turner, A.J., Szabo, E., and Reed, E., 1998, Platinum-DNA adduct, nucleotide excision repair and platinum based anti-cancer chemotherapy, *Cancer Treat Rev.* 24:331-344.

Gupta, S., Campbell, D., Derijard, B., and Davis, R.J., 1995, Transcription factor ATF2 regulation by the JNK signal transduction pathway, *Science* 267:389-393.

Hibi, M., Lin, A., Smeal, T., Minden, A., and Karin, M., 1993, Identification of an oncoprotein- and UV-responsive protein kinase that binds and potentiates the c-Jun activation domain, *Genes Dev.* 7:2135-2148.

Jennerwein, M.M., and Eastman, A., 1991, A polymerase chain reaction-based method to detect cisplatin adducts in specific genes, *Nucleic Acids Res.* 19:6209-6214.

Lee, S., Elenbas, B., Levine, A., and Griffith, J., 1995, p53 and its 14kDa C-terminal domain recognize primary DNA damage in the form of insertion/deletion mismatches, *Cell* 81:1013-1021.

Levine, A.J., 1993, The tumor suppressor genes, *Annu. Rev. Biochem.* 62:623-651.

Levine, A.J., 1997, p53, the cellular gatekeeper for growth and division, *Cell* 88:323-331.

Livingstone, C., Patel, G., and Jones, N., 1995, ATF-2 contains a phosphorylation-dependent transcriptional activation domain, *EMBO J.* 14:1785-1797.

Lotem, J., and Sachs, L., 1993, Hematopoietic cells from mice deficient in wild-type p53 are more resistant to induction of apoptosis by some agents, *Blood* 82:1092-1096.

Lowe, S.W., Ruley, H.E., and Jacks, T., and Housman, D.E., 1993, p53-mediated apoptosis modulates the cytotoxicity of anti-cancer agents, *Cell* 74:957-967.

Lowe, S.W., Bodis, S., McClatchy A., Remington, L., Ruley, H.E., Fisher, D.E., Housman, D.E., and Jacks, T., 1994, p53 status and the efficacy of cancer therapy *in vivo*, *Science* 266:807-810.

McKay, R.A., Miraglia, L.J., Cummins, L.L., Owens, S.R., Sasmor, H., and Dean, N.M., Characterization of a potent and specific class of antisense oligonucleotide inhibitor of human protein kinase C-alpha expression, *J. Biol. Chem.* 274:1715-1722.

Miyake, H., Hara, I., Gohji, K., Yamanaka, K., Arakawa, S., and Kamidono, S., 1998, Enhancement of chemosensitivity in human bladder cancer cells by adenoviral-mediated p53 gene transfer, *Anticancer Res.* 18:3087-3092.

Newell, C.L., Deisseroth, A.B., and Lopez-Berestein, G., 1994, Interaction of nuclear proteins with an AP-1/CRE-like promoter sequence in the human TNF-alpha gene, *J. Leukocyte Biol.* 56:27-35.

Nguyen, D.M., Spitz, F.R., Yen, N., Cristiano, R.J., and Roth, J.A., 1996, Gene therapy for lung cancer: enhancement of tumor suppression by a combination of sequential systemic cisplatin and adenovirus-mediated p53 gene transfer, *J. Thorac. Cardiovasc. Surg.* 112:1372-1376, discussion 1376-1377.

Nielsen, L.L., Lipari, P., Dell, J., Gurnani, M., and Hajian, G., 1998, Adenovirus-mediated p53 gene therapy and paclitaxel have synergistic efficacy in models of human head and neck, ovarian, prostate, and breast cancer, *Clin. Cancer Res.* 4:835-846.

O'Connor, P.M., Jackman, J., Bae, I., Myers, T.G., Fan, S., Mutoh, M., Scudiero, D.A., Monks, A., Sausville, E.A., Weinstein, J.N., Friend, S., Fornace, A.J., Jr., and Kohn, K.W., 1997, Characterization of the p53 tumor suppressor pathway in cell lines of the National Cancer Institute anticancer drug screen and correlations with the growth-inhibitory potency of 123 anticancer agents, *Cancer Res.* 57:4285-4300.

Oshita, F., and Saijo, N., 1994, Rapid polymerase chain reaction assay to detect variation in the extent of gene-specific damage between cisplatin- or VP-16-resistant and sensitive lung cancer cell lines, *Jpn J. Cancer Res.* 85:669-673.

Potapova, O., Haghghi, A., Bost, F., Liu, C., Birrer, M.J., Gjerset, R., and Mercola, D., 1997, The JNK/stress-activated protein kinase pathway functions to regulate DNA repair and inhibition of the pathway sensitizes tumor cells to cisplatin, *J. Biol. Chem.* **272**:14041-14044.

Potapova, O., Bost, F., Dean, N., and Mercola, D., 1998, Inhibition of the JNK pathway blocks cell cycle progression in human tumor cells, *Proc. AACR*, 89th Annual Meeting, abstract #1720, p. 251.

Reed, E., 1998, Platinum-DNA adduct, nucleotide excision repair and platinum based anti-cancer chemotherapy, *Cancer Treatment Reviews* **24**: 331-344.

Roth, J.A., Swisher, S.G., Merritt, J.A., Lawrence, D.D., Kemp, B.L., Carrasco, C.H., El-Naggar, A.K., Fossella, F.V., Glisson, B.S., Hong, W.K., Khuri, F.R., Kurie, J.M., Nesbitt, J.C., Pisters, K., Putnam, J.B., Schrump, D.S., Shin, D.M., and Walsh, G.L., 1998, Gene therapy for non-small cell lung cancer: a preliminary report of a phase I trial of adenoviral p53 gene replacement, *Semin. Oncol.* **25**:33-37.

Saves, I., and Masson, J.M., 1998, Mechanisms of resistance to xenobiotics in human therapy, *Cell Mol Life Sci.* **54**:405-426.

Scanlon, K.J., Kashani-Sabet, M., 1988, Elevated expression of thymidylate synthase cycle genes in cisplatin-resistant human ovarian carcinoma A2780 cells, *Proc. Natl. Acad. Sci. USA.* **85**:650-653.

Scanlon, K.J., Kashani-Sabet, M., Miyachi, H., Sowers, L.C., and Rossi, J., 1989, Molecular basis of cisplatin resistance in human carcinomas: model systems and patients, *Anticancer Res.* **9**:1301-1312.

Scanlon, K.J., Jiao, L., Funato, T., Wang, W., Tone, T., Rossi, J.J., and Kashani-Sabet, M., 1991, Ribozyme-mediated cleavage of c-fos mRNA reduces gene expression of DNA synthesis enzymes and metallothionein, *Proc. Natl. Acad. Sci. USA.* **88**:10591-10595.

Smeal, T., Binetruy, B., Mercola, D., Birrer, M., and Karin, M., 1991, Oncogenic and transcriptional cooperation with Ha-ras requires phosphorylation of c-Jun on serines 63 and 73, *Nature* **354**:494-496.

Smeal, T., Binetruy, B., Mercola, D., Grover-Bardwick, A., Heidecker, G., Rapp, U.R., and Karin, M., 1992, Oncoprotein-mediated signalling cascade stimulates c-Jun activity by phosphorylation of serines 63 and 73, *Mol. Cell. Biol.* **12**:3507-3513.

Stark, G.R., 1993, Regulation and mechanisms of mammalian gene amplification, *Adv. Cancer Res.* **61**:87-113.

Stein, C.A., and Kreig, A.M., 1994, Problems in interpretation of data derived from *in vitro* and *in vivo* use of antisense oligodeoxynucleotides, *Antisense Res. Dev.* **4**:67-69.

Van Dam, H., Wilhelm, D., Herr, I., Steffen, A., Herrlich, P., and Angel, P., 1995, ATF-2 is preferentially activated by stress-activated protein kinases to mediate c-jun induction in response to genotoxic agents, *EMBO J.* **14**:1798-1811.

Wilhelm, D., van Dam, H., Herr, I., Baumann, B., Herrlich, P., and Angel, P., 1995, Both ATF-2 and c-Jun are phosphorylated by stress-activated protein kinases in response to UV irradiation, *Immunobiology* **193**:143-148.

RUTH GJERSET¹, ALI HAGHIGHI¹, SVETLANA LEBEDEVA¹, DAN MERCOLA^{1,2}

1. Sidney Kimmel Cancer Center, 10835 Altman Row, San Diego, CA 92121
2. University of California, San Diego Cancer Center, 9500 Gilman Drive, La Jolla, CA 92093

**Gene Therapy Approaches to Sensitization of Human Prostate
Carcinoma to Cisplatin by Adenoviral Expression of p53
and by Antisense Jun Kinase Oligonucleotide Methods**

Running Title: Sensitization of Prostate Carcinoma by p53 and Antisense Jun Kinase

Key Words: cancer/prostate carcinoma/p53 adenovirus/antisense Jun Kinase/Chemotherapy sensitization

Corresponding Author
Dan Mercola
phone: (858) 410-8141
fax: (858) 450-3251
danmercola@skcc.org

In "Methods in Molecular Biology: Genomics Protocols," ed. M. Starkey, Humana Press, UK (2000).

1. INTRODUCTION

One of the challenges of medical research today is to find ways of bringing our genetic knowledge of cancer to clinical application and to develop improved therapies by exploiting gene-based strategies. By offering increased specificity and reduced toxicity, gene-based approaches promise alternatives when conventional treatments fail. Gene therapy also offers improved responses to conventional treatments when used in combination with gene therapy. Chief among the cancers in urgent need of improved treatment options is prostate cancer, the most commonly diagnosed cancer in men.

Advanced prostate cancer is resistant to most forms of hormone therapy, radiation therapy, and conventional chemotherapy. In fact, many of the most powerful chemotherapeutic drugs commonly used for other cancers are not effective against prostate cancer. Among these agents is cisplatin (*cis*-diamminedichloroplatinum, CDDP, Platinol™, *cis*-platinum), which causes DNA damage in rapidly dividing cells by forming primarily bifunctional intrastrand adducts between adjacent guanines and guanine-adenine dinucleotides. Cisplatin is highly effective against ovarian cancer and bladder cancer and can achieve cures when used against testicular cancer. Cisplatin has also been applied to colon and brain tumors, but is not in routine use for these applications (1-2). A method for affecting increased sensitivity to cisplatin and for inhibiting or reversing resistance to cisplatin would provide an extended application for this drug, an important agent with well-known properties.

The cellular response to stress and DNA damage now appears to be central to the issue of resistance to DNA damaging chemotherapies such as cisplatin, suggesting that genetic approaches that target these pathways may be effective in reversing resistance and enhancing the benefits of these agents. Here we describe the potential of reversing drug resistance through gene therapies that target two major stress and DNA damage-response pathways—the Jun NH₂-terminal kinase /stress activated protein kinase (JNK/SAPK) pathway and the DNA damage-induced apoptotic pathway mediated by the p53 tumor suppressor. There are suggestions that inhibition of the Jun kinase pathway and/or restoration of the p53 pathway may offer new biological approaches to therapy sensitization in prostate cancer. These approaches would expand the potential of presently available treatments and offer alternatives when conventional treatment protocols fail. These approaches are illustrated by the use of a p53 adenoviral expression vector and by the use of highly efficient antisense JNK oligonucleotides.

1.1. In vitro combination studies with p53 adenovirus and cisplatin

The p53 tumor suppressor has attracted considerable attention not only for its tumor suppressor properties, but also for its ability to sensitize tumor cells to apoptosis following treatment with chemotherapy and radiation (3-8). Recent studies suggest that p53 gene therapy could have a broad application as a therapy sensitizer in cancer, a possibility that greatly expands the clinical application of p53-based approaches. Because many cancers, including prostate cancer, acquire p53 mutations as the disease progresses and becomes resistant to therapy, p53 gene therapy in combination with chemotherapy could have advantageous application for these advanced cancers. Numerous *in vitro* studies now support the application of p53-gene therapy as a therapy sensitizer for cancer.

The results of screening tumor cells for sensitivity to various chemotherapeutic agents following exposure of cells to a replication-defective adenovirus encoding wild-type p53 (Adp53) compared to control vector, Ad-βgal (Ad-β-galactosidase) is summarised in Fig. 1. The cells were treated under conditions where some 50-70% of them show transgene expression, as evidenced by X-gal staining of parallel cultures infected with Ad-βgal. Viability is scored by the MTS assay (9). Under these conditions, it was found that growth suppression by Adp53 alone is incomplete and that 7-day viabilities of Adp53-treated cultures were about 60-80% of control vector-treated cultures. Numerous tumor cell types lacking wild-type p53 expression, including the prostate cancer line PC-3, can be growth suppressed and sensitized to chemotherapeutic drug treatment following restoration of

wild-type p53 activity, consistent with role of p53 in mediating DNA damage recognition and apoptosis (Fig. 1).

1.2. In vivo combination studies using p53 adenovirus and cisplatin in a nude mouse model for prostate cancer

Recently it has been shown that p53 is highly effective at suppressing the growth of human prostate xenografts in nude mice but fails to achieve complete tumor eradication by itself (10, 11). We have tested the possibility that more complete suppression can be achieved by combining p53 gene therapy with the DNA damaging chemotherapy, cisplatin. In the experiment shown in Fig. 2, with these treatment doses, both Adp53 and cisplatin administered as single agents lead to a significant reduction in tumor growth relative to tumors receiving only control vector ($p < 0.001$). When combined, Adp53 and cisplatin lead to an even greater reduction in tumor growth, which was significantly better than either agent used alone ($p < 0.02$). The vector doses in this experiment were low (equivalent to about 10-30 pfu per cell) and completely without side effects, as judged by periodic weight measurements of the animals and histological examination of tissues, suggesting that higher doses or more prolonged treatment could have been applied without adverse side effects. This *in vivo* study therefore confirms the *in vitro* observations and supports the clinical application of p53 adenovirus combination approaches to tumors expressing mutant p53.

Adenovirus-based approaches are among the most promising for clinical applications of gene therapy. Adenoviruses are relatively easy to prepare, are stable, can be obtained in high titer, and provide high gene transfer efficiencies. Adenoviruses are also well tolerated in patients and have been used in phase I clinical trials with few side effects even with repeated doses (12-18). Improvements in tissue targeting of adenovirus will extend the application of adenovirus-based approaches to a broad range of clinical situations. Nevertheless, Adenovirus mediated p53 gene transfer has already shown efficacy in clinical trials for lung cancer, hepatocellular carcinoma, and head and neck cancer (18).

1.3. In vitro studies combining inhibition of the Jun kinase pathway with chemotherapy

Another important cellular pathway involved in the DNA damage response is the Jun kinase/stress-activated protein kinase (JNK/SAPK) pathway, which is often upregulated in prostate cancer (19- 20). This pathway represents one of the Mitogen-activated Protein Kinase pathways (MAPK) and plays a role in growth factor signaling, oncogene expression, and cellular transformation, as well as the DNA damage response (9).

Numerous reports document the activation of the Jun kinase pathway in cells following treatment with a variety of DNA damaging agents, including UV radiation, ionizing radiation, methylethane sulfate (MMS), N-nitro-N'-nitroso-guanidine (MNNG), Ara-C (1- β -D-arabinofuranosylcytosine), and cisplatin (19). A major substrate of JNK is the transcription factor c-Jun, which is greatly activated upon phosphorylation of serine residuals 63 and 73. We have demonstrated that tumor cells that stably express a nonphosphorylatable dominant negative mutant c-Jun are defective in repair of cisplatin adducts, consistent with their increased sensitivity to cisplatin. The DNA repair assay that we used was based on the observations that cisplatin adducts will inhibit the Taq polymerase such that the decrease in yield of the PCR product is directly proportional to the degree of platination of the template. The density of adducts can then be calculated based on a Poisson distribution predicted from a random process of platination (21). Thus (P) the relative PCR signal strength (damaged template relative to undamaged template) is related to the platination level (n), the number of adducts per PCR amplicon-sized fragment by the formula $P = e^{-n}$. In our case we amplified a 2.7 kb fragment of the HPRTase gene, a fragment providing a sufficiently large target size to enable us to detect significant decreases in PCR signals from templates from cisplatin-treated cells. Amplification of a smaller fragment of 150 bp in length, a fragment too small to register significant levels of platination under our conditions, served as a control for the efficiency of the PCR amplification. Table 1 summarizes the frequency of adduct formation calculated after quantitating the PCR signal strengths (results of two experiments performed in triplicate). As shown in the table,

cisplatin adducts form at a greater frequency on genomic DNA in mutant Jun expressing cells than in parental cells. In addition, mutant Jun expressing cells show no repair of adducts in a 6 h recovery period following a 1 h treatment with cisplatin, whereas parental cells repair about half of the adducts in that time period.

These results have been confirmed using a plasmid recovery DNA repair assay. In this assay, cells are transfected with CAT reporter plasmids that have been damaged *ex vivo* by previous treatment with 25 μM cisplatin for 3 h. Reporter gene expression 24 and 48 h post transfection is taken as an indication of DNA repair. As shown in Fig. 4, cells that express mutant Jun are suppressed relative to parental cells in their ability to repair the damaged plasmid, consistent with the PCR-based DNA repair assays.

While the mechanism by which the Jun kinase pathway affects DNA repair is not known, there are several candidate target genes whose roles in DNA synthesis and repair could account for observations that we have made. As listed in Table 2, the promoters of number DNA synthesis and repair genes, contain AP-1 or ATF2/CREB regulatory elements. These include DNA polymerase β , topoisomerase I, topoisomerase II, uracyl glycosylase, PCNA, metallothioneine and others. In several cases, such as DNA polymerase β , exposure of cells to UV radiation is known to induce the gene, and ATF2/CREB sites are required for this induction. Thus a number of genes involved in DNA excision repair may be coordinately upregulated upon activation of the Jun kinase pathway following cisplatin damage. Some or all of these could serve as potential targets for gene therapy approaches to drug sensitization of cancer.

1.4. In vivo studies combining inhibition of the Jun kinase pathway by antisense with chemotherapy

In a parallel arm of the *in vivo* study shown in Fig. 2, we tested the anti-tumor efficacy of downregulation of Jun kinase combined with cisplatin. In this study we down regulated Jun kinase with antisense oligonucleotides targeting either the Jun kinase 1 (JNK1) and/or Jun kinase 2 (JNK2) family of Jun kinase isoforms. These compounds were previously developed and characterized as described (22- 23).

An important methodological consideration is the use of high affinity antisense oligonucleotides that completely suppress target mRNA and protein at low concentration. In collaborative studies with Isis Pharmaceuticals, Inc., we have developed a systematic method that now has been adapted to a multiwell procedure. The salient features are that a large series of phosphorothioate oligonucleotides complementary to 20 nt stretches of JNK1 and JNK2 spaced approximately every 50 bp along the transcribed portion of the gene are prepared on a small scale. Thus, the target gene sequence must be known. These trial oligonucleotides are then tested for the ability to suppress steady state transcript levels in culture cells 24 h *after* a 4-hour lipid-mediated transfection (22, 23). Most of these trial oligonucleotides we tested were not efficient at promoting suppression of target mRNA at low (0.2 – 0.4 μM) concentration. However, it was readily possible to identify antisense compounds that were over 90% efficient at eliminating target mRNA at these low concentrations after a single 4 h transfection. This step is key in order to avoid any temptation to use less efficacious antisense compounds by increasing the concentration to high levels ($>1 \mu M$) where many nonspecific interactions leading to aberrant cellular localization and weak membrane-protein complex formation have been observed (24). Moreover, compounds that require $>1 \mu M$ cannot be considered as potential drugs owing to the generation of nonspecific interactions and owing to the many drawbacks in attempting to achieve local concentrations on the order of $\sim 1 \mu M$ *in vivo*. These considerations are likely important in understanding the many difficulties some workers have had in “getting antisense to work.” For the studies summarized here, it was possible to select highly efficient antisense oligonucleotides that are complementary to a sequence that is invariant in all isoforms of JNK1 or JNK2 thereby making it possible to reduce or eliminate all isoforms of JNK1 or JNK2 with a single antisense oligonucleotide. Next, the elapsed time of suppression of target mRNA and target

protein was determined (23). These studies showed that a single antisense treatment suppressed target mRNA and protein from approximately 24 h to 72 h thereby defining a 2 d window in which antisense-mediated effects could be observed (22- 23; Potapova *et al.*, unpublished observations). However, for growth studies where cell numbers are counted or tumor volume measured, any loss of growth due to inhibition of a growth-promoting target protein will remain apparent as decreased total growth for at least 3 weeks (22).

Since a variety of human tumor cells, including PC-3 cells, were sensitized to the cytotoxic effects of DNA-damaging cisplatin *in vitro* upon inhibition of the JNK pathway (9), it was decided to test whether xenografts of PC-3 cells could be sensitized to cisplatin. Moreover, since many of the potential JNK-regulated genes encode gene products that facilitate DNA synthesis (Table 2), it appeared logical to expect that inhibition of JNK *in vivo* may affect tumor growth even in the absence of cisplatin (25). This experiment was carried out as a separate arm of the same *in vivo* study as for the evaluation of Adp53 in Fig. 2.

Following inoculation of the mice with the PC-3 cells, the animals were monitored until visible and palpable tumors developed. At this point and for all subsequent observations, tumor volumes were estimated from the length and width of the tumors (*see* Section 3.2). Treatment consisted of intraperitoneal injection of oligonucleotide solution (*see* Section 2.2) daily for 6 of 7 days per week. On the 7th day, oligonucleotide treatment was omitted and the mice received either vehicle or cisplatin (*see* Section 3.2). Treatment (systemic antisense oligonucleotide 25 mg/Kg of an equimolar mixture of antisense JNK1 and antisense JNK2 termed combined-antisense JNK1 + JNK2, or a scrambled-sequence oligonucleotide or vehicle (PBS) alone) was initiated upon development of readily visible and palpable tumors (Fig. 5). Every seventh day, antisense treatment was omitted and a subgroup of 15 animals receiving the combined-antisense treatment also received cisplatin, i.e., the same dose cisplatin and timing as for the p53 treatment regimen. As a control, separate group of animals received cisplatin alone. In order to confirm that systemic antisense treatment led to inhibition of JNK activity, JNK kinase activity of tumor extracts was determined 18 h after antisense treatment. These studies demonstrated an 89% reduction of steady state tumor JNK activity in tumors of antisense-treated animals compared to the activity of PC-3 cells, and an 80% reduction compared to the tumor JNK activity of scrambled sequence oligonucleotide-treated animals (Fig. 5).

We observed that treatment with antisense oligonucleotides, either antisense JNK2 or combined-antisense treatment, led to marked inhibition of tumor growth and these results were superior to the results for cisplatin alone. When the growth curves of Fig. 5 were integrated, it was found, for example, that combined-treatment led to 78% inhibition whereas cisplatin treatment led to 47% tumor growth inhibition. These results are significantly less ($p<0.002$) than controls (vehicle alone, scrambled sequence oligonucleotide) and are significantly different from each other ($p<0.02$; ANOVA). The effect of antisense JNK can be attributed largely to antisense JNK2 (Fig. 5). The dominance of JNK2 has been observed in human lung carcinoma cells (22) and in a series of nine human prostate carcinoma cell lines (26). When antisense cisplatin treatments were combined, growth inhibition was further enhanced to 89% of maximum growth inhibition (Fig. 5). Thus, these *in vivo* studies suggest that it may be possible both to inhibit growth and to sensitize solid tumors to chemotherapy by eliminating the Jun kinase pathway.

1.5. Combined inhibition of Jun kinase and restoration of p53

The approaches described here have implications for therapeutic approaches targeting the DNA damage response in tumor cells. Upregulation of the DNA repair machinery may accompany tumor progression and the development of drug resistance. This process may involve, in part, AP-1 and ATF2/CREB regulated DNA synthesis and repair genes. In fact earlier studies by Scanlon and coworkers demonstrated that downregulation of AP-1 activity using a c-fos ribozyme was effective at sensitizing ovarian carcinoma cells to cisplatin, and this correlated with downregulation of DNA polymerase β , topoisomerase I, and thymidylate synthetase, all known to have AP-1 sites in their promoter regions (27) (Table 2).

Independent of Jun kinase DNA damage response, loss of the p53 tumor suppressor contributes to resistance to DNA damaging therapies by removing an important component of the DNA damage recognition machinery. Because p53 induces apoptosis in response to the level of DNA damage, it is likely that the success or failure of DNA repair contributes to the suppressive effects of p53.

These results support the combined application of p53 gene therapy along with antisense therapy to inhibit the Jun kinase pathway, or some downstream target of the pathway. When used in combination with conventional chemotherapies such as cisplatin, the combined approach, which can be foreseen today may extend the application of conventional treatments to prostate cancer and provide a new strategy for treatment of therapy resistance advanced disease.

2. MATERIALS

1. Adenoviral vectors (Deborah Wilson, Introgen Therapeutics, Inc., Houston Texas) (*see Note 1*).
2. Antisense oligos (*see Note 2*):
JNK1- 5'-CTCTCTGTAGGCCGCTTGG-3'
JNK2- 5'-GTCCGGGCCAGGCCAAAGTC-3'
3. Delbecco's modified minimum medium supplemented with 10% fetal calf serum (Irvine Scientific, Inc., Irvine, CA).
- PC-3 human prostate carcinoma cells, as well as other cell lines used in *in vitro* assays (T47D breast cancer cells, DLD-1 colon cancer cells, and T98G glioblastoma cells) were grown at 37°C in an environment of 10% CO₂.
4. Animals: 5-6 week athymic female post-weaning Harlan Sprague Dawley mice (Harlan Laboratories, Indianapolis, IN).
5. 10X PBS: 2 g anhydrous KH₂PO₄, 11.4 g anhydrous Na₂HPO₄, 2 g KCl, 80 g NaCl. Make up the vol to 1 L with H₂O. Dilute 1:10 before use.
6. X-gal staining solution: 1 mg/mL X-gal (5-bromo-4-chloro-3-indoyl-β-D-galactopyranoside), 5 mM potassium ferricyanate, 5 mM potassium ferrocyanate, 2 mM MgCl₂ in PBS.
7. Taq polymerase (Qiagen).
8. 250 μM dNTPs ((Pharmacia Biotech. Inc.).
9. PCR Reaction mix: 25 μL reactions contain 0.03–0.25 μg DNA, 25 pmol each of forward and reverse primer, 250 μM dNTPs (Pharmacia Biotech. Inc.), 1.25 U Taq polymerase (Qiagen), 1X buffer (Qiagen), Solution Q (Qiagen).
10. Choramphenicol acetyltransferase (CAT) assay reaction mix (per reaction): 70 μL cell lysate, 30 μL 5 mM Chloramphenicol, 0.4 μL ³H-AcetylCoA (200 mCi/mmol; NEN® Life Science Products, Inc.), 0.6 μL (4.4 μg/μL) nonradioactive AcetylCoA (Pharmacia Biotech. Inc.).
11. Whole Cell Extract (WCE) buffer: 20 mM HEPES, pH 8.0, 75 mM NaCl, 2.5 mM MgCl₂, 0.05 % (v/v) Triton X-100, 0.5 mM dithiothreitol, 20 mM β-glycerophosphate, 0.1 mM Na₃VO₄ 2 μg/mL leupeptine, 100 μg/mL paramethylsulfonyl fluoride.

12. Jun Kinase Assay buffer: 20 mM HEPES, pH 7.7, 20 mM MgCl₂, 20 mM β-glycerophosphate, 20 mM p-nitrophenyl phosphate, 0.1 mM Na₃VO₄, 2 mM DTT, 20 μM ATP, 5 μCi of [γ^{32} P] ATP.
13. Oligonucleotide transfection (lipofection) solution: mix 10 μg/mL Lipofectin (Gibco BRL, Gaithersburg, MD) reagent in MEM (Gibco BRL, Gaithersburg, MD) with an equal volume of oligonucleotide solution, incubating this mixture at room temperature for 15 min and diluting it with lipofectin solution to a final oligonucleotide concentration of 0.4 μM.
14. X-gal staining solution: 1 mg/mL 5-bromo-4-chloro-3-indoyl-β-D-galactopyranoside, 5 mM potassium ferricyanate, 5 mM potassium ferrocyanate, 2 mM MgCl₂ in PBS.
15. Lipofection solution for plasmid transfection: Prepare 1 μg/μL stock of DOTAP lipofection reagent (Boehringer Mannheim Corp, Indianapolis, IN). To prepare the mix (per well) of a 24-well tissue culture plate:
 - a. Plasmid/HEPES mix: 1.25 μL (1 μg/μL) plasmid + 11.25 μL 5 mM HEPES, pH 7.8.
 - b. DOTAP/HEPES mix: 7.5 μL DOTAP (1 μg/μL) + 17.5 μL 5 mM HEPES, pH 7.8.

Mix entire contents of (a) and (b) together, and incubate for 30 min at room temperature.

3. METHODS

3.1. 96-well growth assay

1. Plate cells in complete medium 1 day prior to vector treatment in 24-well tissue culture plates so that their density at the time of treatment is about 70-80% of confluence.
2. Treat the cells with Ad p53 or Ad βgal for 2 to 3 h (100 pfu per cell).
3. Incubate the cells for additional 2 d in one of the Adβgal-treated wells
4. Remove the medium and wash the wells 2 times with PBS.
5. Fix the cells by overlaying with a solution containing 3.7% paraformaldehyde (v/v) in PBS for 15 min.
6. Wash the wells with PBS and overlay with X-gal staining solution.
7. Incubate the cells at 37°C overnight to allow development of blue stain in β-galactosidase-expressing cells for estimating the infection efficiency.
8. Following treatment with vector, plate the cells at low density (1000 cells per well) in 96-well plates and treat (in triplicate) with drug for 1-4 h depending on the drug, followed by incubation for an additional 5-7 d (see Note 1).
9. Incubate cells for an additional 6 d and score viability by addition of the tetrazolium dye MTT for 1 h and determining the A₂₆₀ of the formazan product as described by the manufacturer (Promega).

3.2. Subcutaneous tumor model in nude mice

1. Inoculate 5 × 10⁶ PC-3 prostate cancer cells (mutant p53) sub-cutaneously on the back of nude mice by injecting 100 μl of a cell suspension in PBS at 5 × 10⁷ cells/mL.
2. Allow tumors develop 5 d to a size of 50-100 mm³.

3. Estimate tumor vol by measuring the length and width of the tumor with a caliper and calculate by using the formula, volume = $\pi/6$ (length x width²).
4. Initiate treatment (designated day 1) and monitor tumor volume every 2-3 d (*see Note 2*).
5. For oligonucleotide treatment, inject mice IP at 25 mg/Kg and based on the average weight of all mice by daily intraperitoneal injection with a solution at a concentration yielding the total dose in 0.2 mL of PBS. Treat control animals with either vehicle alone or the scrambled sequence control oligonucleotide.

3.3. Analyses of DNA repair by PCR stop assay

1. Prepare genomic DNA from about 5×10^5 cultured cells using the QIAamp blood kit (Qiagen) essentially following the manufacturer's protocol, except lyse cells directly on the plate in the presence of PBS, Qiagen protease and lysis buffer supplied in the kit.
2. Following purification, adjust the DNA concentration to 0.25 mg/mL in sterile water and store at -20°C until use.
3. Carry out quantitative PCR as described (32) for the measurement of cisplatin adduct formation on specific regions of DNA (*see Note 3*). For each primer pair, verify that product formation is directly proportional to input template by performing a pilot experiment with serial two fold dilutions of template, followed by electrophoresis on a 1% agarose gel containing 0.5 µg/mL ethidium bromide.
4. Quantify bands using a Kodak digital camera and analysis software or an equivalent apparatus for the integration of band intensity from photographic film.
5. For the PCR reaction, use primers at a concentration of 0.03 to 0.25 µg per 25 µl reaction depending on the amount of template used in the PCR reaction.
6. Carry out the PCR reaction following amplification program:
 1 cycle 94°C, 1 min 30 s
 25 cycles 94°C, 1 min
 57°C, 1 min
 70°C, 2 min 30 s
 1 cycle 94°C, 1 min; 57°C, 1 min; 70°C, 7 min.

Use two independent templates for each treatment condition and set up each for analysis in triplicate with one template as an internal PCR control in order to generate a 270 bp fragment of the dihydrofolate reductase gene (*see Note 4*).

3.4. Analysis of DNA repair using CAT reporter assay

1. Treat 100 µg of CAT reporter plasmid (in which the CAT gene is expressed from the RSV promoter), with 25 µM cisplatin in 300 µL total of PBS on ice for 3 h to create cisplatin-damage reporter DNA.
2. Precipitate the DNA by adding 150 µl of 7.5 M NH₄Ac and 450 µl isopropanol.
3. Leave the mixture at -20°C for 1 h.
4. Centrifuge the DNA at 14,000g for 30 min.
5. Perform 2 washes with 70% ethanol, followed by a final wash in absolute ethanol.

6. Resuspend the DNA in sterile H₂O and use for transfections.
7. Process untreated DNA the same way but without the addition of cisplatin and use this plasmid preparation as a control.
8. Plate the cells in 24-well plates the day prior to transfection so that their density at the time of transfection is 50% (about 10⁵ cells per well).
9. Set up transfections in triplicate wells either with 1 to 1.25 µg undamaged plasmid or damaged plasmid for the 24 h time point together with a second set of triplicate wells transfected for the 48 h time point, using the DOTAP liposomal transfection reagent (*see* Section 2.5.9).
10. Add 500 µL media to entire contents of step 7 and mix well.
11. Wash cells in the well of 24-well plate twice with 1X PBS.
12. Add 537.5 µL of transfection in (step 8) to the well.
13. Incubate the reactin overnight in the 37°C, 10%CO₂ incubator.
14. Aspirate off the transfection mix and wash cells twice with 1X PBS.
15. Aspirate off the PBS, and replace with 1 mL fresh complete culture medium.
16. Incubate for 24-48 h at 37°C, 10%CO₂.
17. Remove the medium, wash the cells twice with PBS and store dry plate at -70°C until required.

3.5. CAT Assay

1. Thaw the plates from step 17 above for 5 min at 37°C.
2. Add 100 µL of 1X Reporter Lysis Buffer (Promega) to each well of a 24-well plate.
3. Shake the plate vigorously for 15 min.
4. Transfer entire 100 µL of lysate to microcentrifuge tubes.
5. Spin lysates for 2 min at 14,000g (4°C).
6. Transfer supernatants to fresh tubes.
7. Heat supernatants for 10-15 min at 65°C to destroy deacetylase activity. If there is particulate material present after this heating step, centrifuge again and collect the supernatants.
8. Measure the protein concentration of each sample using the Biorad Protein Assay (Biorad Laboratories), following manufacturers instructions.
9. Equalize protein concentration of the samples using 1X Reporter Lysis Buffer (Promega). Add 31 µL of CAT reaction mix to 70 µL of the above samples.
10. Incubate the mix at 37°C for 2 h.

11. Add entire sample to 1 mL 7M urea.
12. Add 1 mL toluene:PPO (8 g PPO per mL toluene). Shake well and count using a scintillation counter. The resulting counts are proportional to accumulated CAT expression and, therefore, total CAT activity.

3.6. Antisense Oligonucleotide transfection

1. Wash 70% confluent cultures (24 h after plating) in tissue culture plates twice with PBS.
2. Incubate the cells with lipofectin- 0.4 μ M oligonucleotide solution (*see Section 2*) at 37°C in 10% CO₂ from 4 h to overnight (*see Note 5*).
3. Following lipofection, wash the cells once with serum-free MEM and culture in complete medium (*see Note 5*).

3.7. Jun Kinase Assay

1. Transfect cells with oligonucleotides as described above (Section 3.5).
2. Wash the cells with ice-cold PBS and suspend in WCE buffer.
3. Determine the protein concentration of the cell extracts by the Bradford dye method (Bio-Rad Laboratories Inc.) (*see Note 6*).
4. Carry out the kinase assay as described below (28, 29):
 - a. Mix 50 μ g of whole cell extract (WCE) with 10 μ g of GST-c-Jun (1-223) for 3 h at 4°C.
 - b. Wash 4 times and incubate the beads with 30 μ L of kinase reaction buffer for 20 min at 30°C.
5. Stop the reaction by addition of 20 μ L of Laemmli sample buffer.
6. Elute the phosphorylated GST-c-Jun protein by boiling the sample for 5 min.
7. Resolve the components by 10% SDS-polyacrylamide gel electrophoresis (SDS-PAGE).
8. Quantify the ³²P-phosphorylated GST-c-Jun by digitization and integration of the respective “band” values of the autoradiograph of the dried gel (*see Note 3*).

4. NOTES

1. These vectors are replication defective Adenoviral recombinants in which the early region genes E1A and E1B required for viral replication have been deleted and replaced with an expression cassette containing the transgene of interest. In the case of the p53 adenovirus (Adp53), the expression cassette consisted of the human wild-type p53 coding sequence, flanked by the cytomegalovirus (CMV) promoter, and the Simian virus 40 (SV40) polyadenylation signal. In the case of the control adenovirus (Ad β gal), the expression cassette consisted of the bacterial β -galactosidase coding sequence flanked by the CMV promoter and SV40 polyadenylation signals. In the case of the control adenovirus (AdLuc), the expression cassette consisted of the firefly luciferase coding sequence flanked by the Rous sarcoma virus (RSV) promoter and SV-40 polyadenylation sequences. Viral stocks were stored at -70° C and repeated freezing and thawing

were avoided. The concentrations of the stocks, expressed in plaque-forming units per mL (PFU/mL) were $1\text{-}2 \times 10^{11}$.

2. The sequences were determined in preliminary studies utilizing a messenger walk procedure as described (see ref. 28, 29). Since *in vivo* studies require large amounts of oligonucleotide, a single "scrambled sequence" control sequence was chosen consisting of a scrambled 20 nt sequence previously used as a control in the analysis of antisense PKC α : 5' TCGCATCGACCCGCCACTA- 3'. Both ASJNK sequences contain a single CpG sequence thought to have potential immunostimulatory properties that may, therefore, influence xenograft growth by immunological mechanisms. The control oligonucleotide used here has a nucleotide composition closely approximating the average of antisense JNK1 and JNK2 but contains three CpG dinucleotides sequences thereby providing a control for the potential influence of CpG sequences. All three oligonucleotides were prepared and purified as previously described (34-35).
3. Wells that do not receive drug serve as a control to which drug treated wells are compared. Example drug treatments are as follows: 5-fluorouracil (AdrucilTM, Pharmacia Biotech. Inc.) 10 mM for 1 h; Doxorubicin (Doxorubicin hydrochloride, Aldrich) 3.7 μM for 1 h, cisplatin (PlatinolTM, Bristol Laboratories) 30 μM for 1 h for PC-3 and 20 μM for 1 h for T98G.
4. An example treatment consisted of cisplatin (PlatinolTM, diammine-platinum dichloride, aqueous solution 1mg/mL, Bristol Myers Squibb Company) intraperitoneal administration on days 1 and 8 at a dose of 4mg/kg (LD10), i.e., 88 μ l per 22 g mouse. The dose corresponds to approximately 20% of the IC50 of cisplatin for mice and is the maximum tolerable doses for a repeated weekly treatment. Vector (Adp53 or AdLuc) was administered intratumorally at a dose of 10^8 pfu per injection on days 3, 5, and 7 and again on days 10, 12, and 14. Vector was diluted into sterile cold PBS prior to injection so that injection volumes were 100 μ l.
5. Because Taq polymerase is blocked at cisplatin adducts, the relative efficiency of PCR amplification of genomic DNA from cisplatin-treated versus control cells drops in proportion to platination levels. The relative PCR efficiency is equal to the frequency of undamaged strands, P, within a population. P is related to the average number of cisplatin adducts, n, per fragment, by the Poisson formula: $P = e^{-n}$, or $-(\ln P) = n$. A drop in the PCR signal to 0.6 of control would therefore reflects an average cisplatin adduct density of $-(\ln 0.6) = 0.51$ adducts per fragment. PCR signals ranging from 0.9 to 1.0 of control are generally indistinguishable from the control, due to standard deviations in the range of ± 0.1 . Since a PCR signal equal to 0.9 of control reflects an adduct density of 0.1 adduct per fragment, we consider that the assay is not sensitive to adduct densities of less than 0.1 adduct per fragment. In most cases with genomic DNA from cisplatin-treated cells, the assay requires PCR amplifying a fragment of around 2-3 kb in length.
6. This fragment is too small to register significant levels of damage under the conditions we use, and its amplification product varies by less than 5-10% amongst the various templates.
7. Generally a 4 h exposure is required for the reduction of target JNK mRNA by >80%. This is observed after 24 h of lipofection as judged by Western analysis. Resistant cell types are treated for longer periods and this approach is *favored* over increasing the oligonucleotide concentration or altering the oligonucleotide:lipofectamine ratio.
8. Typically all preparations yield very similar protein concentrations but volumes should be used so as to provide equal amounts of total cellular protein in all samples prior to subsequent analysis.
9. Prepare in advance GST-c-Jun fusion proteins by expression and purification (Qiagen plasmid DNA purification system kit) from *E. coli* and by addition of Glutathione Sepharose[®] 4B beads (Pharmacia Biotech, Inc.).

10. For digitization software that provides interactive designation of the bands by, for example, drawing boxes, subtract background by using half-sized boxes placed exactly above and below the band question or by subtracting one-half of the sum of same sized boxes placed above and below the band in question. Subtract background values in all cases thereby yielding "net" band values. Determine the Relative Jun Kinase Activity by normalizing the resulting net band values by division by similar results for control cases such as the scrambled-sequence or mock transfected cell case.

Acknowledgements

This work was supported in part by grants from the U.S. Public Health Service, NCI CA69546 (R.A.G.), NCI CA63783 (D.A.M.), and NCI CA76173 (D.A.M.), by the U.S. Army Breast Cancer Research Program DAMD17-96-1-6038 (R.A.G.), and by Introgen Therapeutics, Inc. (R.A.G.) and by the Fellowship Program of the Sidney Kimmel Cancer Center.

We thank Kluwer Academic/Plenum Publishers, Inc. (New York, Boston, Dordrecht, London, Moscow) to reprint Figures 1 and 2 and Tables 1 and 2 from "Cancer Gene Therapy: Past Achievements and Future Challenges" (*Advances in Experimental Medicine and Biology*, Vol 465), N. Habib, editor (2000).

We thank Angela Narehood for excellent editorial assistance.

REFERENCES

1. Fischer, D. S., Knobf, M. T., and Durivage, H. J. *The Cancer Chemotherapy Handbook*, 4th ed, St. Louis, MO: Mosby, Inc., 1993.
2. Cantrell, J. E., Hart, R. D., Taylor, R. F., Harvey, J. H., Jr. Pilot trial of prolonged continuous-infusion 5-fluorouracil and weekly cisplatin in advanced colorectal cancer. *Cancer Treatment Reports* 71(6)(1987): 615-618.
3. Clarke, A.R., Purdie, C.A., Harrison, D.J., Morris, R. G., Bird C. C., Hooper M. L., Wyllie, A. H. Thymocyte apoptosis induced by p53-dependent and independent pathways. *Nature* 362(6423) (April 1993): 849-852.
4. Gjerset, R. A., Turla, S. T., Sobol, R. E., Scalise, J. J., Mercola, D. M., Collins, H., and Hopkins, P. J. Use of wild-type p53 to achieve complete treatment sensitization of tumor cells expressing endogenous mutant p53. *Mole. Carcinog* 14 (1995): 275-285.
5. Dorigo, O., Turla, S. T., Lebedeva, S., and Gjerset, R. A. Sensitization of rat glioblastoma multiforme to cisplatin in vivo following restoration of wild-type p53 function. *J Neurosurg* 88 (1998): 535-540.
6. Lotem, J. and Sachs, L. Hematopoietic cells from mice deficient in wild-type p53 are more resistant to induction of apoptosis by some agents. *Blood* 82 (1993): 1092-1096.
7. Lowe, S. W., Bodis, S., McClatchy, A., Remington, L., Ruley, H. E., Fisher, D. E., Housman, D. E., and Jacks, T. p53 status and the efficacy of cancer therapy *in vivo*. *Science* 266 (1994): 807-810.
8. Lowe, S. W., Ruley, H. E., Jacks, T., Housman, D. E. p53-mediated apoptosis modulates the cytotoxicity of anti-cancer agents. *Cell* 74 (1993): 957-967.
9. Potapova, O., Haghghi, A., Bost, F., Liu, C., Birrer, M. J., Gjerset, R., Mercola, D. The Jun kinase/stress-activated protein kinase pathway functions to regulate DNA repair and inhibition of the pathway sensitizes tumor cells to cisplatin. *J Biol Chem* 30 (1997): 14041-14044.
10. Asgari, K., Sesterhenn, I. A., McLeod, D. G., Cowan, K., Moul, J. W., Seth, P., Srivastava, S. Inhibition of the growth of pre-established subcutaneous tumor nodules of human prostate cancer cells by single injection of the recombinant adenovirus p5 expression vector. *In. J Cancer* 71 (1997): 377-382.
11. Ko, S. C., Gotoh, A., Thalmann, G. N., Zhai, H. E., Johnston, D. A., Zhang, W. W., Kao, C., Chung, L. W. Molecular therapy with recombinant p53 adenovirus in an androgen-independent, metastatic human prostate cancer model. *Hum Gene Ther* 7(14) (September 1996): 1683-1691.
12. Swisher, S. G., Roth, J. A., Nemunaitis, J., Lawrence D. D., Kemp, B. L., Carrasco, C. H., Connors, D. G., El-Naggar, A. K., Fossella, F., Glisson, B. S., Hong, W. K., Khuri, F. R., Kurie, J. M., Lee, J. J., Lee, J. S., Mack, M., Merritt, J. A., Nguyen, D. M., Nesbitt, J. C., Perez-Soler, R., Pisters, K. M., Putnam, J. B., Jr., Richli, W. R., Savin, M., Wough, M. K. Adenovirus-mediated p53 gene transfer in advanced non-small cell lung cancer. *J Natl Cancer Inst* 91(9) (May 1999): 763-771.
13. Kauczor, H. U., Schuler, M., Heussel, C. P., von Weymar, A., Bongartz, G., Rochlitz, C., Huber, C., Thelen, M. CT-guided intratumoral gene therapy in non-small-cell lung cancer. *Eur Radiol* 9 (1999): 292-296.
14. Roth, J. A. Restoration of tumor suppressor gene expression for cancer. *Forum (Genova)* 8 (1998): 368-376.
15. Schuler, M., Rochlitz, C., Horowitz, J. A., Schelgel, J., Perruchoud, A. P., Kommooss, F., Bolliger, C. T., Kauzor, H. U., Dalquen, P., Fritz, M. A., Swanson, S., Herrmann, R., and Huber, C. A phase I study of adenovirus-mediated wild-type p53 gene transfer in patients with advanced non-small cell lung cancer. *Hum Gene Ther* 9 (1998): 2075-2082.
16. Roth, J. A., Swisher, S. G., Merritt, J. A., Lawrence, D. D., Kemp, B. L., Carrasco, C. H., El-Naggar, A. K., et al. Gene therapy for non-small cell lung cancer: a preliminary report of a phase I trial of adenoviral p53 gene replacement. *Semin. Oncol.* 25 (1998), 33-37.
17. Zwaka, R. M. and Dunlop, M. G. Gene therapy for colon cancer. *Hematol.Oncol.Clin. North Am* 12 (1998): 595-615.
18. Clayman, G. L., el-Naggar, A. K., Lippmann, S. M., Henderson, Y. C., Frederick, M., Merritt, J. A., Zumstein, L. A., Timmons, T. M., Liu, T. J., Ginsberg, L., Roth, J. A., Hong, W. K., Bruso, P., Goepfert, H. Adenovirus-mediated p53 gene transfer in patients with advanced recurrent head and neck squamous cell carcinoma. *J Clin Oncol* 16(6) (June 1998): 2221-2232.
19. Bost, F., Potapova, O., Liu, C., Zhang, Y.-M., Charbono, W., Dean, N., McKay, R., and Mercola, D. High Frequency regression of established human prostate carcinoma PC-3 xenografts by systemic treatment with antisense jun kinase. *The Prostate* 38 (1999): 320-321.
20. Loda Magi-Galluzzi C., Mishra R., Fiorentino M., Montironi R., Yao H., Capodieci P., Wishnow K., Kaplan I., and Stork P. J., Loda M. Mitogen-activated protein kinase phosphatase 1 is overexpressed in prostate cancers and is inversely related to apoptosis. *Lab Invest* 76(1) (1997): 61-70.
21. Jennerwein, M. M. and Eastrman, A. A polymerase chain reaction-based method to detect cisplatin adducts in specific genes. *Nucleic Acids Res* 19 (1991): 6209-6214.
22. Bost, F., McKay, R., Bost, M., Potapova, O., Dean, N., and Mercola, D. Jun Kinase-2 isoform is preferentially required for epidermal growth factor-induced proliferation of human A549 lung carcinoma cells. *Mol Cell Biol* 19 (1999): 1938-1949.
23. Bost, F., McKay, R., Dean, N., and Mercola, D. Antisense methods for the discrimination of phenotypic properties of closely related gene products: The Jun Kinase Family. *in Methods in Enzymology*, J. N. Abelson & M. I. Simon (Eds. in Chief), for volume "Antisense Technology," M. I. Phillips (vol. Ed.) (2000) 314: 541-542.
24. Stein, C. A. Does antisense exist? *Nature Medicine* 1(1)(1995): 1119-1121.
25. Bost, F., Dean, N., McKay, R., and Mercola, D. Activation of the Jun Kinase/Stress-Activated Protein Kinase pathway is Required for EGF-Autocrine Stimulated Growth of Human A549 Lung Carcinoma Cells. *J Biol Chem* 272 (1999): 33422-33429.
26. Yang, YM., Bost, F., Liu, C., and Mercola, D. The Jun Kinase pathway promotes growth of prostate carcinoma cell lines. *Cancer Gene Therapy* 5(6)(1998): S31 (Abstract PD-96).
27. Scanlon, K., Jiao, L., Funato, T., Wang, W., Tone, T., Rossi, J., and Kashani-Sabet, M. Ribozyme-mediated cleavage of c-fos mRNA reduces gene expression of DNA synthesis enzymes and metallothionein. *Proc Natl Acad Sci U.S.A.* 88 (1991): 10591.
28. Binetruy, B., Smeal, T., and Karin, M. Ha-Ras augments c-Jun activity and stimulates phosphorylation of its activation domain. *Nature* 351 (1991): 22-27.
29. Gjerset, R.A., Lebedeva, S., Haghghi, A., Turla, S.T., and Mercola, D. Inhibition of the Jun kinase pathway blocks DNA repair, enhances p53-mediated apoptosis and promotes gene amplification. *Cell Growth and Diff* 10 (1999): 545-554.
30. Deepak K. Srivastava, Teresa Y. Rawson, Stephen D. Showalter, and Samuel H. Wilson . Phorbol Ester Abrogates Up-regulation of DNA Polymerase by DNA-alkylating Agents in Chinese Hamster Ovary Cells. *J Biol Chem* 270 (1995):16402-16408.
31. Kedar, P.S., Widen, S.G., Englander, E.W., Fornace, A.J., Jr., Wilson, S.H. The ATF/CREB transcription factor-binding site in the polymerase beta promoter mediates the positive effect of N-methyl-N'-nitro-N-nitrosoguanidine on transcription. *Proc Natl Acad Sci U S A* 88(9)(1991): 3729-3733.
32. Mu, D., Tursun, M., Duckett D.R., Drummond, J.T., Modrich, P., Sancar, A. Recognition and repair of compound DNA lesions (base damage and mismatch) by human mismatch repair and excision repair systems. *Mol Cell Biol* 17(2)(1997): 790-769.
33. Baumgartner, B., Heiland, S., Kunze, N., Richter, A., Knippers, R. Conserved regulatory elements in the type I DNA topoisomerase gene promoters of mouse and man. *Biochem Biophys Acta* 1218(1)(May 1994): 123-127.

34. Heiland S., Knippers R., Kunze N. The promoter region of the human type-I-DNA-topoisomerase gene. Protein-binding sites and sequences involved in transcriptional regulation. *Eur J Biochem* 217(3)(1993): 813-822.
35. Hochhauser, D., Stanway, C.A., Harris, A.L., and Hickson, I.D. Cloning and characterization of the 5'-flanking region of the human topoisomerase II alpha gene. *J Biol Chem* 267 (1992): 18961-18965.
36. Popanda, O., Thielmann, H.W. The function of DNA topoisomerases in UV-induced DNA excision repair: studies with specific inhibitors in permeabilized human fibroblasts. *Carcinogenesis* 12 (1992): 2321-2328.
37. Unpublished: Genebank Acc. #T29334, Inst. Genomics Res., 1995.
38. Liang, G., Wolfgang, C.D., Chen, B.P., Chen, T.H., Hai, T. ATF3 gene. Genomic organization, promoter, and regulation. *J Biol Chem* 271(3)(January 1996): 1695-1701.
39. Nilsson, M., Ford, J., Bohm, S., Toftgard, R. Characterization of a nuclear factor that binds juxtaposed with ATF3/Jun on a composite response element specifically mediating induced transcription in response to an epidermal growth factor/Ras/Raf signaling pathway. *Cell Growth Differ* 8(1997): 913-920.
40. Hsu, J.C., Bravo, R., Taub, R. Interactions among LRF-1, JunB, c-Jun, and c-Fos define a regulatory program in the G1 phase of liver regeneration. *Mol. Cell Biol* 12(10)(1992): 4654-4665.
41. Chu, H.M., Tan, Y., Kobierski, L.A., Balsam, L.B., Comb, M.J. Activating transcription factor-3 stimulates 3',5'-cyclic adenosine monophosphate-dependent gene expression. *Mol Endocrinol* 8(1)(1994): 59-68.
42. Kharbanda S., Rubin E., Gunji H., Hinz H., Giovannella B., Pantazis, P., Kufe D. Camptothecin and its derivatives induce expression of the c-jun protooncogene in human myeloid leukemia cells. *Cancer Res* (1991) 51(24): 6636-6642.
43. Pearson, B.E., Nasheuer, H.P., Wang, T.S. Human DNA polymerase alpha gene: sequences controlling expression in cycling and serum-stimulated cells. *Mol Cell Biol* 11(4)(1991): 2081-2095.
44. Kharbanda S.M., Sherman M.L., Kufe D.W. Transcriptional regulation of c-jun gene expression by arabinofuranosylcytosine in human myeloid leukemia cells. *J Clin Invest* 86(5)(1990): 1517-1523.
45. Haug, T., Skorpen, F., Kvaloy, K., Efstad, I., Lund, H., Krokan, H.E. Human uracil-DNA glycosylase gene: sequence organization, methylation pattern, and mapping to chromosome 12q23-q24.1. *Genomics* 36(3)(1996): 408-416.
46. Scanlon, K.J., Ishida, H., Kashani-Sabet, M. Ribozyme-mediated reversal of the multidrug-resistant phenotype. *Proc Natl Acad Sci U S A* 91(23)(1994): 11123-11127.
47. Lee, W., Haslinger, A., Karin, M., Tijan, R. Activation of transcription by two factors that bind promoter and enhancer sequences of the human metallothionein gene and SV40. *Nature* 325(6102)(1987): 368-372.
48. Feuerstein, N., Huang D., and Prystowsky M.B. Rapamycin Selectively Blocks Interleukin-2-induced Proliferating Cell Nuclear Antigen Gene Expression in T Lymphocyte. *J Biol Chem* 270 (1995): 9454-9458.
49. Huang, D., Shipman-Appasamy, P. M., Orten, D. J., Hinrichs, S. H., Prystowsky, M. B. Promoter activity of the proliferating-cell nuclear antigen gene is associated with inducible CRE-binding proteins in interleukin 2-stimulated T lymphocytes. *Mol Cell Biol* 14(6)(June 1994): 4233-4338.
50. Park, J. S., Luethy, J. D., Wang, M. G., Fargnoli, J., Fornace, A. J., Jr., McBride, O. W., Holbrook, N. J. Isolation, characterization and chromosomal localization of the human GADD153 gene. *Gene* 116(2)(July 1992): 259-267.
51. Luethy, J.D., Holbrook, N.J. The pathway regulating GADD153 induction in response to DNA damage is independent of protein kinase C and tyrosine kinases. *Cancer Res* 54(7 Suppl)(1994): 1902s-1906s.
52. Gately, D.P., Jones, J.A., Christen, R., Barton, R.M., Los, G., Howell, S.B. Induction of the growth arrest and DNA damage-inducible gene GADD153 by cisplatin in vitro and in vivo. *Br J Cancer* 70(6)(December 1994):1102-6.
53. Delmastro, D.A., Li, J., Vaisman, A., Solle, M., Chaney, S.G. DNA damage inducible-gene expression following platinum treatment in human ovarian carcinoma cell lines. *Cancer Chemother Pharmacol* 39(3)(1997): 243-253.
54. Kolodner, R.D., Hall, N.R., Lipford, J., Kane, M.F., Rao, M.R., Morrison, P., Wirth, L., Finan, P.J., Burn, J., Chapman, P. Structure of the human MSH2 locus and analysis of two Muir-Torre kindreds for msh2 mutations. *Genomics* 3(1994): 516-26.
55. Lamerdin, J.E., Montgomery, M.A., Stilwagen, S.A., Scheidecker, L.K., Tebbs, R.S., Brookman, K.W., Thompson, L.H., Carrano, A.V. Genomic sequence comparison of the human and mouse XRCC1 DNA repair gene regions. *Genomics* 25(2)(January 1995):547-554.
56. Leach, F.S., Nicolaides, N.C., Papadopoulos, N., Liu, B., Jen, J., Parsons, R., Peltomaki, P., Sistonen, P., Aaltonen, L.A., Nystrom-Lahti, M., et al. Mutations of a mutS homolog in hereditary nonpolyposis colorectal cancer. *Cell* 75(6)(1993): 1215-25.
57. Iwakuma, T., Shiraishi, A., Fukuhara, M., Kawate, H., Sekiguchi, M. Organization and expression of the mouse gene for DNA repair methyltransferase. *DNA Cell Biol* 15(10)(1996): 863-872.
58. Lefebvre, P., Zak, P., Laval, F. Induction of O6-methylguanine-DNA-methyltransferase and N3-methyladenine-DNA-glycosylase in human cells exposed to DNA-damaging agents. *Cell Biol* 12(3)(1993): 233-41.
59. Scherer, S.J., Seib, T., Seitz, G., Dooley, S., Welter, C. Isolation and characterization of the human mismatch repair gene hMSH2 promoter region. *Hum Genet* 97(1)(1996): 114-116.
60. Mello, J.A., Acharya, S., Fishel, R., Essigmann, J.M. The mismatch-repair protein hMSH2 binds selectively to DNA adducts of the anticancer drug cisplatin. *Chem Biol* 3(7)(1996): 579-589.
61. Dalton, T.P., Li, Q., Bittel, D., Liang, L., Andrews, G.K. Oxidative stress activates metal-responsive transcription factor-1 binding activity. Occupancy *in vivo* of metal response elements in the metallothionein-I gene promoter. *J Biol Chem* 271(42)(October 1996): 26233-26241.
62. Gjerset, R. and Mercola, D., Sensitization of Tumors to Chemotherapy through Gene Therapy, in *Advances in Experimental Medicine and Biology*, vol. 465, Chapter 24, pp. 273 - 292, volume theme: Cancer Gene Therapy: Past Achievements and Future Challenges. N. Habib, Ed. Plenum Publishing Corp. NY. (2000).

FIGURE LEGENDS

Figure 1. Viability assay showing that Ad-p53 suppresses growth and enhances sensitivity to DNA damaging chemotherapeutic drugs in p53-mutant-expressing cells (DLD-1 colon carcinoma cells, T47D breast cancer cells, PC-3 prostate cancer cells, and T98G glioblastoma cells). Infection efficiencies were 60-70%, and drug treatments 1 day post-infection were as follows: 5-fluorouracil (5FU) 10 μ M 1 hr, doxorubicin (dox) 3.7 μ M 1 hr, cisplatin (CDDP) 30 μ M 1 hour for PC-3 cells and 20 μ M 1 hr for T98G cells. Viability was assayed 6 days post drug treatment in all cases except PC-3, where viability was assayed 4 days post drug treatment, and expressed as a percent of control cells treated with Ad- β gal.

Figure 2. Suppression of PC-3 prostate tumor growth in nude mice by Ad-p53 + cisplatin. Vector (Ad-p53 or control Ad-Luc, 10⁸ pfu per tumor) was administered intratumorally on days 3,5,7,10, and cisplatin was administered intraperitoneally on days 1,8.

Figure 3. Cell survival (viability) assay showing that expression of mutant Jun (dnJun) sensitizes clonal T98G cells (■) to cisplatin. As controls, Similar viability results are shown for wild-type c-Jun overexpressing clonal T98G cells (◆), and empty vector expressing clonal T98G cells (●). The open symbols indicate the corresponding experiments with the inactive transplatin control indicating that decreased survival by inhibition of the JNK pathway is specific to cisplatin-generated DNA damage (after ref. 22).

Figure 4. Plasmid reactivation assay using CAT (chloramphenicol acetyltransferase) reporter plasmid damaged *ex vivo* by treatment with cisplatin. Reporter gene expression, assayed 24 h post-transfection, indicates that mutant Jun-expressing clonal T98G cells are suppressed in their ability to repair and express the CAT transgene.

Figure 5. Application of Antisense JNK and cisplatin chemotherapy to established xenografts of PC-3 human prostate carcinoma cells. Groups of 10-11 or 15 athymic female mice that had been inoculated with PC-3 cells and allowed to develop visible tumors were started on treatment ("start" arrow) of either one of the indicated antisense oligonucleotide solutions by daily IP injection or cisplatin weekly or a control consisting of vehicle alone or a scrambled sequence oligonucleotide. The average size of the tumors for each treatment group are plotted from the time of inoculation to the end of treatment ("end" arrow). The percent inhibition of growth was calculated by integrating each curve and expressing the result as 100 x (1-(growth/growth of control)). These experiments were carried out in parallel with the p53 adenovirus-treated PC-3 tumors.

Figure 6. Relative 4 day growth following Ad-p53 treatment or Ad- β gal treatment (control) of PC-3 prostate carcinoma cells (parental), PC-3 empty vector transduced cells, and PC-3 mutant Jun-expressing cells (PC-3 mjun). Growth was assayed using the MTT assay.

Table 1. Cisplatin-DNA adducts per 2.7 Kbase

<i>Treatment</i>	<i>T98G Parental Cells</i>	<i>T98G Mutant Jun Cells</i>
200 μ M cisplatin 1 hour	0.48 ± 0.08	0.63 ± 0.2
200 μ M cisplatin 1 hour, 6 hour recovery	0.20 ± 0.05	0.55 ± 0.2

Table 2. DNA repair associated genes which contain potential JNK-regulated sequences (after reference 62)

<i>Repair Associated Gene</i>	<i>Element</i>	<i>Sequence (consensus sequence)²</i>	<i>Position</i>	<i>LLG Score</i>	<i>Reference for Function</i>
DNA Polymerase β	AP-1/TRE	CTGACTCA (- t g a c t c a)	337	2.0	Known to be functional and TPA-activated classic TRE (30).
	ATF/CREB	TTACGTAA (t t a c g t c a)	282	2.0	Known to be genotoxic-activated (30-31).
DNA Polymerase α (32)	ATF/CREB	CACGTCA (t/g a c g t c a)	-82		Function of ATF/CREB (32) unknown.
		GGGGTCA (t g a g t c a)	-149		AP-1 sites thought to be significant in DNA repair: DNA polymerase is over-expressed in cisplatin resistant cells and anti-Fos ribozyme sensitizes (27).
Topoisomerase I	AP-1	GGGGGC GG (t g a g t c a)	753	2.0	(33-34)
	AP-1	TGACCCA (t g a c t c a)	217	2.0	(33-34)
	ATF/CREB	TGACGTCA (t g a c g t c a)	792	2.0	known to be functional & stress-activated (33-34).
Topoisomerase II α	ATF/CREB	TGACGCCG (t g a c g t c a)	286	2.0	(35-36); Topo II is UV-inducible and functions early in UV-induced DNA damage repair.
	AP-1	TGATTGG (t g a g t c a)	337	2.0	(35)
Topoisomerase II β	AP-1	TGACTCA (t g a c t c a)	3		(37)
	AP-1	AGAGTCA (t g a g t c a)	65	1.6	(37)
ATF-3	AP-1	TGAGTAA (t g a c g t c a)	-1600		(38-39) ATF-3 is stress-induced, anisomycin (JNK activator) induced, and induced by ATF-2/c-Jun coexpression suggesting a functional role for the ATF/CREB site. ATF-3/c-Jun heterodimers bind ATF/CREB sites and activate transcription (40-41) and ATF-3/c-Jun and ATF-3/JunD heterodimers have been shown to bind TTAGTTAC, a ATF/CREB sequence, which mediates EGF/ras/raf-stimulated transcription (42), however, a role in induction of DNA repair genes is not known.
	AP-1	ATAGTCA (t g a c g t c a)	-1353		
	AP-1	AGACTAA (t g a c g t c a)	-605		
	AP-1	GAGTCA (t g a c g t c a)	-380		
	ATF/CRE	TTACGTCA (t t a c g t c a)	-92		
c-Jun	ATF/CREB	TTACCTCA (t t a c g t c a)		2.0	(43-45); the "functional" association with DNA repair is strong induction of c-Jun by genotoxins known to activate JNK/SAPK.
Uracil Glycosylase (46)	AP-1	TGGGTCA (t g a g t c a)	141	2.0	Activation regulation not known.
PCNA	AP-1	TGACTCA (t g a c t c a)	489	2.0	DNA polymerase- A accessory protein function.
Proliferating Cell Nuclear Antigen	ATF/CREB	TGAGGTCAGGG	209	1.64	(47-48); IL-2, a potent JNK/SAPK

<i>Repair Associated Gene</i>	<i>Element</i>	<i>Sequence (consensus sequence)²</i>	<i>Position</i>	<i>LLG Score</i>	<i>Reference for Function</i>
	ATF/CREB	(tg a c g t c a ---) GTGACGTAC (-tt a c g t c a --)	1253	1.60	activator, induces PNCA expression via ATF/CREB promoter sites which is blocked by rapamycin.
GADD153 (49) Growth Arrest and DNA-damage" Inducible Gene	ATF/CREB	ACTCCTGACCTT (tg t a c g t c a -----)	207	1.63	Induction requires phosphorylation-dependent event that is not PKA, PKC (50), or p38 (51) mediated consistent with a role for JNK/SAPK (50). Moreover GADD153 is induced by MMS (50) & cisplatin (52-53). The role of the ATF/CREB site is unknown. GADD153 is phosphorylated and activated by p38 in response to stress (54).
XRCC1 (55- 56) X-ray Damage Repair Cross Complementing Gene Product.	ATF/CREB	ACGTCA (a c g t c a)	1815	2.0	The site at 466 is consistent with c-Jun/ATF-3 vs. ATF-2 (TESS).
	ATF/CREB	GGACGTCAA (tg a c g t c a)	1814	2.0	Functional roles of these ATF/CREB and AP-1 sites are not known .
	ATF/CREB	CCTGACCTCA (-t g a c g t c a)	2029	1.64	
	ATF/CREB	GCTGACGTAG (--t g a c g t c a -)	466	1.60	
		CCAATCA (t g/t a c/g t c a)	93	2.0	
MGMT (57) O6-Methylguanine-DNA-Methyl-transferase	ATF/CREB	TGCGTCA (t g a c g t c a)	1661	2.0	MGMT is induced by genotoxic agents (58). The site at 1674 is consistent with c-Jun/ATF-3 (TESS). The functional significance of these sites is unknown.
	ATF/CREB	GTGACATCAT (-t g a c t c a -)	1195		
	AP-1	TGAGTCA (t g a g t c a)	734	2.0	
	AP-1	TTACTCA (t t a c t c a)	285	1.73	
MSH2 (59-60)	ATF/CREB	TGGCGTCA (t g a c t c a)	108	1.62	TESS does not recognize c-Jun participation at 108 site. Role in cisplatin induced repair unknown.
	AP-1	TGAATCA (t g a c/g t c a)	569	2.0	MSH2 has been reported to selectively bind to cisplatin-DNA adducts (32, 59).
	AP-1	TGATGAAA (t g a c/g t c a)	884	1.62	
Metallothionein IIA	AP-1	GAGCCGCAAGT (g a g t c a ----- t) GACTTCTAGCG g a c t c a a g t c CGGGGGCGTG a - - - - - t g)	188	2.0	(61); TPA and UV-light activated.

¹ Repair associated protein for which only partial promoter sequences are known (i.e. in Genbank) without recognizable AP-1 regulated sites include ADP ribose polymerase, tif2/refl, SSRP, Ercc1 and thymidylate synthetase.

² AP-1 consensus: TG/TAC/GTCA; CREB/ATF-2 consensus: TG/TACGTCA.

³ Positions are based on TESS numbering of promoter sequences unless preceded by (-).

Abbreviations:

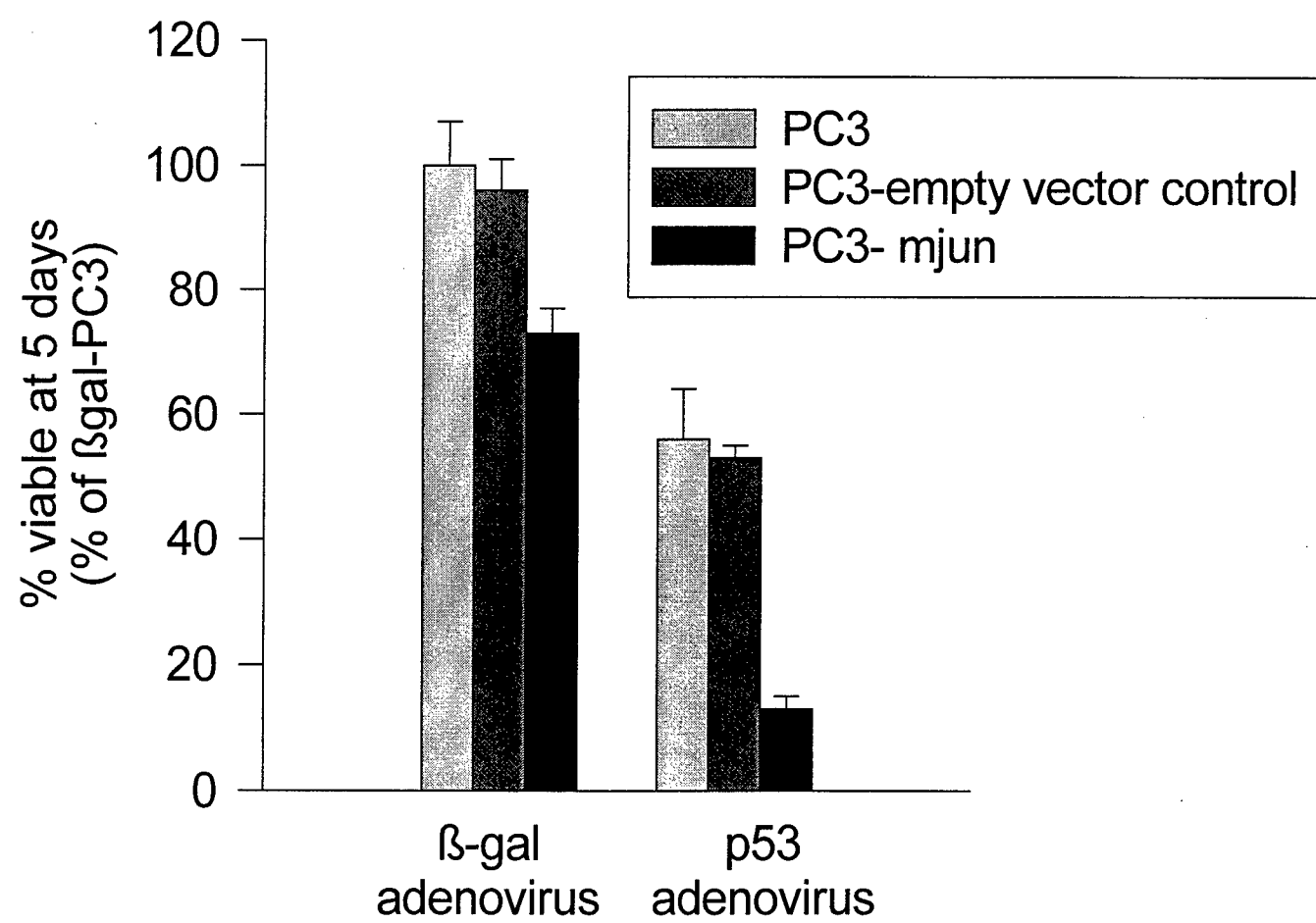
AP-1, activator protein-1 complex, a Jun and a Fos family member

CREB/ATF, cAMP response element binding proteins

LLG, Log likely-hood score which is 2 for a perfect match of the candidate response element with the consensus sequence (TESS criteria) and all ambiguous matches yield a score of 0

MMS - methyl methanesulfonate

TESS - Transcription Element Search System



ABSTRACT SUBMITTED TO THE AACR SPECIAL CONFERENCE ON DNA REPAIR
DEFECTS, January 14-19, 2000. San Diego CA.

T98G glioblastoma cells defective in DNA repair show enhanced p53-mediated growth suppression and apoptosis. Ali Haghghi, Svetlana Lebedeva, Dan Mercola, Ruth A. Gjerset, Sidney Kimmel Cancer Center, 10835 Altman Row, San Diego CA 92121.

We have examined how the cellular DNA damage response and repair pathways might be exploited in combination with tumor suppressor gene replacement to achieve enhanced anti-tumor responses of therapy resistant tumors. We have made use of the T98G glioblastoma tumor cell clones, which have lost wild-type p53 and PTEN activity, and which were inhibited in Jun Kinase (JNK)-mediated c-Jun N-terminal phosphorylation (JNP) by stable modification with a non-phosphorylatable mutant of c-Jun. Our earlier studies have shown that these clones have an increased sensitivity to DNA damaging agents such as cisplatin, but not to agents that target microtubules such as taxanes. The increased sensitivity to DNA damage correlates with a defect in DNA repair, suggesting a role for the Jun Kinase pathway in DNA repair in these cells. These clones also display an elevated frequency of gene amplification suggesting that the DNA repair defect leads to an accumulation of strand breaks that are known to promote gene amplification events. Furthermore, the mutant Jun-modified clones show greater growth suppression and apoptosis in response to wild-type p53, compared to the parental T98G cells from which they were derived. Taken together, these results suggest that a synergistic therapeutic benefit might be achieved when DNA damage recognition is restored as with p53, and DNA repair is inhibited. Through RT-PCR and Western analysis we have examined differentially expressed genes such as bcl2, bax and p21, whose inhibition or overexpression in mutant Jun-modified clones might account for the effects we observe. We find that these clones have elevated p21waf1, decreased levels of bcl2, and an increased bax/bcl2 ratio, that could contribute to increased apoptosis.



DEPARTMENT OF THE ARMY
US ARMY MEDICAL RESEARCH AND MATERIEL COMMAND
504 SCOTT STREET
FORT DETRICK, MARYLAND 21702-5012

REPLY TO
ATTENTION OF:

MCMR-RMI-S (70-1y)

26 Aug 02

MEMORANDUM FOR Administrator, Defense Technical Information Center (DTIC-OCA), 8725 John J. Kingman Road, Fort Belvoir, VA 22060-6218

SUBJECT: Request Change in Distribution Statement

1. The U.S. Army Medical Research and Materiel Command has reexamined the need for the limitation assigned to technical reports written for this Command. Request the limited distribution statement for the enclosed accession numbers be changed to "Approved for public release; distribution unlimited." These reports should be released to the National Technical Information Service.
2. Point of contact for this request is Ms. Kristin Morrow at DSN 343-7327 or by e-mail at Kristin.Morrow@det.amedd.army.mil.

FOR THE COMMANDER:

Encl

Phylis Rinehart
PHYLLIS M. RINEHART
Deputy Chief of Staff for
Information Management

ADB274369	ADB274596
ADB256383	ADB258952
ADB264003	ADB265976
ADB274462	ADB274350
ADB266221	ADB274346
ADB274470	ADB257408
ADB266221	ADB274474
ADB274464	ADB260285
ADB259044	ADB274568
ADB258808	ADB266076
ADB266026	ADB274441
ADB274658	ADB253499
ADB258831	ADB274406
ADB266077	ADB262090
ADB274348	ADB261103
ADB274273	ADB274372
ADB258193	
ADB274516	
ADB259018	
ADB231912	
ADB244626	
ADB256677	
ADB229447	
ADB240218	
ADB258619	
ADB259398	
ADB275140	
ADB240473	
ADB254579	
ADB277040	
ADB249647	
ADB275184	
ADB259035	
ADB244774	
ADB258195	
ADB244675	
ADB257208	
ADB267108	
ADB244889	
ADB257384	
ADB270660	
ADB274493	
ADB261527	
ADB274286	
ADB274269	
ADB274592	
ADB274604	